

**Investigations on the effects of sodium hydrogen sulfide
on human fibroblast-like synoviocytes and in two murine
models of arthritis**

Doctoral thesis at the Medical University of Vienna
for obtaining the academic degree

Doctor of Philosophy (PhD)

Submitted by

DI (FH) Daniela Sieghart

Supervisor:

Ao. Univ.-Prof. Dr. Günter Steiner

Department of Internal Medicine III, AKH Vienna, Austria

Ludwig Boltzmann Gesellschaft

Cluster for Rheumatology, Balneology and Rehabilitation

Kurbadstrasse 14, 1100 Vienna, Austria

Vienna, 09.2014

*Die Endlosigkeit des wissenschaftlichen Ringens sorgt unablässig dafür,
dass dem forschenden Menschegeist seine beiden edelsten Antriebe
erhalten bleiben und immer wieder von Neuem angefacht werden:
Die Begeisterung und die Ehrfurcht.*

Max Planck

(1858 - 1947)

Table of Contents

TABLE OF CONTENTS	III
LIST OF FIGURES	VI
LIST OF TABLES	VIII
ABSTRACT	IX
ZUSAMMENFASSUNG	X
PUBLICATIONS ARISING FROM THIS THESIS	XII
ABBREVIATIONS	XIII
ACKNOWLEDGMENTS	XV
1 INTRODUCTION	1
1.1 Normal Joint Structure	1
<i>1.1.1 Fibroblast-like Synoviocytes (FLS)</i>	2
1.2 Osteoarthritis (OA)	3
<i>1.2.1 The Pathogenesis of OA and the Importance of FLS</i>	4
<i>1.2.2 The Role of IL-1 in OA</i>	5
<i>1.2.3 The Role of IL-6 in OA</i>	6
<i>1.2.4 The Role of Matrix Metalloproteinases in OA</i>	6
<i>1.2.5 Treatment of OA</i>	7
1.3 Rheumatoid Arthritis (RA)	8
<i>1.3.1 The Pathogenesis of RA</i>	9
<i>1.3.2 Treatment of RA</i>	10
<i>1.3.3 Animal Models of RA</i>	10
1.4 Hydrogen Sulfide (H₂S)	11
<i>1.4.1 Sulfur Bath Therapy</i>	14
<i>1.4.2 Exogenous H₂S Donors and their Relevance in Research</i>	16
2 AIMS	18

3 RESULTS	19
3.1 Short-term NaHS treatment increases IL-6 expression and secretion in primary osteoarthritic FLS	19
3.2 NaHS reduces spontaneous IL-6 secretion in resting FLS	21
3.3 NaHS reduces spontaneous chemokine secretion	22
3.4 NaHS treatment does not affect viability of FLS	22
3.5 NaHS treatment decreases IL-1β-induced FLS activation	24
3.6 NaHS reduces IL-1β-induced MAPkinase activation	27
3.7 NaHS treatment abolishes the IL-1β-induced architectural changes of FLS grown in 3-D extracellular matrix micromasses	31
<i>3.7.1 Phosphorylation of Akt is induced by NaHS treatment in FLS grown in 3-D micromass cultures</i>	33
<i>3.7.2 IL-1β-induced stimulation of MMP-2 production is inhibited by NaHS treatment</i>	34
3.8 NaHS affects serum cytokine levels in healthy mice challenged with LPS	35
3.9 NaHS treatment of mice with collagen-induced arthritis	36
<i>3.9.1 Hydrogen sulfide treatment does not affect levels of anti-collagen IgG antibodies</i>	37
<i>3.9.2 Hydrogen sulfide does not influence clinical outcome but seems to increase incidence of arthritis</i>	38
<i>3.9.3 NaHS treatment significantly increases number of osteoclasts but does not influence other histological parameters</i>	39
<i>3.9.4 NaHS treatment does not affect immune cell composition in lymph nodes of mice with collagen-induced arthritis</i>	40
3.10 NaHS treatment of mice with K/BxN serum transfer arthritis	41
<i>3.10.1 NaHS treatment does not influence disease severity or clinical outcome</i>	42
<i>3.10.2 NaHS treatment substantially reduces bone erosion and cartilage loss but has less impact on joint inflammation</i>	42
<i>3.10.3 NaHS treatment increases inflammatory monocytes in blood and spleen</i>	44
4 DISCUSSION	45
4.1 The role of hydrogen sulfide in inflammatory response	45
4.2 Hydrogen sulfide interferes with signaling pathways	46

4.3 Hydrogen sulfide inhibits IL-1β-induced experimental hyperplasia of FLS in micromass cultures	47
4.4 Effects of hydrogen sulfide treatment in animal models of arthritis	47
4.5 Concluding remarks	48
5 METHODS AND MATERIALS	49
5.1 Cell-Culture and treatment	49
5.2 Apoptosis Assay Using Flow Cytometry	49
5.3 Real-time RT PCR	49
5.3.1 <i>RNA Isolation</i>	49
5.3.2 <i>Reverse Transcription</i>	50
5.4 Enzyme-linked Immunosorbent Assay	51
5.5 Proteome Profiler Array	51
5.6 Western-Blotting	52
5.7 Micromass Cultures	53
5.7.1 <i>Immunohistochemistry</i>	53
5.8 Animal Models	53
5.8.1 <i>Collagen-induced Arthritis</i>	53
5.8.2 <i>Serum transfer arthritis</i>	54
5.8.3 <i>Clinical evaluation</i>	55
5.8.4 <i>Sample Collection</i>	55
5.8.5 <i>Histological and Immunological Analysis</i>	56
5.9 Statistical Analysis	57
5.10 Chemicals and Reagents	58
5.11 Buffers and solutions	60
5.12 Equipment	63
6 REFERENCES	64
7 CURRICULUM VITAE	79

List of Figures

Figure 1 Anatomy of a synovial joint (knee)

Figure 2 The development of osteoarthritis is a multistep process

Figure 3 The role of FLS in the pathogenesis of OA

Figure 4 Schematic representation of a normal joint and a joint with pathologic RA

Figure 5 Structure and catalytic equation of H₂S

Figure 6 The generation of hydrogen sulfide can be catalysed by at least three different metabolic pathways

Figure 7 Gasotransmitter H₂S has multiple functions

Figure 8 Kinetics of spontaneous H₂S release from incubated NaHS and GYY4137

Figure 9 Short-term NaHS treatment increases pro-inflammatory cytokine expression and production of OA-FLS

Figure 10 NaHS treatment decreases the production of IL-6 in restive FLS and this effect is transient

Figure 11 NaHS treatment significantly reduces production of chemokines IL-8 and RANTES

Figure 12 NaHS does not affect viability of FLS at therapeutically relevant concentrations

Figure 13 NaHS decreases IL-6 secretion in activated FLS

Figure 14 NaHS decreases MMP-2 and MMP-14 expression in activated FLS

Figure 15 NaHS treatment reduces IL-8 and RANTES secretion in activated FLS

Figure 16 IL-1 β -induced phosphorylation of several MAPkinases can be ameliorated by NaHS treatment

Figure 17 NaHS affects MAPkinases signaling

Figure 18 IL-1 β induces MAPkinases phosphorylation but decreases levels of p-Akt2

Figure 19 NaHS treatment deactivates MAPkinases induced by IL-1 β stimulation in FLS

Figure 20 NaHS treatment reduced the IL-1 β -induced activation of MKK3/6 and GSK-3 β and increased the activation of Akt

- Figure 21** FLS grown in 3-D micromass culture develop lining hyperplasia when activated which could be inhibited by NaHS treatment
- Figure 22** NaHS treatment induced Akt phosphorylation in micromass cultures
- Figure 23** NaHS treatment reduced IL-1 β -induced MMP-2 production in FLS micromasses
- Figure 24** NaHS treatment reduced serum cytokine levels in LPS-triggered mice
- Figure 25** Schematic illustration of treatment pattern for collagen-induced arthritis
- Figure 26** IgG antibody levels expressed as arbitrary units in the serum of DBA/1 mice
- Figure 27** NaHS treatment does not influence outcome of CIA but seems to increase incidence
- Figure 28** Histological evaluation of hind paws of CIA mice
- Figure 29** Flow cytometry analysis of immune cell composition in lymph nodes of NaHS treated mice or control mice
- Figure 30** Schematic illustration of treatment pattern for serum transfer arthritis
- Figure 31** NaHS treatment has no significant impact on disease severity or outcome
- Figure 32** Hydrogen sulfide influences joint degeneration in mice with serum transfer arthritis
- Figure 33** Numbers of inflammatory monocytes in blood and spleen of serum transfer arthritis mice
- Figure 34** Schematic illustration of a right hind paw from mus musculus

List of Tables

Table 1 Oligonucleotide sequences for q RT-PCR

Table 2 Primary antibodies for Western blot analysis

Table 3 Sulfur treatment and arthritis induction

Table 4 Antibodies used in flow cytometry

Table 5 Chemicals and reagents used for this work

Abstract

Hydrogen sulfide (H₂S) is a member of the gasotransmitter family and has emerged as a promising agent for resolution of inflammation in different diseases. H₂S is frequently applied to patients suffering from osteoarthritis (OA) in form of sulfur bath therapies, but information about its effectiveness is still poor. It was the objective of this study to investigate the effects of H₂S on fibroblast-like synoviocytes (FLS), which are key players in OA pathogenesis by responding to pro-inflammatory stimuli such as interleukin (IL)-1 β with excessive production of cytokines and matrix degrading enzymes. Furthermore, this study aimed to investigate the *in vivo* effects of H₂S in two murine models of arthritis.

Primary FLS derived from OA patients were used for *in vitro* experiments. FLS activation was induced by IL-1 β . FLS treated with the exogenous H₂S donor sodium hydrogen sulfide (NaHS) were analysed by flow cytometry, enzyme-linked immunosorbent assay and quantitative real-time RT-PCR. The activation of several MAPkinases and other serine/threonine kinases was assessed by human proteome profiler array and Western-blotting. Treatment-induced effects on cellular structure and synovial architecture were investigated in 3-dimensional (3-D) extracellular matrix micromasses. Additionally, the *in vivo* effects of H₂S were investigated in two murine arthritis models, collagen-induced arthritis and serum transfer arthritis.

NaHS treatment reduced spontaneous and IL-1 β -induced production of IL-6, IL-8 and RANTES (regulated on activation, normal T cell expressed and secreted) in different experimental settings and decreased the expression of MMP-2 and MMP-14. IL-1 β stimulation induced the phosphorylation of most MAPkinases. NaHS treatment reduced the IL-1 β -induced MAPK activation in FLS but increased phosphorylation of pro-survival factor Akt. When cultured in spherical micromasses, FLS intentionally established a synovial lining layer-like structure; stimulation with IL-1 β altered the architecture of micromasses leading to hyperplasia of the lining layer which was reverted by exposure to NaHS. In addition, NaHS suppressed IL-1 β -induced upregulation of MMP-2 whereas it stimulated phosphorylation of Akt. Furthermore, in mice with serum transfer arthritis NaHS treatment significantly diminished the number of osteoclasts leading to greatly reduced bone erosion, while the amount of inflammation was only slightly decreased.

The data obtained indicate, on the one hand, anti-inflammatory effects of hydrogen sulfide on activated synovial fibroblasts that result from selective manipulation of the MAPK and the PI3K/Akt pathway and on the other hand suggest direct effects on bone metabolism by interfering with osteoclastogenesis.

Zusammenfassung

Schwefelwasserstoff (Dihydrogensulfid, H₂S) gehört zu der Familie der Gasotransmitter und ist in eine Vielzahl biologischer Prozesse involviert. Zudem haben sich H₂S freisetzende Verbindungen in verschiedenen Krankheitsmodellen als vielversprechende Kandidaten für einen möglichen therapeutischen Einsatz erwiesen. H₂S wird bei der Behandlung von Patienten mit degenerativen und entzündlichen Erkrankungen des rheumatischen Formenkreises, insbesondere Arthrosen, in Form von Schwefelbadtherapien eingesetzt, jedoch ist die bisherige Erkenntnis bezüglich seiner Wirksamkeit begrenzt und wenig über die zugrunde liegenden zellulären und molekularen Mechanismen bekannt.

Synoviale Fibroblasten spielen eine wichtige Rolle in der Entstehung der Arthrose wie auch der rheumatoiden Arthritis indem sie auf die Aktivierung durch Entzündungs-induzierende Faktoren wie z.B. Interleukin (IL)-1 β mit der vermehrten Produktion von Zytokinen und Matrix abbauender Enzyme reagieren. Es war daher das primäre Ziel dieser Arbeit, die Effekte von H₂S auf synoviale Fibroblasten zu untersuchen. Ein weiteres Ziel war die Untersuchung möglicher *in vivo* Effekte der H₂S Behandlung an Hand von zwei Tiermodellen der rheumatoiden Arthritis.

Für Zellkulturexperimente wurden primäre synoviale Fibroblasten verwendet, welche aus Patienten mit Arthrose im Zuge von Gelenkersatzoperationen gewonnen worden waren. Diese wurden mit IL-1 β aktiviert und mit Natriumhydrogensulfid (NaHS) behandelt, welches in wässriger Lösung H₂S freisetzt, und mit Hilfe von Durchflusszytometrie, ELISA und quantitativer Real-Time RT-PCR untersucht. Die Aktivierung verschiedener MAP Kinasen und anderer Serin/Threonin Kinasen wurde mittels Proteom Profiler Array und Western Blot analysiert. Für die Untersuchung möglicher Effekte von NaHS auf Zellstruktur und Gewebearchitektur der synovialen Fibroblasten wurden die Zellen in 3-dimensionalen Kulturen über mehr als 2 Wochen inkubiert. Mögliche Effekte auf die Entwicklung und den Verlauf von entzündlicher, destruierender Arthritis wurden in zwei verschiedenen Mausmodellen untersucht.

Eine Behandlung mit NaHS führte zum Rückgang der spontanen sowie der durch IL-1 β -induzierten Produktion von IL-6, IL-8 und RANTES. Zusätzlich wurde die Expression der Matrix-Metalloproteinasen (MMP)-2 und -14 inhibiert. Die Aktivierung von synovialen Fibroblasten durch IL-1 β bewirkte eine deutliche Erhöhung der Phosphorylierung der meisten MAP Kinasen, wohingegen die Phosphorylierung von Akt leicht reduziert wurde. Gleichzeitige Behandlung mit NaHS reduzierte die IL-1 β -induzierte Aktivierung der MAP Kinasen, erhöhte aber deutlich die Phosphorylierung von Akt, welcher ein wichtiger Faktor für das Überleben der Zelle ist. Synoviale Fibroblasten, welche in 3-dimensionalen Kulturen mit IL-1 β stimuliert wurden, zeigten eine Kondensation von Zellen an der Oberfläche,

ähnlich der pathologisch erhöhten Anzahl an Zellschichten im Synovium von Patienten mit rheumatoider Arthritis. Diese Zellkondensation konnte durch Behandlung der Kulturen mit NaHS vollständig unterbunden werden.

In den an zwei Arthritis Modellen durchgeführten therapeutischen Studien konnte im Modell der Serumtransfer Arthritis durch Behandlung mit NaHS die erosive Knochenschädigung durch Inhibierung der Osteoklastenaktivierung verhindert werden, wohingegen kein signifikanter Einfluss auf das entzündliche Geschehen festgestellt wurde.

Die erhaltenen Daten zeigen, dass Hydrogensulfid die durch IL-1 β induzierte Aktivierung synovialer Fibroblasten hemmen kann, welche auf die Manipulation der MAP Kinasen sowie des PI3K/Akt Signaltransduktionsweges zurückzuführen sind. Weiters legen die Ergebnisse der Tierversuche nahe, dass NaHS einen direkten Einfluss auf die Osteoklastenbildung haben könnte, wodurch vorwiegend die erosive Natur der Arthritis reduziert wird.

Publications arising from this thesis

Sieghart D, Liszt M, Wanivenhaus A, Broell H, Kiener H, Kloesch B, Steiner G Hydrogen sulfide decreases IL-1 β -induced activation of fibroblast-like synoviocytes from patients with osteoarthritis. *Journal of Cellular and Molecular Medicine* (in press)

Kloesch B, Liszt M, Krehan D, Broell J, Kiener H, Steiner G (2012a) High concentrations of hydrogen sulphide elevate the expression of a series of pro-inflammatory genes in fibroblast-like synoviocytes derived from rheumatoid and osteoarthritis patients. *Immunology letters* **141**: 197-203

Abbreviations

OA	Osteoarthritis
RA	Rheumatoid arthritis
FLS	Fibroblast-like synoviocytes
IL	Interleukin
TNF	Tumor necrosis factor
MMP	Matrix-metalloproteinase
TIMP	Tissue inhibitors of metalloproteinases
MIP	Macrophage inflammatory protein
ECM	Extracellular matrix
ACR	American College of Rheumatology
EULAR	European League against Rheumatism
DMOADs	Disease modifying OA drugs
NSAIDs	Non-steroidal anti-inflammatory drugs
CCP	Cyclic citrullinated peptide
SE	Shared epitope
MHC	Major histocompatibility complex
CIA	Collagen-induced arthritis
CFA	Complete Freund`s adjuvant
AIA	Antigen induced arthritis
PIA	Pristane-induced arthritis
GPI	Glucose-6-phosphate isomerase
ED ₅₀	Effective dose 50
LD ₅₀	Lethal dose 50
H ₂ S	Hydrogen sulfide
NaHS	Sodium hydrogen sulfide
Na ₂ S	Sodium sulfide
GY4137	Morpholin-4-ium 4 methoxyphenyl(morpholino) phosphino-dithioate
TST	Sulfurtransferase
TSMT	Thiol-S-methyltransferase
MST	3-mercaptopyruvate sulfurtransferase
CSE	Cystathionine-γ-lyase
CBS	Cystathionine-β-synthetase
CAT	Cysteine aminotransferase
NO	Nitric oxide
MAPK	Mitogen-activated protein kinase

ERK	Extracellular-signal regulated kinase
MSK	Mitogen- and stress activated protein kinase
RSK	Ribosomal protein S6 kinase
MKK	Mitogen-activated protein kinase kinase
GSK	Glycogen synthase kinase
HSP	Heat shock protein
NF- κ B	Nuclear factor kappa-B
JNK/SAPK	c-Jun N-terminal kinase/stress-activated protein kinase
ELISA	Enzyme-linked immunosorbent assay
qRT-PCR	Quantitative real-time RT-PCR
DMEM	Dulbecco's modified Eagle's medium
FBS	Fetal bovine serum
NEAA	Non-essential amino acids
PBS	Phosphate buffered saline
7-AAD	7-Aminoactinomycin
RT	Room temperature
3-D	3-dimensional
Poly-HEMA	Poly-2-hydroxyethylmethacrylate
H&E	Hematoxylin and eosin
TRAP	Tartrate-resistant acid phosphatase
LC	Langerhans cells
Treg	Regulatory T cells
SD	Standard deviation
SEM	Standard error of mean

Acknowledgments

First and foremost, I would like to thank my supervisor Günter Steiner for giving me the opportunity to perform this research project and my PhD thesis. Thank you for your constant support and guidance.

I am also very grateful to the members of my thesis committee, Gerhard Zlabinger and Hans Bröll for their encouragement, support and critical evaluation of this project.

For financing of this project I would like to thank the Ludwig Boltzmann Society and the European Union.

A special thanks I would like to address to all my colleagues at the Ludwig Boltzmann Institute for Rheumatology and Balneology: Burkhard Klösch, Melissa Liszt, Elisabeth Dietersdorfer, Tatjana Becker, Silvia Löbsch and at the Division of Rheumatology, Department of Internal Medicine III at the Medical University Vienna: Hans Kiener, Birgit Niederreiter, Karolina v. Dalwigk, Brigitte Meyer, Anita Fischer, Victoria Saferding, Roman Kreindl, Eliana Goncalves Alves, Silvia Hayer, Markus Hoffmann and Love Amoyo-Minar.

And of course I am much obliged to my family and friends. A huge thanks to all of them!

1 Introduction

1.1 Normal Joint Structure

Joints are complex structures made up of bone covered by cartilage, synovium and ligaments, which in combination provide the strength to bear weight and to support mobility in one or more directions. There exist three types of joints differentiated by the way the bones are joined. Fibrous joints are linked by dense regular connective tissue whereas cartilaginous joints are linked by cartilage. The main characteristics of synovial joints, like the knee, are the formation of synovial cavities filled with viscous synovial fluid which mainly contains hyaluronan and lubricin. The knee joint consists of three bones: the femur, the tibia and the fibula (Figure 1). Ligaments and tendons, parallel bundles of collagen fibers, connect the bones to synovium and muscles. Intraarticular structures such as the meniscus provide additional stability. With low friction articulation, joints enable movement of the body with minimal effort (Hettinga, 1979).

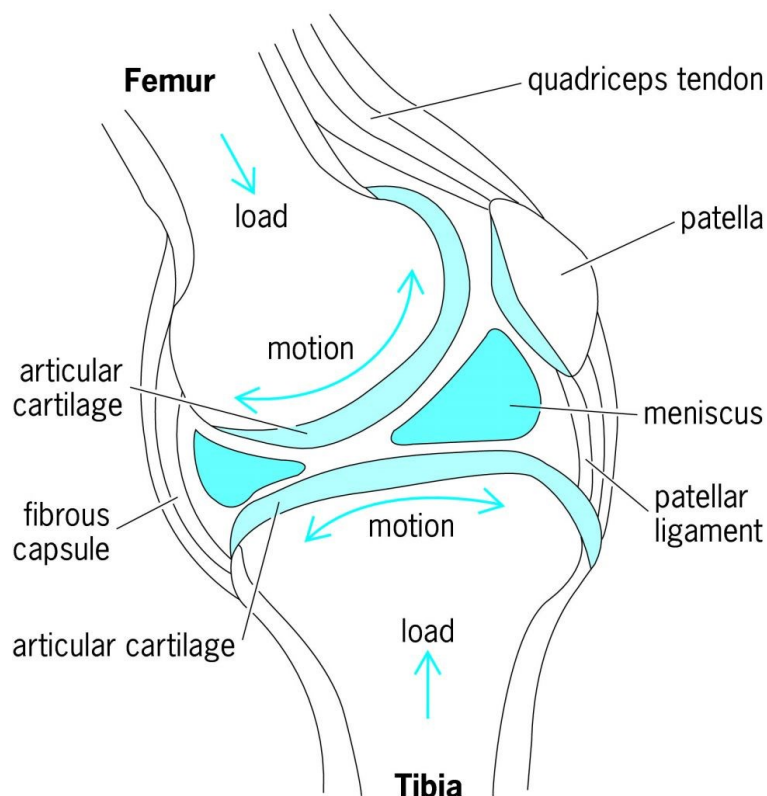


Figure 1 Anatomy of a synovial joint (knee)

The knee joint consists of three bones: femur, tibia and fibula which are covered with articular cartilage. Muscle and strong flexible ligaments like the meniscus provide joint motion and the stability to bare weight. Adapted from McGraw-Hill Concise Encyclopedia of Bioscience. © 2002 by the McGraw-Hill Companies, Inc.

The synovium is a soft tissue which encapsulates the joint and traps the synovial fluid within the cavity. It provides structural stability and brings nutrients to the cartilage. The surface of the synovial membrane is covered with the intimal lining layer, composed of a mixture of two cell types: Type A or macrophage-like cells and Type B or fibroblast-like synoviocytes (FLS). The major function of type A cells is the phagocytosis of cell debris and waste. In addition, they express major histocompatibility complex (MHC) II molecules and possess antigen-presenting capacity (Iwanaga et al, 2000). The cells are embedded in extracellular matrix (ECM) interspersed with collagen fibrils which keeps the surface smooth and non-adherent. The intimal lining layer is separated by the sublining layer through a net of small blood vessels.

Covered by the synovial fluid, the cartilage is an avascular connective tissue that provides covering for the bone. Articular cartilage is comprised of collagen, chondroitin sulfate, proteoglycans, water molecules and chondrocytes. It receives its oxygen and nutrients from the surrounding joint fluid by diffusion during movement. Its function is to protect the joint from impact and loading (Bartok & Firestein, 2010; Martel-Pelletier et al, 1999).

1.1.1 Fibroblast-like Synoviocytes (FLS)

Fibroblast-like synoviocytes, also named synovial fibroblasts arise from the mesenchymal lining and are located in the intimal lining layer of the synovial membrane. FLS are characterized by the expression of UDP-glucose 6-dehydrogenase, which is required for the synthesis of hyaluronic acid and CD55 (decay accelerating factor) (Bottini & Firestein, 2013). Furthermore, synovial fibroblasts express vimentin, collagens IV and V, lubricin, vascular adhesion molecule 1, intracellular adhesion molecule 1, various cytokines like interleukin (IL)-6, IL-15 or IL-16, chemokines like IL-8 and RANTES (regulated on activation, normal T cell expressed and secreted) as well as matrix metallo-proteinases (MMPs). FLS aggregation relies on the adhesion molecule cadherin-11 (Kiener & Brenner, 2005; Kiener et al, 2006), which is also used as a surface marker to distinguish synoviocytes from other fibroblast lineages. For *in vitro* analysis, human or murine FLS can be isolated from synovial tissue. After three to four passages the population of macrophage-like cells is overgrown by fibroblast-like cells, which can be kept in culture for several months. The purity of cells can be determined by flow cytometry, using specific FLS markers as for example CD90.2, V-CAM and I-CAM1. In addition, the expression of vimentin can be used to determine purity of *in vitro* cultured FLS (Rosengren et al, 2007).

FLS derived from healthy donors were found to migrate and invade Matrigel matrix, and build a complex synovial lining structure of one to three cell layers thick. Formation of this lining could be enhanced by tumor necrosis factor (TNF)- α . Other fibroblast lineages such as lung or skin fibroblasts do not show this ability (Kiener et al, 2010).

1.2 Osteoarthritis (OA)

Rheumatic and musculoskeletal diseases (RMDs) are the major cause of disability and OA is ranked on place 11 regarding cause of years lived with disability in the world (Palazzo et al, 2014). This most common joint disease has accompanied mankind ever since being detectable even in fossilized skeletons of our ancestors. OA is a degenerative joint disease whose pathogenesis is a multistep process, characterized by an imbalance of synthesis and degradation of ECM leading to the loss of articular cartilage and subchondral bone (Figure 2) as well as secondary inflammation of the synovium, termed synovitis (Alaaeddine et al, 1999; Roman-Blas et al, 2007).

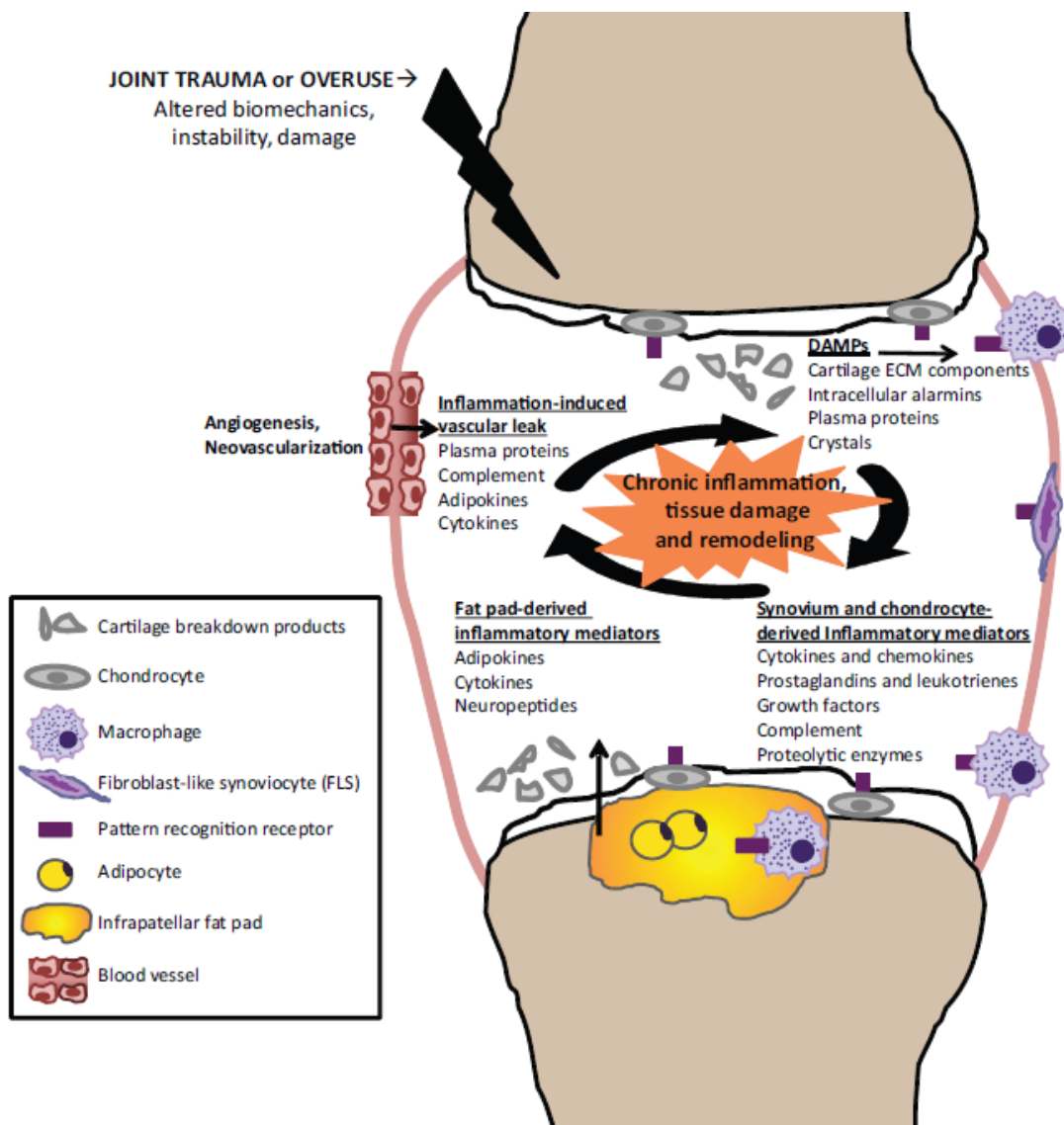


Figure 2 The development of osteoarthritis is a multistep process

Idiopathic or trauma-induced OA have a chronic inflammatory component triggered by damage-associated molecular patterns (DAMPs) or alarmins which induce FLS and chondrocytes to produce high amounts of inflammatory mediators like cytokines or proteolytic enzymes (Sokolove & Lepus, 2013).

OA affects approximately 5 % of the Austrian population and is particularly a disease of the elderly, being diagnosable to some extent in the majority of people over the age of 70. Numerous risk factors are known to play a role in different stages of the disease. Besides aging, also obesity or sex were found to be major risk factors for OA. Women have a higher prevalence and incidence to develop OA which is mainly caused by estrogen insufficiency. In addition, genetic predispositions like mutations in collagens II, IV, V or VI, deletions of genes encoding for proteins of ECM or growth differentiation factor 5 as well as IL-1 or COX-2 point mutations may contribute to OA development (Abramson & Attur, 2009).

Common symptoms of OA are pain, tenderness, functional disability, occasional effusion and morning stiffness leading to a reduced quality of life, making it the leading cause of impaired mobility in the elderly. OA typically affects only one or a few joints; in the majority of cases it affects hands, spine and the large weight bearing joints like knees and hip. It is a progressive disease and decreased movement secondary to pain and locking can favor muscle atrophy. There are four main radiographic features of OA: joint space narrowing, osteophyte formation, subchondral sclerosis and the formation of subchondral cysts (Boegard & Jonsson, 1999).

The American College of Rheumatology (ACR) classification criteria of knee OA (Altman et al, 1986) based on clinical and radiographic characteristics include knee pain for the most days of prior month, radiographic osteophytes at the joint margins, synovial fluid of osteoarthritis (at least 2: clear, viscous, WBC <2,000 cells / ml), morning stiffness of the knee (for at least 30 min) and/or crepitus on active joint motion. According to the ACR it has to be distinguished between primary or idiopathic OA, at which the origin of the disease is unknown, and secondary OA, relying on a previous trauma.

1.2.1 The Pathogenesis of OA and the Importance of FLS

The pathogenesis of primary OA is not completely understood and it was long time considered a non-inflammatory joint disease simply induced by wear and tear. Recent research revealed that OA involves various elements of the inflammatory response including up-regulation of cytokines and chemokines driven by IL-1 β and TNF- α increased levels of which were detected in the synovial fluid of OA patients. Both cytokines potentially induce a positive feedback-loop by stimulating their own production and induce FLS (Afif et al, 2007) to produce other cytokines like IL-6 (Tan et al, 1990), IL-8, cartilage degradative products, inducing angiogenesis (VEGF) and growth (PDGF, TGF- β) or inducing activation of immune cells. Furthermore, OA FLS show reduced susceptibility to apoptosis, which may lead to pannus hyperplasia similar to that seen in rheumatoid arthritis (RA) (Figure 3).

Although OA is affecting a large part of the population, most research on the role of FLS in joint disease has been done in RA, which is a highly inflammatory autoimmune disease

where FLS additionally display a pathogenic phenotype hallmarked by hyperplasia and enhanced invasiveness.

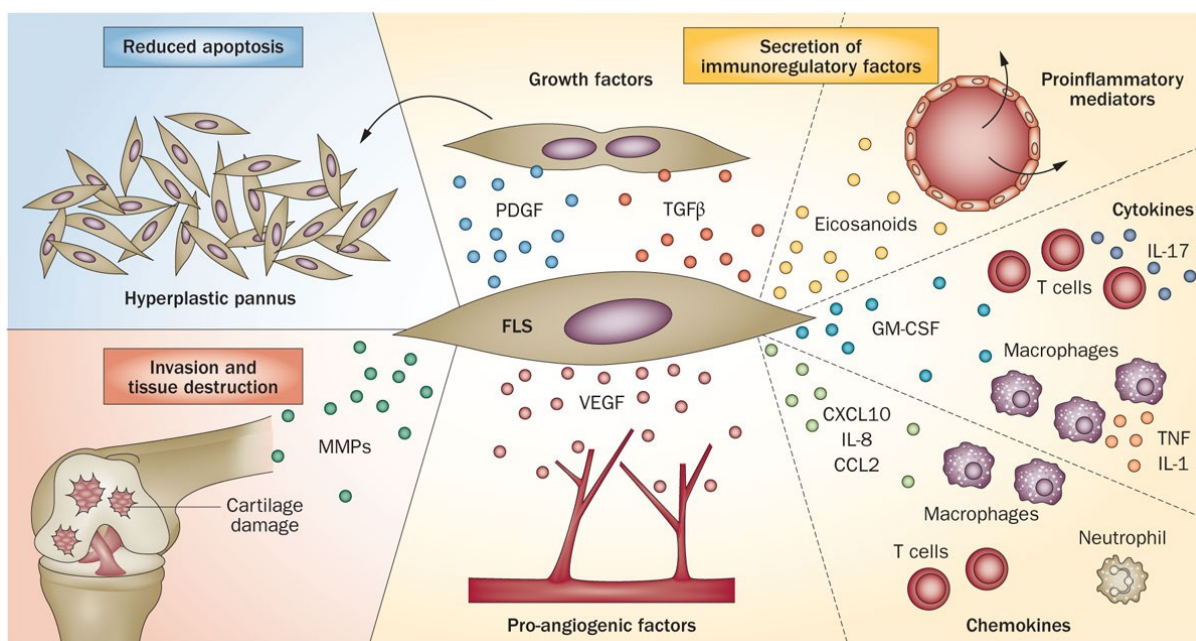


Figure 3 The role of FLS in the pathogenesis of rheumatic diseases (Bottini & Firestein, 2013).

FLS are key players in the progression of rheumatic diseases inducing inflammation via secretion of various cytokines and chemokines such as IL-8 or RANTES which act as chemoattractants promoting the invasion of immune cells such as macrophages or neutrophils. Furthermore, FLS contribute to cartilage degradation by the secretion of MMPs, induce angiogenesis, and especially in RA show reduced apoptosis leading to pannus hyperplasia.

1.2.2 The Role of IL-1 in OA

Cytokines play a central role regulating adaptive and innate immune responses. Dysregulation of cytokines has been implicated with the pathogenesis of several inflammatory and immunologic diseases. The family of cytokines includes interleukins, chemokines, interferons, TNF and lymphokines.

IL-1 is a glycoprotein that plays a major role in inflammatory responses by inducing the synthesis of cytokines, chemokines or proteases. The IL-1 superfamily consists of 11 members with IL-1 α and IL-1 β being the most studied one. Both bind to the IL-1 receptor I (IL-1RI) and their activation is naturally regulated by IL-1R antagonist (Contassot et al, 2012). In OA, IL-1 β seems to be associated with cartilage degradation by stimulating IL-1 β -sensitive FLS to secrete MMP-1, MMP-3 and MMP-13 together with other degradative enzymes. Elevated levels of IL-1 β were found in the synovial fluid, synovial membrane, subchondral bone and cartilage of OA patients. In addition, IL-1 β induces the production of other cytokines and chemokines like IL-6, IL-8, RANTES and MCP-1 (Kapoor et al, 2011).

Interestingly, it was described that the deletion of IL-1 β or the IL-1 β converting enzyme (ICE) increased the severity of surgically induced knee OA in mice (Clements et al, 2003).

1.2.3 The Role of IL-6 in OA

The pleiotropic cytokine IL-6 participates in a broad spectrum of biological events, such as immune responses, haematopoiesis and acute-phase reactions (Hirano, 2010). In general, cytokines are regulatory proteins which under physiological conditions are produced temporarily and are catabolized quickly. In contrast, permanent overproduction of IL-6 has been implicated in the pathogenesis of a variety of diseases, including several chronic inflammatory diseases and cancer. Elevated levels of IL-6 were found in the synovial fluid of OA patients (Doss et al, 2007; Venn et al, 1993).

Expression of IL-6 is dependent on the activation of the mitogen-activated protein kinase (MAPK) pathways (Fan et al, 2004) as well as the nuclear factor (NF)- κ B pathway (Lauder et al, 2007; Liacini et al, 2002; Miyazawa et al, 1998). Soluble IL-6 forms a complex with a membrane IL-6 receptor which then binds to gp130, triggering signal transduction (Ferraccioli et al, 2010).

The physiological effects of IL-6 in the joint include the stimulation of osteoclast formation, the inhibition of TNF- α , IL-1 and the activation of IL-1 receptor alpha and IL-10. Furthermore, IL-6 favours the recruitment of mononuclear cells as well as the activation of T cells by inducing the cells to shift from G0 to G1 phase (Romano et al, 1997). In addition, IL-6 is a potent mediator of MMP synthesis and inhibition which aberrant production of can promote pathologic degradation of cartilage and bone.

1.2.4 The Role of Matrix Metalloproteinases in OA

MMPs belong to the family of zinc dependent endopeptidases and participate in physiological reconstruction processes within the normal joint being centrally involved in the turnover of ECM. The MMP family of enzymes consists of 28 members, their aberrant activation has been found to coincide with several pathologic conditions, including RA. The activity of MMPs is regulated by four different endogenous tissue inhibitors of MMP (TIMP). MMP-2 is a potent mediator of basement-membrane degradation (Zhang et al, 2004) and together with MMP-14 (Knauper et al, 1996) was found to be dependent on the activation of the c-Jun N-terminal kinase/stress-activated protein kinase (JNK/SAPKinase) pathway. Type IV collagenases/gelatinases MMP-2 and MMP-14 were described to be negatively regulated by the MAPK pathway (Ispanovic & Haas, 2006). The proteolytic activity at sites of synovial attachment to cartilage was found to be mediated by a complex consisting of MMP-14, MMP-2 and TIMP-2.

1.2.5 Treatment of OA

Today, therapeutic options for OA are still very limited. New guidelines for treatment of OA were published by the OA Research Society International (OARSI) in 2014 (McAlindon et al, 2014). Since currently inhibition of disease progression is not possible (Wang et al, 2011), treatment is targeted mainly at reduction of bone destruction, secondary inflammation and pain. Most prominent therapeutics are: disease modifying OA drugs (DMOADs), hyaluronic acid, chondroitin sulfate, calcitonin, bisphosphonates, analgesics like morphine or fentanyl, corticosteroids or non-steroidal anti-inflammatory drugs (NSAIDs) which inhibit the generation of prostaglandins by blocking COX-1 and COX-2 such as ibuprofen or diclofenac (Blackburn, 1996; Flood, 2010; Monfort et al, 2008; Rainbow et al, 2012; Zhang et al, 2007).

Besides medical interactions physical therapy and balneotherapy are important options for holistic treatment. According to the OARSI guidelines, balneotherapy is recommended for multi-joint OA with co-morbidities (McAlindon et al, 2014). Clinical trials for the effectiveness of OA treatments are rare because of difficulties in monitoring disease progression (Francon & Forestier, 2009). If the disability is severe and medical interventions are ineffective joint replacement surgery is performed.

1.3 Rheumatoid Arthritis (RA)

RA is a systemic autoimmune disease characterized by chronic inflammation of the synovial membrane (Figure 4), hyperplasia of the synovial lining and overactivation of osteoclasts, resulting in pain, impairment and the irreversible destruction of articular cartilage and bone (Georganas et al, 2000).

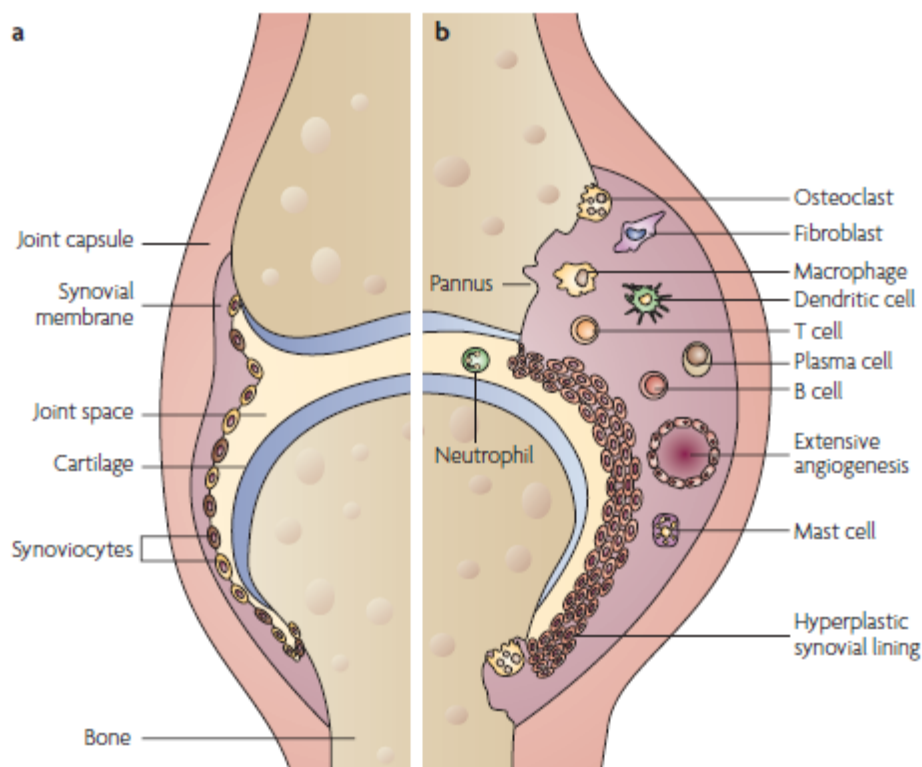


Figure 4 Schematic representation of a normal joint and a joint with pathologic RA (Strand et al, 2007)

Healthy joint (a) compared to a joint affected by RA (b) with classical features of the disease: joint space narrowing, immune cell invasion and hyperplasia of the synovial membrane.

The prevalence in the population is about 1%, with women being two times more prone to be affected. Typically, RA manifests in a polyarthritis, predominantly affecting the small joints of the hands and feet (Ngian, 2010). Another very severe consequence of RA can be additional organ manifestation, e.g. skin, eyes, lungs, heart and even accelerated atherosclerosis (Gabriel & Michaud, 2009), leading to decreased life expectancy (Bartok & Firestein, 2010).

1.3.1 The Pathogenesis of RA

The etiology of RA is still not fully understood. The development of RA is driven by changes in the synovium which displays an aberrant structure hallmarked by FLS hyperplasia and aggregation of immune cells, especially T lymphocytes. B lymphocytes are also found at a lower percentage, their clonal expansion suggesting an antigen-driven maturation (Bartok & Firestein, 2010). In general, the breakdown of self-tolerance is a fundamental process in the pathogenesis of autoimmune disease. Under normal conditions, T lymphocytes, potent for recognition of self-peptide, undergo negative selection in the thymus (central selection). Another defence mechanism is peripheral tolerance, mediated by regulatory T (Treg) cells or the engagement of inhibitory receptors like CTLA-4, inducing T cells to become unresponsive or anergic. If cells somehow escape these mechanisms, this results in chronic activation of T lymphocytes which may lead to development of systemic autoimmune disease. Besides the presence of autoantibodies against immunoglobulin IgG-Fc (rheumatoid factor), type II Collagen or Vimentin, a high percentage of patients present antibodies to citrullinated epitopes (anti-citrullinated protein antibodies, ACPA) which are currently the most specific markers for RA (Ding et al, 2009; Irigoyen et al, 2005).

Immunosenescence – the aging of the immune cells - is thought to contribute to the loss of self-tolerance in T cells, which would explain the correlation between age and prevalence in RA (Colmegna & Weyand, 2011). However, aberrant T lymphocytes are considered to play a central role in the initiation of RA (Fournier, 2005; Joosten et al, 2008; Kao et al, 2007) fostering further activation of macrophage-like synoviocytes and FLS through secretion of pro-inflammatory mediators and autoreactive B cells which produce pathogenic autoantibodies..

FLS derived from RA patients display a unique aggressive phenotype and are critically involved in joint destruction through aberrant production of several cytokines, chemokines and proteolytic enzymes that degrade ECM (Arend & Dayer, 1995; Bartok & Firestein, 2010). Reduced cell death leads to the accumulation of FLS in the intimal lining layer which can be 10-20 cells deep. Especially the resulting increase in production of IL-6 (Madhok et al, 1993) and MMPs (Bartok & Firestein, 2010) are hallmarks of RA-FLS, the primary effectors of cartilage destruction. Konttinen *et al.* (Konttinen et al, 1999) described MMP-1, MMP-9, MMP-13, MMP-14 and MMP-15 as being expressed in RA synovial membrane.

Genetic background clearly plays an important role in this heterogeneous disease (Julia & Marsal, 2013; Viatte et al, 2013). The so-called shared epitope (SE), consisting of a five amino acid motif in the third allelic hypervariable region of the HLA-DR beta chain (Ling et al, 2010) was the first genetic predisposition described. It was found being associated with a strong susceptibility to severe RA. Furthermore, a relatively strong association was found for PTPN22 (Begovich et al, 2004). Other relevant associations include immune genes such

as IL-23R, CTLA-4, TRAF1, STAT-4, IRF5 and CCR6 as well as the enzyme peptidyl-arginine deaminase (PADI4) that converts arginine residues into citrulline thereby creating neo-epitopes specifically targeted by patients with RA (Kurko et al, 2013).

1.3.2 Treatment of RA

Different scores for defining disease activity were proposed by the ACR and the European League against Rheumatism (EULAR). They include parameters like morning stiffness, pain, tenderness, swelling and erythrocyte sedimentation rate (Shammas et al, 2010).

Within the last decade, treatment strategies for RA have markedly improved. The introduction of biological therapies such as TNF, IL-6 or IL-1 cytokine antagonists or the depletion of T and B cells have decreased severity of disease and the progression of symptoms in about half of patients (Bartok & Firestein, 2010). Another group of anti-rheumatic agents are DMARDs like methotrexate, infliximab and rituximab. DMARDs are able to decelerate disease progression and joint destruction. Corticosteroids have both anti-inflammatory and joint protective effects and are often applied while waiting on DMARDs reaction (Majithia & Geraci, 2007; O'Dell, 2004). NSAIDs are used for treatment of acute inflammation and pain reduction but they fail to prevent joint destruction. In even worse cases surgical interventions are needed.

1.3.3 Animal Models of RA

Experimental models for RA are indispensable for research and provide a better understanding of the etiology of disease and possible treatment strategies (Hu et al, 2013). Due to the heterogeneity of RA, a wide range of arthritis models exists. There are two groups of models: inducible models based on immunization with complete Freund's adjuvant (CFA) and transgenic / knock-out models. The clinically most relevant and most widely used models are collagen-induced arthritis (CIA), adjuvant-induced arthritis, pristane-induced arthritis (PIA), antigen induced arthritis (AIA), K/BxN serum transfer arthritis and the TNF-transgenic mouse model.

CIA in mice is a well-established model in which collagen type II is injected twice subcutaneously, primary immunization and boost, respectively. 12-16 days after the boost an RA like disease develops. The incidence of CIA is between 70% and 80% (Rosloniec et al, 2001; Williams, 2004). In this model IL-6 is significantly increased at day one after induction suggesting that IL-6 is important at the early phases of disease. Knock-out experiments in mice confirmed this hypothesis and revealed a significant reduction of IL-17-producing T cells in IL-6^{-/-} mice (Ferraccioli et al, 2010).

In pristane-induced arthritis a single injection with the mineral oil pristane in rats leads to the development of arthritis after two weeks which shows an acute phase followed by a chronic relapsing disease course (Olofsson & Holmdahl, 2007).

The AIA model in mice is a unilateral model in which following systemic immunization with methylated bovine serum albumin arthritis is induced by injection of the antigen directly into the knee joint. Animals show pronounced synovial hyperplasia and severe cartilage degradation (Ferraccioli et al, 2010).

K/BxN mice express the T-cell receptor transgene KRN and MHC class II molecule Ag⁷ and spontaneously develop severe erosive arthritis. Disease is caused by autoantibodies directed against glucose-6-phosphate isomerase which are found in high titers in the serum of K/BxN mice. Serum transfer to C57BL/6 mice rapidly induces severe monophasic arthritis (Monach et al, 2008).

Aberrant production of the pro-inflammatory cytokine TNF was found to be sufficient to induce the development of arthritis which was first demonstrated in Tg197 human TNF-transgenic mice overexpressing human TNF on a C57BL/6 background. These animals spontaneously develop severe, erosive polyarthritis that closely mimics human RA (Li and Schwarz, 2003). Treatment with monoclonal antibodies against human TNF can completely block the outbreak of disease.

1.4 Hydrogen Sulfide (H₂S)

Hydrogen sulfide was long time known as a highly toxic gas, being produced by fermentation in cesspools or sewage pipes, with intoxication leading to respiratory arrest and subsequent death. Several reported accidents are responsible for its bad reputation. Since 2002, hydrogen sulfide belongs to the gasotransmitter family like nitric oxide or carbon oxide. H₂S has the capacity to bind to several groups of proteins, thereby influencing their function and activation. H₂S influences the activation of the NF-κB pathway, leucocyte rolling, ATP release, vasodilatation and presumably other cellular mechanisms. Knowledge about its importance in the pathology of several diseases has increased in the last decade with H₂S being recognized as modulator of disease apart from being just a by-product of cellular degradation. For example, elevated levels of endogenous H₂S were detected in synovial fluid of RA patients (Whiteman et al, 2010a) which might have beneficial effects e.g. by inducing neutrophil apoptosis or tissue repair (Wallace et al, 2012).

Today, H₂S represents an interesting target for research and is not simply considered as a by-product of cellular metabolism. The molecule shows great structural similarities to water (Figure 5) but H₂S, being much less polar than water, dissociates in aqueous solution into hydrogen cation (H⁺) and hydrosulfide anion (HS⁻), which in a further step (only at high pH values) breaks down to H⁺ and sulfide ion (S²⁻). The catalytic activities of these reactions are

$K_{a1} = 1.3 \times 10^{-7} \text{ M}$ and $K_{a2} = 1 \times 10^{-19} \text{ M}$ (Caliendo et al, 2010). H_2S is a weak acid with pKa values of 6.76 at 37°C.

Under biological conditions nucleophile HS^- is the predominant sulfide species. HS^- is a very reactive compound which can bind to the metal centres of biological molecules such as proteins and form iron-sulfur clusters which inhibit their function (Hughes et al, 2009).

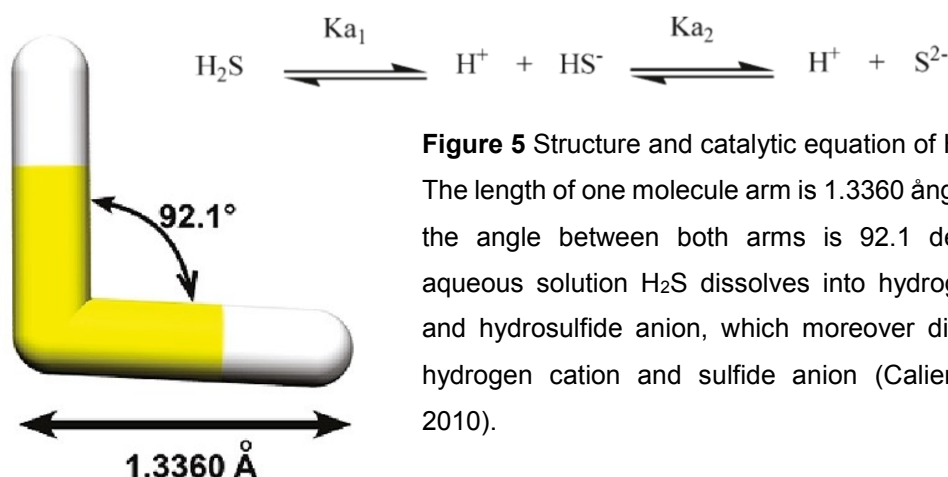


Figure 5 Structure and catalytic equation of H_2S .

The length of one molecule arm is 1.3360 ångström and the angle between both arms is 92.1 degrees. In aqueous solution H_2S dissolves into hydrogen cation and hydrosulfide anion, which moreover dissolves to hydrogen cation and sulfide anion (Caliendo et al, 2010).

In humans and other mammals, H_2S is endogenously synthesized from L-cysteine predominantly by cystathionine- γ -lyase (CSE) (Wang, 2003) and cystathionine- β -synthetase (CBS) (Wang, 2003) (Figure 6). Cysteine aminotransferase (CAT) (Mani et al, 2013) and 3-mercaptopyruvate sulfurtransferase (MST) (Mani et al, 2013) dependent pathways also catalyse the production of H_2S , but to a smaller extent.

CBS hydrolyses L-cysteine to H_2S and L-serine whereas CSE hydrolyses L-cysteine to H_2S plus pyruvate and ammonia. In an alternative pathway, CSE catalyses the conversion of cysteine to thiocysteine, which is then hydrolysed by CSE to cysteine and H_2S (Hughes et al, 2009).

CBS deficiency results in increased concentrations of homocysteine and methionine in plasma and decreased levels of cysteine and might lead to mental retardation and other deficiencies (Hughes et al, 2009).

Endogenous H_2S is mainly oxidized in mitochondria to thiosulfate and subsequently to sulfite and sulfate by thiosulfate cyanide sulfurtransferase (TST). In addition, H_2S can become methylated in the cytosol by thiol-S-methyltransferase (TSMT) to methanethiol and dimethyl sulfide. Physiological levels of endogenous H_2S in humans range between 36 - 42 μM in serum (Zhi et al, 2007). The highest concentrations of endogenous H_2S were found in the human brain (Caliendo et al, 2010).

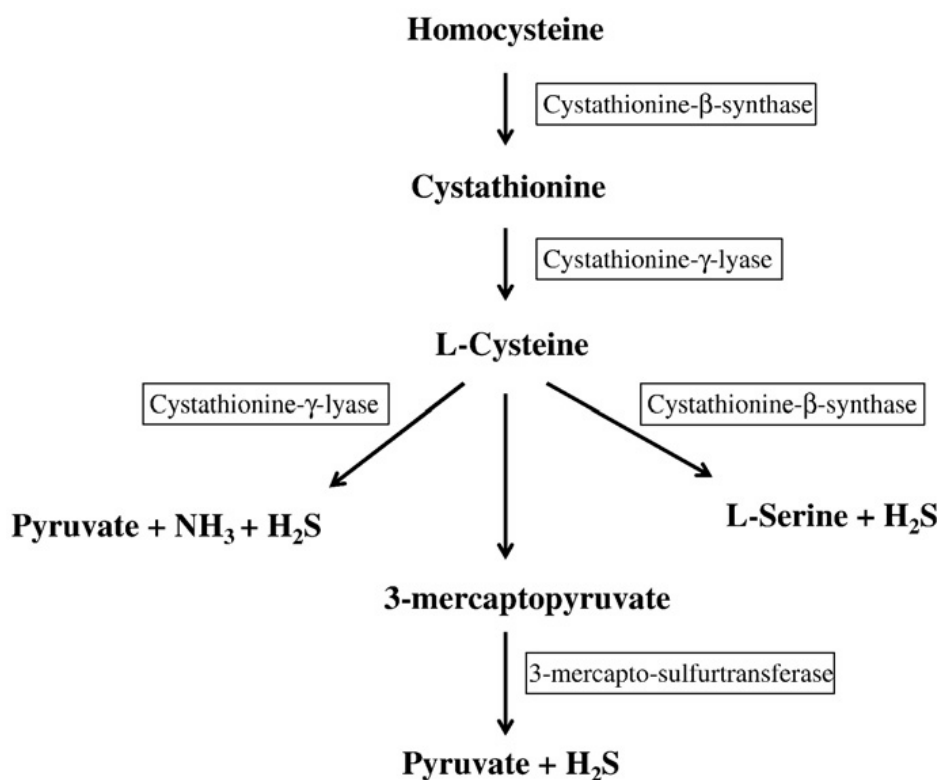


Figure 6 The generation of hydrogen sulfide in mammalian tissue can be catalysed by at least three different metabolic pathways: enzymatic desulfydration of cysteine catalysed by cystathionine- γ -lyase, cystathionine- β -synthase or 3-mercapto-sulfurtransferase. Figure adapted from Hughes et al. 2009 (Hughes et al, 2009).

H₂S is an important signalling molecule (Szabó, 2007), involved in regulation of several physiological processes like blood pressure, insulin secretion, nociception, learning and memory (Whiteman & Winyard, 2011), also playing an important role in modulating inflammation, which was initially contradictory (Lowicka & Beltowski, 2007). In recent years the majority of studies proposed anti-inflammatory effects of H₂S (Figure 7) caused by several key mechanisms: (1) suppression of leukocyte adherence and migration, (2) reduction of pro-inflammatory mediator expression, (3) suppression of nuclear factor kappa-B (NF- κ B) pathway activation as well as (4) the promotion of vasodilation and angiogenesis. In addition, H₂S displayed anti-nociceptive effects by activation of ATP-sensitive potassium channels (Wallace et al, 2012).

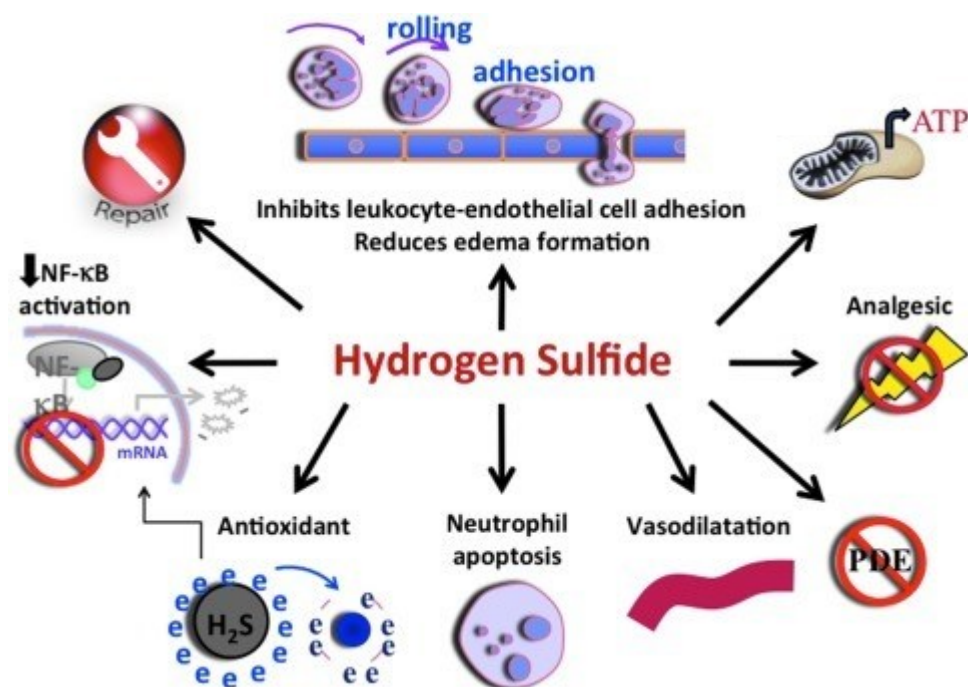


Figure 7 The gasotransmitter H₂S has multiple functions

H₂S displays anti-inflammatory properties by suppressing leukocyte adherence and migration, reducing plasma exudation and the expression of many pro-inflammatory cytokines, chemokines, and enzymes together with suppressing the activation of NF-κB. In addition, H₂S is also a potent antioxidant which can induce apoptosis in neutrophils. Moreover, H₂S exhibits anti-nociceptive effects by activation of ATP-sensitive potassium channels and can act as an energy source (generating ATP) which might contribute to protection and repair of tissue injuries (Wallace et al, 2012).

In synovial fluids derived from RA patients H₂S was found to be four-fold increased. Additionally, H₂S concentrations negatively correlated with neutrophil and total white blood cell counts and positively correlated with tender joint counts (Whiteman & Winyard, 2011).

1.4.1 Sulfur Bath Therapy

Balneotherapy - derived from the Latin word “balneum” for bath - describes the treatment of disease by bathing in mineral spring water. This traditional therapy was already applied by ancient nations like the Greek and Romans (Jackson, 1990).

While drilling for oil, a sulfurous thermal spring was found 1934 in Vienna-Oberlaa. Water analysis revealed that one litre of sulfurous thermal water contains over 60 mg/kg bivalent sulfide (SII), which makes it one of the most powerful sulfur springs in Europe. Patients are treated with sulfur baths at the newly established health resort Therme Wien Med for a duration of 20 min, three times a week for three weeks. Although beneficial effects were

seen in several clinical studies conducted at health resorts all over the world (Francon & Forestier, 2009; Kovacs et al, 2012), the molecular mechanisms underlying this effects are not completely understood. Sulfur baths that are rich in exogenous H₂S are considered as effective therapy in rheumatic disorders (Francon & Forestier, 2009) and are frequently applied to OA patients. The therapy focuses on the reduction of pain, the improvement of mobility and therefore life quality. Balneotherapy is not recommended for active RA patients because elevated water temperatures (about 36 °C) are counterproductive and would increase inflammation and rather enhance than ameliorate the disease.

Since the composition of mineral waters differs between countries or even regions, unambiguous clinical data is difficult to achieve. Therefore, clinical data on the effectiveness of sulfurous thermal water therapy is rare (Fioravanti et al, 2012). A recent study showed a significant reduction in pain for up to 6 months after treatment with sulfur baths (13.2 mg/l S⁻²) in patients with hand OA (Kovacs et al, 2012). Sulfur bath therapy was furthermore shown to reduce oxidative stress in patients with OA by reducing peroxide concentration, superoxide dismutase activity (Ekmekcioglu et al, 2002) as well as plasma homocysteine levels (Leibetseder et al, 2004).

Other sulfur spa therapies like mud packs and hydro-pinothrapy (drinking of sulfurous water) also indicate positive effects on OA patients by decreasing inflammatory parameters like TNF- α and cartilage degradating MMP-2 (Benedetti et al, 2010).

Karagülle *et al.* introduced the first and only animal model for sulfur bath therapy treating rats with adjuvant arthritis. Differences between the three treatment groups (untreated, treatment with sulfurous thermal water, treatment with hot tap water) did not reach statistical significance (Karagülle, 1996).

Until today we still lack knowledge how much of exogenous H₂S or rather its metabolic derivatives reach the joint and how they interact in an inflammatory milieu. Exogenous H₂S has a very high penetration rate. Following uptake by the mucosa and dermis, sulfur molecules are nearly completely oxidized in the epidermis. In Langerhans cells (LC), which are dendritic cells located in the dermis and mucosa, sulfur treatment leads to a modulation of the immune system by inducing the migration of LCs to the lymph node were they stimulate lymphocyte activation.

1.4.2 Exogenous H₂S Donors and their Relevance in Research

For studying the biological activity of H₂S, exogenous sources for example sodium hydrogen sulfide (NaHS) (Szabó, 2007), sodium sulfide (Na₂S) (Andruski et al, 2008) or Morpholin-4-ium 4 methoxyphenyl(morpholino) phosphino-dithioate (GYY4137) (Li et al, 2008) are of interest.

H₂S donors can be distinguished amongst others according to their emission rates. Once in solution, NaHS quickly releases H₂S (Figure 8, left), whereas GYY4137 is a slow-releasing H₂S donor (Figure 8, right).

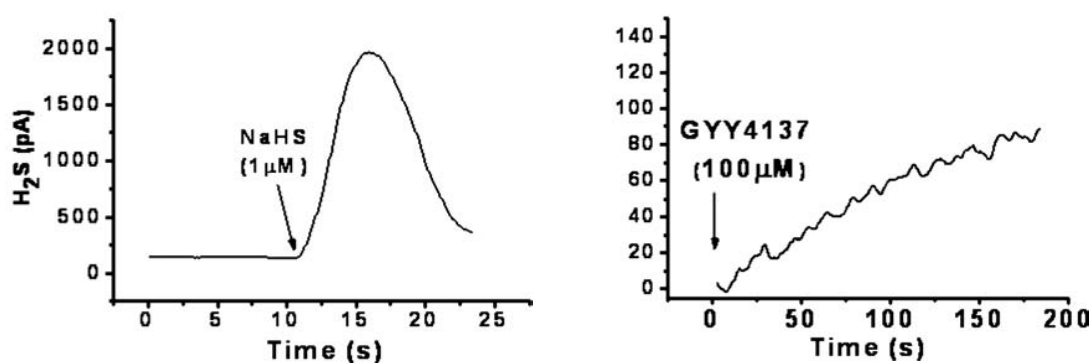


Figure 8 Kinetics of spontaneous H₂S release in aqueous solution from NaHS (left) and GYY4137 (right). The figure was taken from (Whiteman et al, 2010b).

Despite its obvious limitations, the usefulness of NaHS for research has been demonstrated in several experimental studies dealing with inflammation and joint diseases. Previous findings on the effects of NaHS on inflammation *in vitro* are controversial. Anti-inflammatory properties of H₂S by reducing inflammatory parameters (e.g. cytokines) in synovial fibroblasts from RA patients (Kloesch et al, 2010) and human chondrocyte cell line C-28/12 (Kloesch et al, 2012b) were described. Furthermore, treatment with 100 μmol/l NaHS significantly reduced the IL-6 production in LPS-activated RAW264.7 murine macrophages. In contrast, high concentrations of NaHS elevated the expression of TNF-α and IL-1β in these cells (Whiteman et al, 2010b). The duration of exposure also emerged as an important parameter when Kloesch *et al.* in 2012 (Kloesch et al, 2012a) described the increase in pro-inflammatory cytokine expression in one OA and one RA synovial fibroblast cell line following 20 min incubation with NaHS. Moreover, Zhi *et al.* described in 2007 (Zhi et al, 2007) that NaHS treatment of human leukemic monocyte lymphoma cell line U937 increased the activation of NF-κB via the activation of ERK1/2 and IκB-α degradation. Furthermore, it was reported that, during inflammation, oxidative stress induces the conversion of H₂S to sulfite by activated neutrophils (Mitsuhashi et al, 2005).

The role of H₂S in cardiovascular and neurological diseases has been intensely studied (Chen et al, 2013; Giuliani et al, 2013; Gu et al, 2013; Liu et al, 2012; Liu et al, 2013; Zhang et al, 2013a; Zhang et al, 2013b). Regarding involvement in inflammation, experiments using NaHS *in vivo* revealed controversial results. As far, several studies proposed beneficial properties of NaHS ranging from anti-inflammatory potential in mice suffering from lung or pancreas inflammation (Sidhapuriwala et al, 2009) to reduction of oxidative stress in lungs of allergic mice (Benetti et al, 2013). On the other hand, H₂S was found to induce brain damage in rats with encephalopathy (Chen et al, 2011). Investigations on the *in vivo* effects of NaHS revealed an effective dose 50 (ED₅₀) of 35 µmol/kg in rats with carrageenan paw edema (Zanardo et al, 2006). The concentration of NaHS at which 50 % of animals died, the so-called lethal dose 50 [LD₅₀] was described to be 14.6 ± 1 mg / kg in rats (Warenycia et al, 1989). Truong *et al.* (Truong et al, 2007) reported a mouse LD50 of injected NaHS as 0.43 mmol kg⁻¹.

2 Aims

Rheumatic and musculoskeletal diseases (RMDs) are the major cause of disability world-wide. Hydrogen sulfide is a member of the gasotransmitter family and has emerged as a promising agent for resolution of inflammation in different diseases. H₂S is frequently applied to patients suffering from RMDs, especially patients with OA, in form of sulfur bath therapies, but information about its effectiveness is scarce and the underlying mechanisms are poorly understood.

It was therefore the major goal of this thesis to study the cellular and molecular mechanisms of hydrogen sulfide treatment of inflammatory and degenerative joint disorders by investigating its effects on synovial fibroblasts derived from patients with OA, particularly with respect to cytokine production, MMP expression and MAPkinase signaling pathways.

In addition, the study was aimed at increasing our understanding of the interactions between synovial fibroblasts in their extracellular matrix environment in the intimal lining layer by applying a 3-dimensional micromass culture technique.

The ultimate aim was to study *in vivo* the effects of H₂S treatment on inflammation and disease in animal models of arthritis focusing particularly on destructive processes such as cartilage degradation and bone erosion.

3 Results

Most of the work described in this thesis has been published recently. In detail, data shown in Figure 9 were adopted from the following publication:

Kloesch B, Liszt M, Krehan D, et al. (2012a) High concentrations of hydrogen sulphide elevate the expression of a series of pro-inflammatory genes in fibroblast-like synoviocytes derived from rheumatoid and osteoarthritis patients. *Immunology letters* **141**: 197-203

Figures 10 – 15 and 17 – 23 were adopted from the following publication:

Sieghart D, Liszt M, Wanivenhaus A, et al. Hydrogen sulfide decreases IL-1 β -induced activation of fibroblast-like synoviocytes from patients with osteoarthritis. *Journal of Cellular and Molecular Medicine* (in press)

3.1 Short-term NaHS treatment increases IL-6 expression and secretion in primary osteoarthritic FLS

In a pilot experiment we were interested in the effects of short-term NaHS treatment on FLS derived from a single OA patient. Cells seeded at 80 % confluency to 6-well plates were incubated with 1 mM NaHS or its diluent PBS for 20 min. Afterwards, the medium was replaced and FLS were further incubated for one, three, six or 12h. Cells were harvested and expression of IL-6, IL-8, HO-1 and HSP70 were determined by qRT-PCR. IL-6 secretion was determined out of cell culture supernatant by ELISA.

We found stimulative effects of NaHS treatment on the expression (Figure 9A) and secretion (Figure 9B) of IL-6 after three h or three and six h, respectively. IL-8 expression was also increased by 20 min NaHS treatment after three, six and 12 h (Figure 9A). In addition, expression of heme oxygenase (HO)-1 and heat-shock protein (HSP) 70 was upregulated by NaHS (Figure 9C).

The activation of ERK1/2 was analysed by Western-blotting. Therefore, cells seeded at 80 % confluency in 10 cm dishes were treated with 1 mM NaHS for 15, 30, 45 and 60 min following which they were collected and lysed with sample buffer. Expression of ERK and its phosphorylated form was determined, tubulin was used as an internal loading control. NaHS treatment increased the phosphorylation of ERK after 15 to 30 min in a reversible manner (Figure 9D). Hence, short-term NaHS treatment had a positive influence on the activation of ERK1/2 that required further investigations.

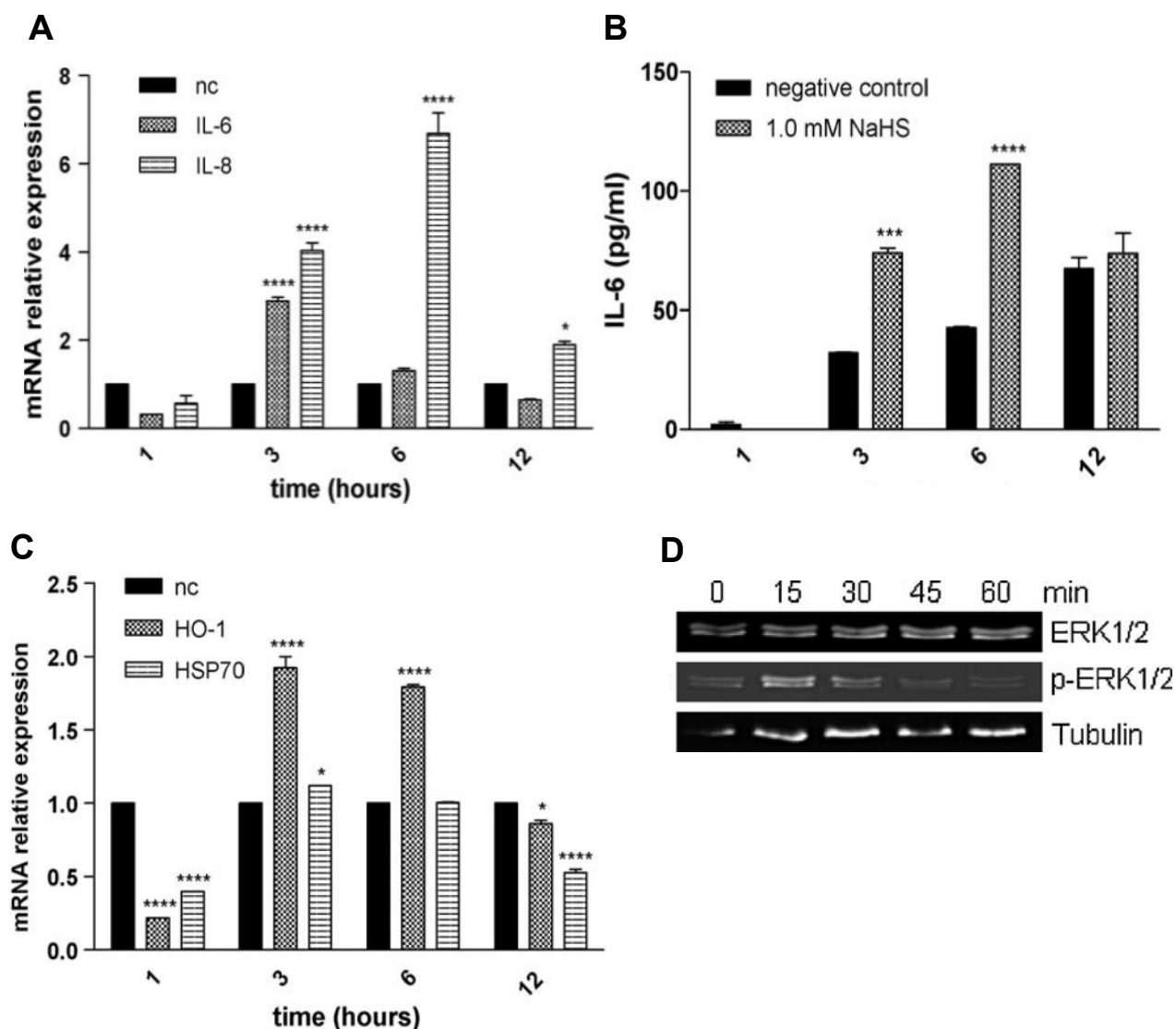


Figure 9 Short-term NaHS treatment increases pro-inflammatory cytokine expression and production of OA-FLS.

Cells were treated with 1 mM NaHS for 20 min following which they were further incubated in fresh medium for one, three, six or 12 h. (A) Expression of pro-inflammatory cytokine IL-6 and chemokine IL-8 was analysed by qRT-PCR. (B) Cell culture supernatants were analysed by ELISA for the secretion of IL-6. (C) The expression of heme oxygenase (HO)-1 and heat shock protein (HSP)70 was detected by qRT-PCR. (D) The activation of MAPkinase ERK1/2 was analysed after cells were treated with 1 mM NaHS for 15, 30, 45 or 60 min. All experiments were performed in duplicates and were repeated once. (A) * $P < 0.05$, ** $P < 0.01$, **** $P < 0.0001$; (B) *** $P < 0.001$, **** $P < 0.0001$; (C) * $P < 0.05$, **** $P < 0.0001$

3.2 NaHS reduces spontaneous IL-6 secretion in resting FLS

FLS derived from patients suffering from OA spontaneously produce low levels of IL-6. Under unstimulated or “resting” conditions, four out of seven primary FLS lines produced detectable amounts of IL-6 and were therefore used in the following experiment. Cells were treated with increasing concentrations of NaHS (0.06 – 1 mM) or phosphate buffered saline (PBS) for one hour (h). Afterwards, the medium was changed and FLS were further incubated in sulfur-free medium for an additional h. Supernatants were collected and analysed by ELISA.

NaHS treatment decreased the production of IL-6 by FLS in a concentration-dependent manner (Figure 10A). Treatment with 1 mM NaHS led to significantly reduced IL-6 levels suggesting potential anti-inflammatory effects of one h NaHS treatment.

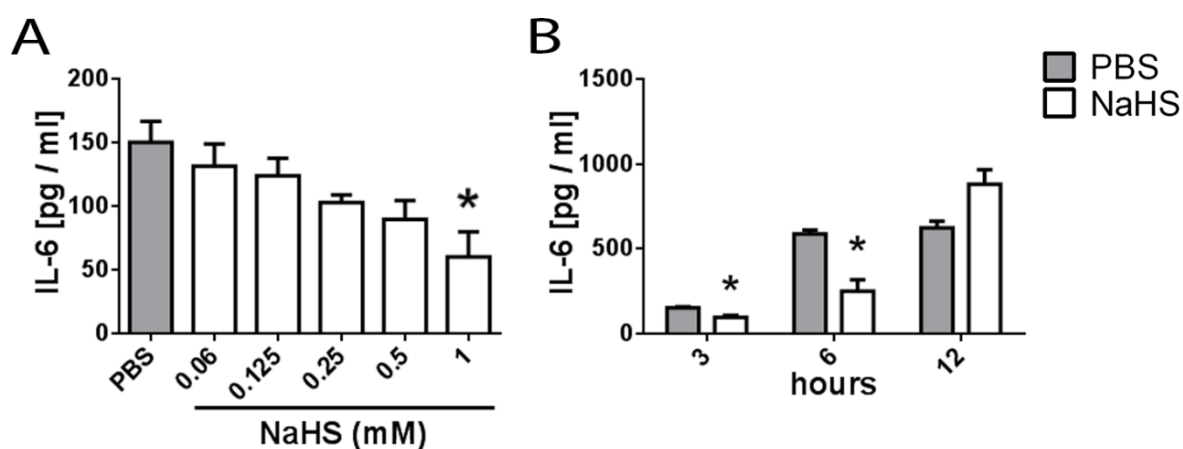


Figure 10 NaHS treatment decreases the production of IL-6 in unstimulated FLS and this effect is transient

IL-6 production was quantified out of cell culture supernatants from cells treated with (A) increasing concentrations of NaHS (0.06 – 1 mM) for one h with consecutive incubation for one h or (B) 1 mM NaHS for one h with consecutive incubation for three, six and 12 h. PBS was used as a control. The graphs comprise data from FLS of four different patients. (A) *P < 0.05; (B) *P < 0.05

Furthermore, it was investigated if this effect is consistent over several hours. Therefore, following one h incubation with 1 mM NaHS or PBS, FLS were further incubated for up to 12 h and supernatants were collected after three, six and 12 h. NaHS treatment significantly reduced spontaneous IL-6 after three and six h. Interestingly, the effect was found to be transient, being no longer detectable after 12 h (Figure 10B).

3.3 NaHS reduces spontaneous chemokine secretion

Chemokines IL-8 and RANTES (or CCL5) are key players in inflammatory diseases acting as chemoattractant for immune cells. Unstimulated FLS secreted detectable amounts of both chemokines and one h treatment with 1 mM NaHS led to significantly decreased secretion of IL-8 and RANTES (Figure 11) after one h recovery in fresh medium.

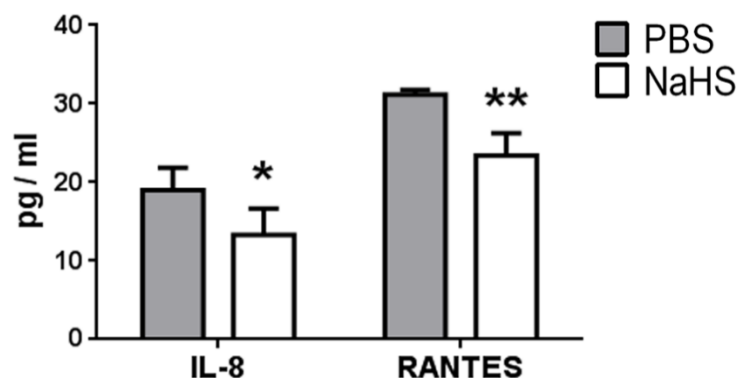


Figure 11 NaHS treatment significantly reduces production of chemokines IL-8 and RANTES

FLS from three different OA patients were treated with PBS or NaHS for one h following which the medium was changed and cells were further incubated for an additional h. IL-8 and RANTES were quantified out of cell culture supernatants and blotted to a graph. The experiment was performed two times in triplicates. *P < 0.05, **P < 0.01

3.4 NaHS treatment does not affect viability of FLS

Since hydrogen sulfide at higher concentrations can be cytotoxic (Caliendo et al, 2010) and effects seen in the first experiments might result from the negative influence of NaHS on cell viability, the next experiment focused on potential apoptotic effects on FLS. Therefore cells were treated with a broad range of NaHS concentrations (0.1 – 4 mM) for one h following which they remained for 24 h in fresh medium. FLS were harvested, stained with annexin V and 7-AAD and analysed by flow cytometry. As positive control, FLS were irradiated with UV light (254 nm) for 10 min. As a negative control, FLS were incubated with PBS.

NaHS concentrations of up to 1 mM did not induce apoptosis in primary FLS whereas 2 and 4 mM NaHS as well as UV treatment induced significantly more early apoptosis (Figure 12A&B) compared to PBS treated samples. Hence, at concentrations used throughout this study, the physiological effects observed were not due to cytotoxicity.

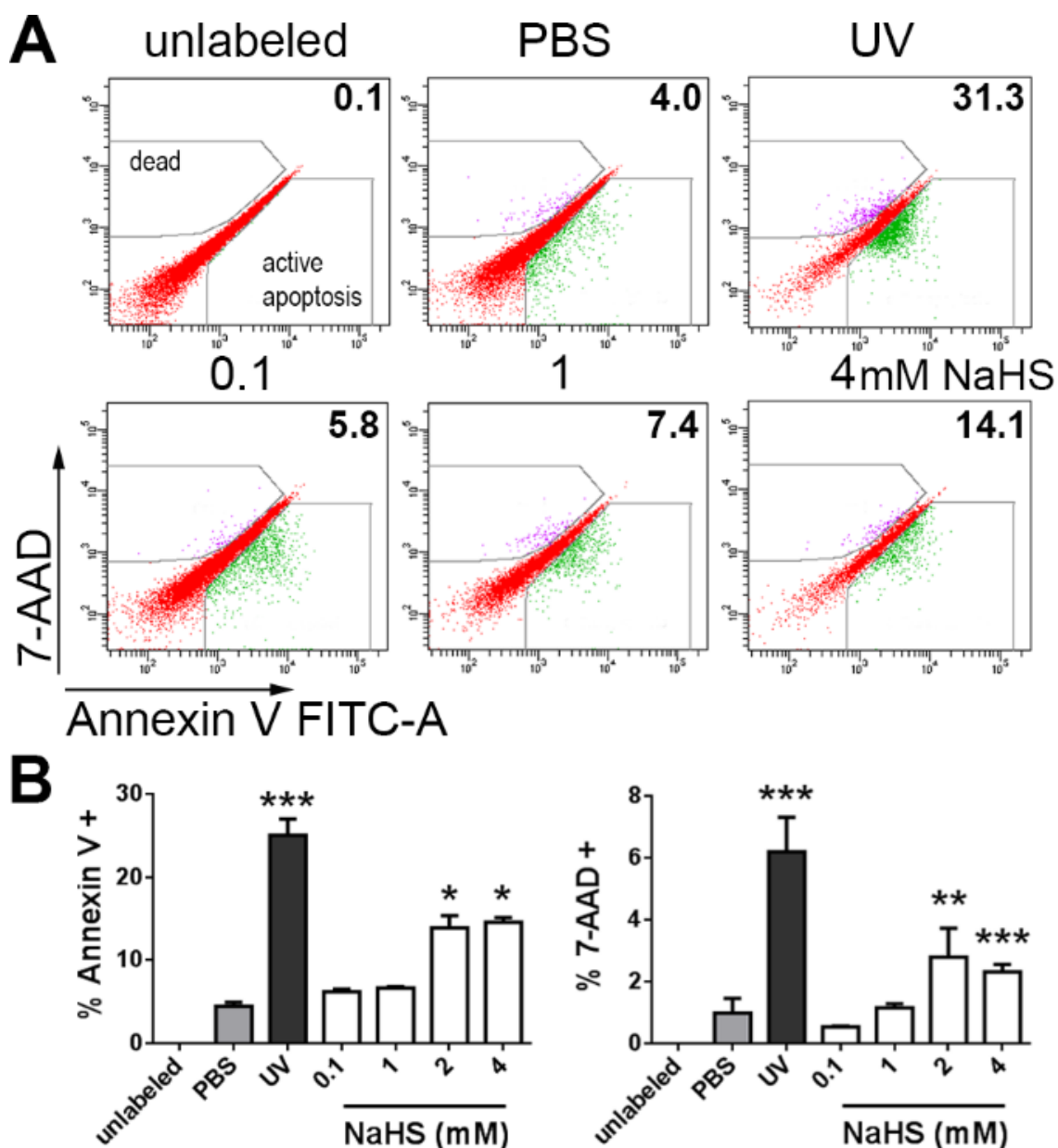


Figure 12 NaHS does not affect viability of FLS at therapeutically relevant concentrations

Viability of FLS was determined by flow cytometry employing annexin V staining, following one h treatment with different concentrations of NaHS. For a negative control, cells were incubated with PBS. For a positive control, cell death was induced by 10 min UV irradiation at 254 nm. (A) FACS scatter plots of one out of three independent experiments: the percentages of early apoptotic cells are indicated. (B) Quantitative evaluation of three independent experiments. (B) *P < 0.05, **P < 0.01, ***P < 0.001

3.5 NaHS treatment decreases IL-1 β -induced FLS activation

During joint inflammation, FLS are activated by pro-inflammatory cytokines or chemokines. IL-1 β plays a crucial role in the development and progression of OA by inducing the expression of matrix degrading enzymes or other cartilage degenerative and inflammatory molecules like IL-6 or IL-8 (Georganas et al, 2000). In the following experiments, FLS were activated with IL-1 β to study this pathologic condition.

Cells were treated simultaneously with NaHS and IL-1 β for one h following further incubation in sulfur-free medium for up to 12 h. Supernatants were obtained at one, three, six and 12 h and were analyzed by ELISA.

IL-1 β activated FLS for up to 12 h, inducing significantly increased secretion of IL-6. In cells treated with NaHS, IL-6 secretion was significantly reduced (Figure 13A) and this inhibitory effect could still be seen after recovery times of three and six h and, though less pronounced, even after 12 h.

We further aimed to investigate if pre-incubation with NaHS has a protective effect on FLS. Therefore, cells were incubated with NaHS for one h following which they were activated with IL-1 β for an additional h. The effects observed were similar to those obtained by simultaneous treatment (Figure 13B) but after recovery of 12 h the decrease was no longer significant.

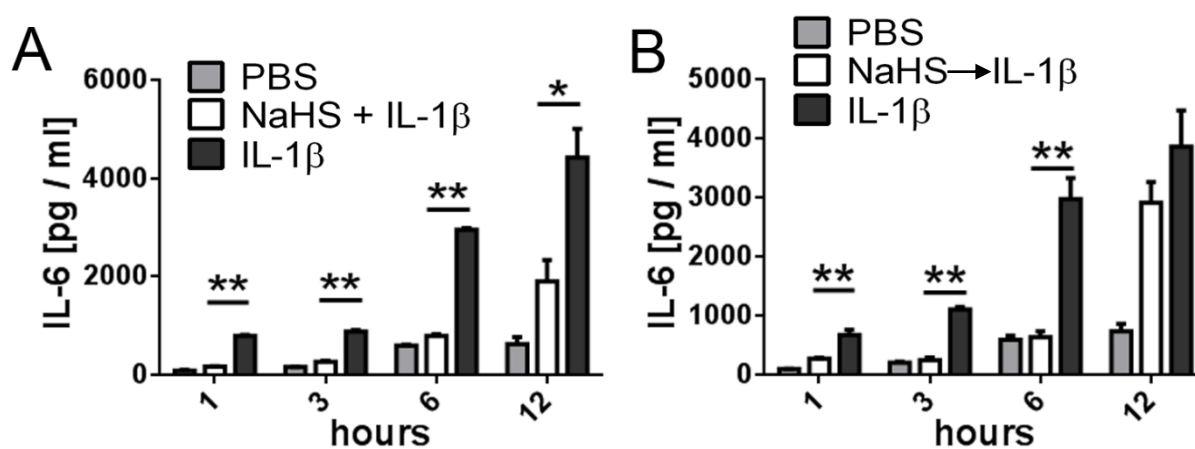


Figure 13 NaHS decreases IL-6 secretion in activated FLS

Determination of IL-1 β -induced IL-6 production by ELISA from cell-culture supernatants after recovery of one, three, six or 12 h. FLS were treated with NaHS (A) simultaneously for one h or (B) were pre-incubated with NaHS for one h, following one h stimulation with IL-1 β . FLS from four different patients were used during this experiments. (A) *P < 0.05, **P < 0.01; (B) **P < 0.01

Overexpression of matrix degrading enzymes like MMPs is a hallmark of several joint diseases (Guerne et al, 1989) and since sulfurylated compounds like chondroitin sulfate were found to affect FLS by reducing the expression of MMPs (Imada et al, 2010), we investigated the ability of NaHS to interfere with tissue remodeling by down-regulating MMP expression. MMP-2 is a mediator of basement-membrane degradation and, besides several types of collagens, degrades precursors of TNF- α and IL-1 β (Amalinei et al, 2010). MMP-2 is activated by binding membrane-anchored MMP-14 – both expressed on synovial fibroblasts (Pap et al, 2000) – and form a membrane bound complex (Zhang et al, 2004) which displays matrix degrading potential (Konttinen et al, 1998; Pap et al, 2000).

Cells were pre-treated with NaHS for one h and subsequently activated with IL-1 β for an additional h. Afterwards, FLS were collected at the previously mentioned time points and cDNA was generated for the analysis by qRT-PCR.

NaHS treatment significantly reduced the expression of MMP-2 and MMP-14 for up to six h (Figure 14). However, after 12 h recovery this inhibitory effect was no longer significant, again suggesting a transient effect.

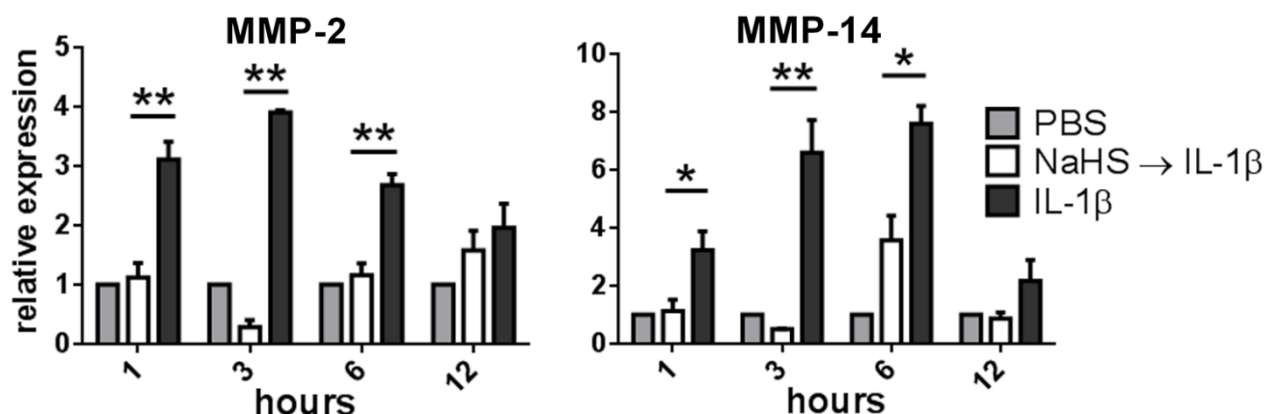


Figure 14 NaHS decreases MMP-2 and MMP-14 expression in activated FLS

FLS were treated with either PBS, IL-1 β or a combination of IL-1 β and NaHS for one h following which they were further incubated in fresh medium for one, three, six or 12 h. Data were normalized to GAPDH expression. FLS from four different patients were used during this experiments. *P < 0.05, **P < 0.01

In addition, the effects of NaHS treatment on the secretion of chemokines IL-8 and RANTES were analysed in cell culture supernatants from FLS treated with 1 mM NaHS or PBS for one h, following activation with IL-1 β for an additional h, and recovery in fresh medium for three h. IL-1 β stimulation induced the secretion of IL-8 and, although to a lesser extent, also of RANTES (Figure 15). Pre-treatment with NaHS significantly reduced the secretion of IL-8 by approximately 20% and almost completely abrogated the IL-1 β induced production of RANTES (Figure 15), providing additional evidence for the anti-inflammatory potency of NaHS treatment on activated FLS.

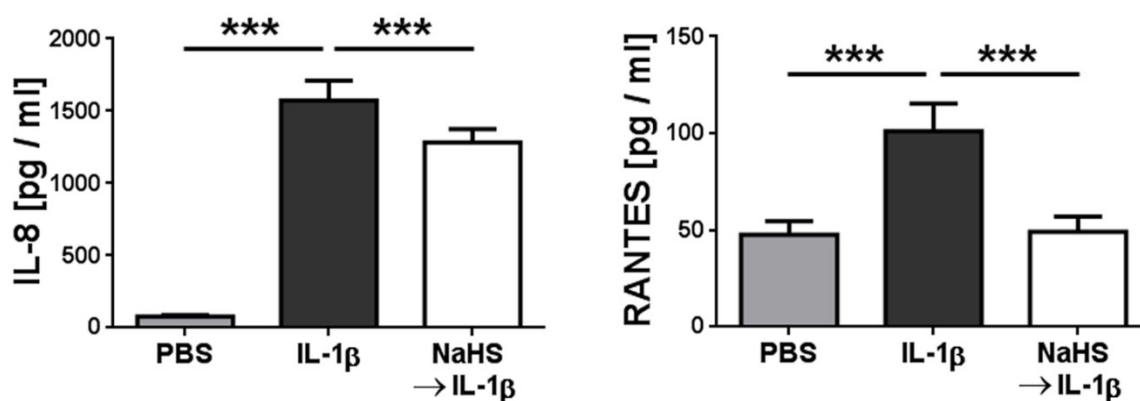


Figure 15 NaHS treatment reduces IL-8 and RANTES secretion in activated FLS

IL-8 and RANTES secretion were measured from cells pre-treated with NaHS or PBS for one h, stimulated with IL-1 β for an additional h and recovered in fresh medium for 3 h. FLS from three different patients were tested two times in triplicates. ***P < 0.001

3.6 NaHS reduces IL-1 β -induced MAPkinase activation

Members of the mitogen-activated protein (MAP) kinase family are key players in inflammatory responses. Since expression of pro-inflammatory factors like IL-6 and several cartilage degrading MMPs partially depends on the activation of the MAPkinase pathway (Georganas et al, 2000), it was of major interest to investigate the effects of NaHS on IL-1 β -induced activation of MAPkinases and other serine/threonine kinases. Human phospho-MAPkinase proteome profiler array was loaded with lysates from cells treated with IL-1 β , NaHS + IL-1 β or PBS for 30 min and resulting pixel densities of spot blots (Figure 16) were quantified and statistically evaluated.

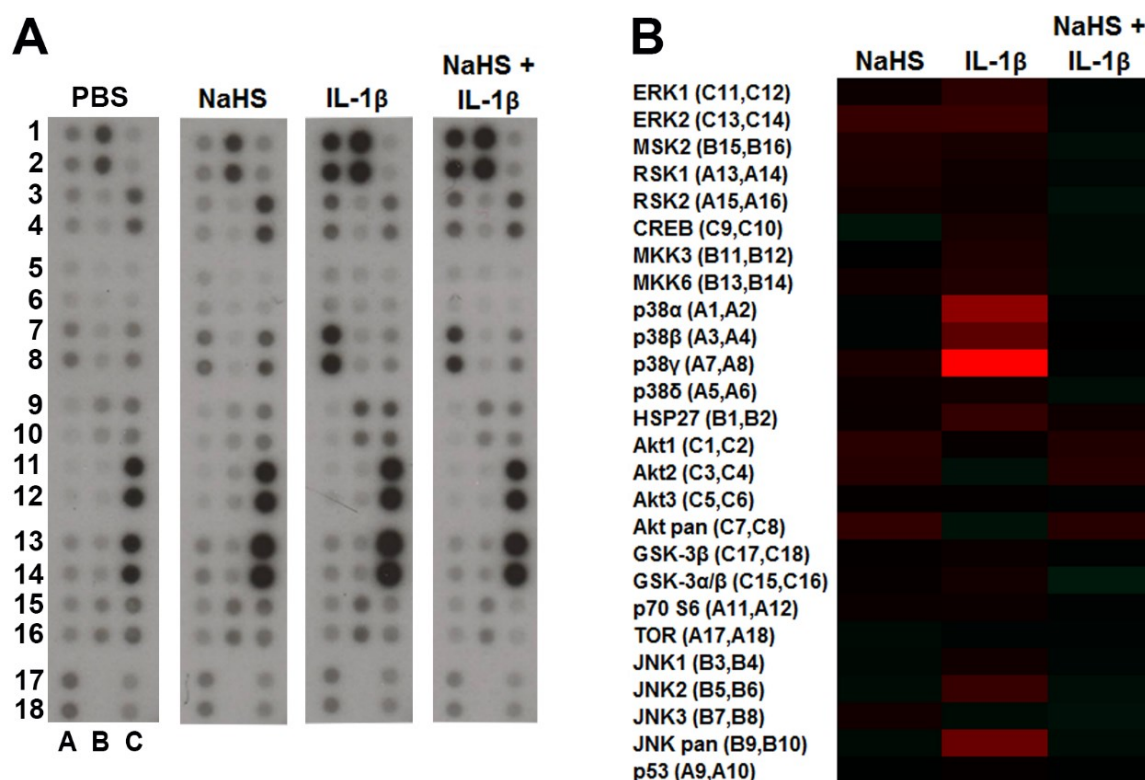


Figure 16 IL-1 β -induced phosphorylation of several MAPkinases can be ameliorated by NaHS treatment

Phosphorylation of 26 different MAPkinases or other serine/threonine kinases were analysed by spot plot assay. (A) FLS were treated with PBS, NaHS, IL-1 β or NaHS + IL-1 β . Subsequently, cell lysates were prepared and incubated with spot blot membranes. Pre-plotted spots were visualised by chemiluminescence. (B) The intensity of spots was quantified and converted to a heat-map of either NaHS- or IL-1 β -treated samples normalized to PBS or NaHS + IL-1 β treated FLS normalized to IL-1 β -stimulated samples, respectively. Plots are representative for FLS from three different patients.

Interestingly, NaHS treatment of unstimulated FLS resulted in the significant activation of members of the ERK pathway (ERK2, MSK2 and RSK1/2) as well as the Akt family whereas phosphorylation of JNK1/2 was found to be slightly downregulated by NaHS treatment, but these changes were statistically not significant (Figure 17).

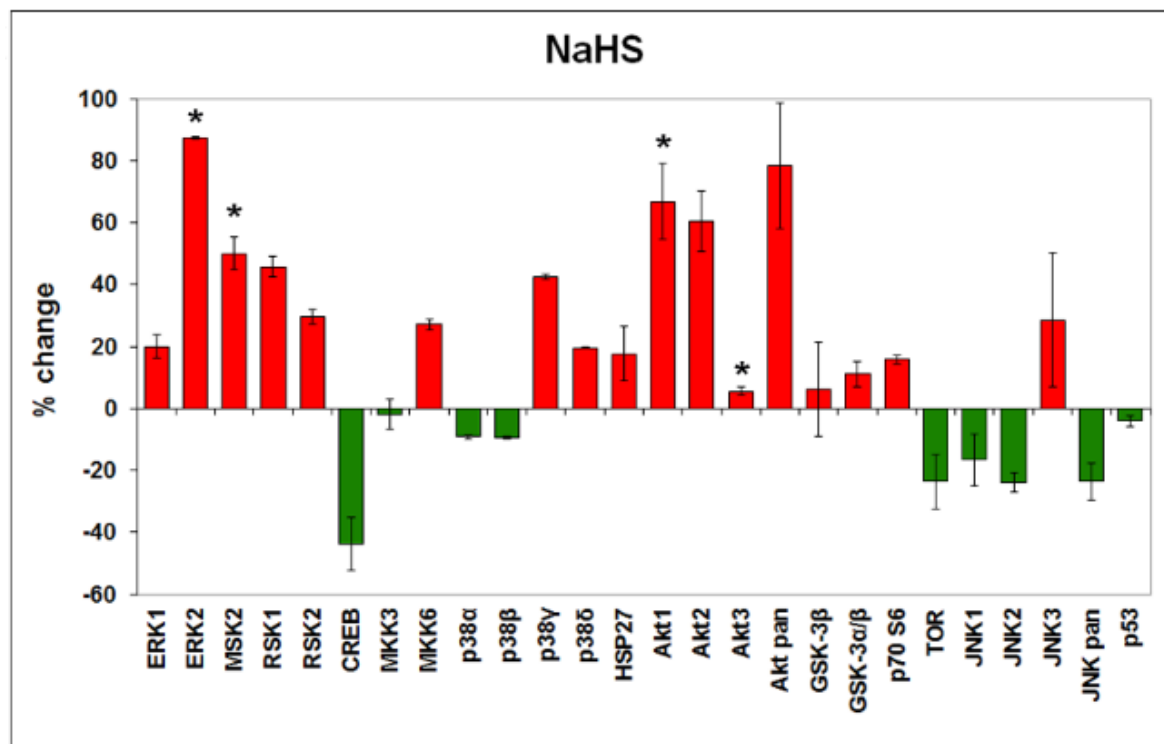


Figure 17 NaHS affects MAPKinases signaling

Phosphorylation of 26 different MAPKinases and other serine/threonine kinases was analysed by spot blot assay. FLS from three different patients were incubated with either PBS or NaHS for 30 min. Changes in pixel density were quantified using the imaging system GeneGnome, statistically evaluated and plotted into graphs (% change) in which NaHS-treated FLS were normalized to PBS-treated cells. Changes of phosphorylation in unstimulated, NaHS-treated FLS showed significant activation (red bars) of several kinases like ERK2, MSK2 or the Akt family. NaHS treatment also resulted in decreased phosphorylation (green bars) of CREB and JNK1/2, but this did not reach the level of statistical significance. *P < 0.05

As expected, in IL-1 β stimulated FLS increased phosphorylation (between 30 and 417%) of several MAPKinases was seen (Figure 18) including extracellular signal-regulated kinase (ERK)1/2, mitogen- and stress activated protein kinase (MSK)2, ribosomal protein S6 kinase (RSK)1, mitogen-activated protein kinase kinase (MKK)3/6, glycogen synthase kinase (GSK)3 α/β , heat shock protein (HSP)27, p38 subunits α , β and γ as well as c-Jun-N-terminal kinase (JNK) 1/2

In contrast, activation of protein kinase B, which is partially encoded by Akt2, appeared to be slightly downregulated by IL-1 β , although this change was statistically not significant (Figure 18). Akt is part of the PI3K/Akt pathway regulating a variety of cellular functions for example survival (Garcia et al, 2010; Miyashita et al, 2003; Zhang et al, 2001).

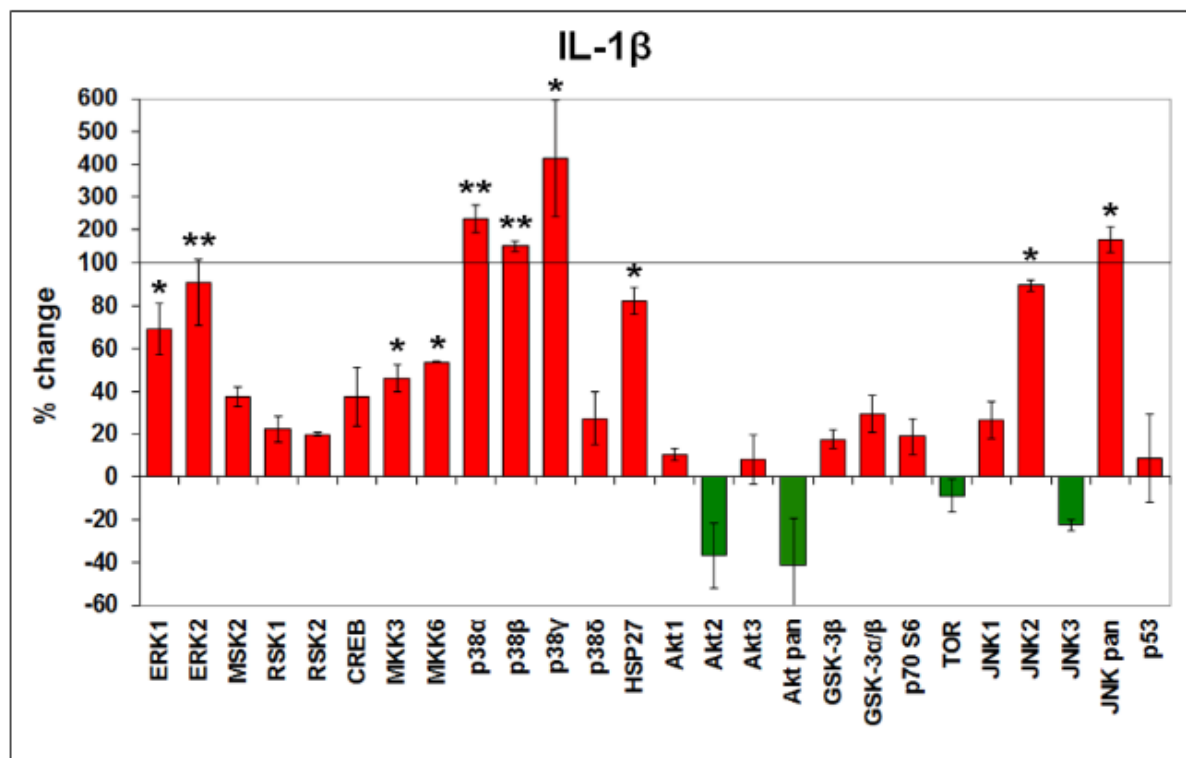


Figure 18 IL-1 β induces phosphorylation of several MAPKs but decreases levels of p-Akt2. Changes in pixel density were quantified, statistically evaluated and plotted into graphs (% change). The phosphorylation of kinases in IL-1 β -stimulated FLS was normalized to the levels of PBS treated controls. Data are representative for FLS from three different patients. *P < 0.05, **P < 0.01

Remarkably, NaHS treatment selectively reduced the IL-1 β -induced activation of some kinases (Figure 19A), particularly MSK2, MKK6 and GSK3 α/β (Figure 19B). As already observed in unstimulated cells, Akt2 phosphorylation was significantly increased by NaHS treatment (Figure 19B). Hence, in contrast to unstimulated cells, in IL-1 β -stimulated FLS the effects of hydrogen sulfide on the activation of several MAPKs were mainly inhibitory whereas the PI3K/Akt pathway seemed to be activated by NaHS both in unstimulated and in stimulated cells.

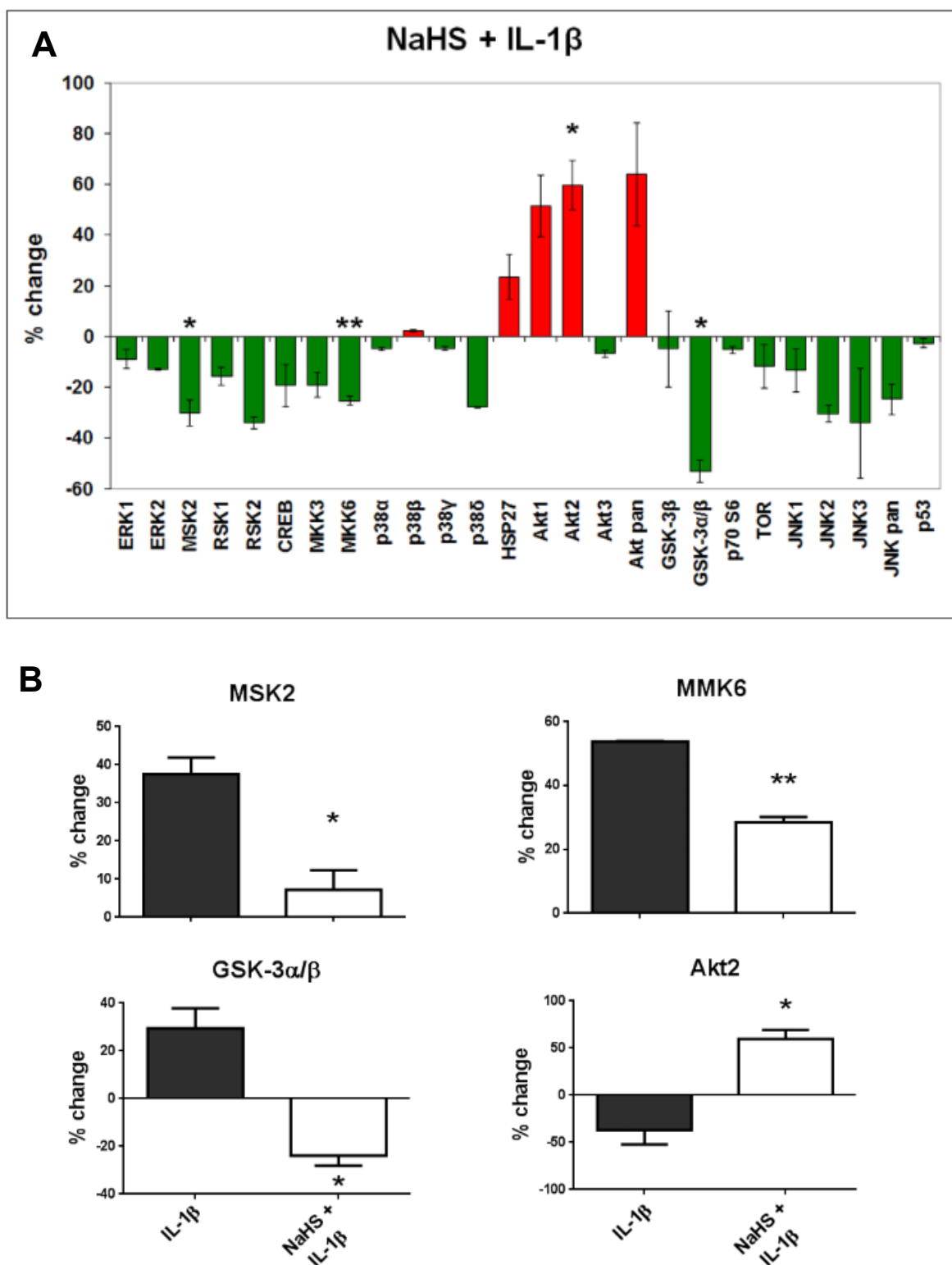


Figure 19 NaHS treatment inhibits phosphorylation of MAPkinases induced by IL-1 β stimulation in FLS

(A) Activated FLS treated with NaHS showed decreased amounts of p-MAPkinases, accompanied by increased levels of p-Akt. Data were normalized to IL-1 β stimulated FLS. (B) Significant differences in the phosphorylation of MSK2, MKK6, Akt2 and GSK-3 α/β between activated FLS and NaHS treated, activated FLS, both normalized to PBS treated controls. Data are representative for FLS from three different patients. *P < 0.05, **P < 0.01

To verify the data obtained by proteome profiler assay, Western-blotting was performed with cell lysates from FLS treated with IL-1 β , NaHS + IL-1 β or PBS for 30 min. FLS from three different patients were used to create three blots for each antibody and the protein amount was quantified by Image J software (data not shown). NaHS treatment on the one hand significantly reduced the IL-1 β -induced activation of MKK3/6 and GSK-3 β but on the other hand increased the activation of pro-survival factor Akt (Figure 20). Hence, the effects seen with proteome profiler array could be verified by Western-blotting.

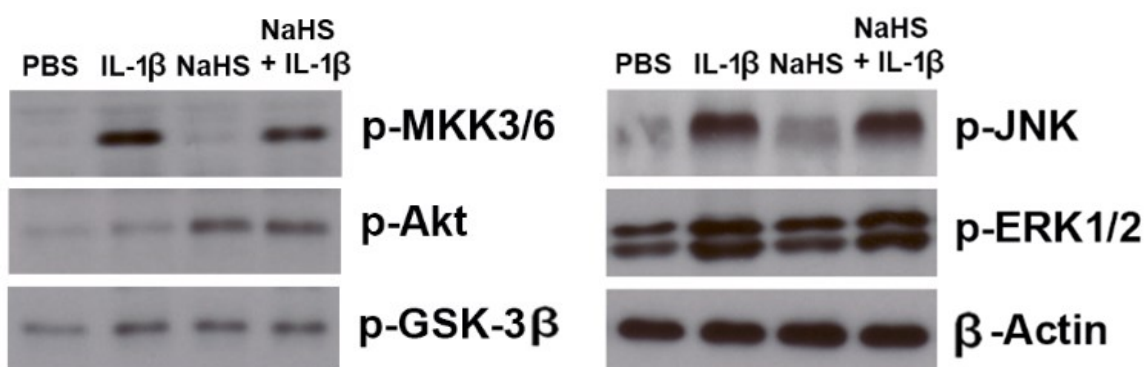


Figure 20 NaHS treatment reduced the IL-1 β -induced activation of MKK3/6 and GSK-3 β and increased the activation of Akt

FLS derived from three OA patients were treated with IL-1 β , NaHS + IL-1 β or PBS for 30 min and cell lysates were loaded on Western blots with antibodies specific to p-MKK3/6, p-Akt, p-GSK-3 β , p-JNK and p-ERK1/2. β -Actin was used as a loading control.

3.7 NaHS treatment abolishes the IL-1 β -induced architectural changes of FLS grown in 3-D extracellular matrix micromasses

FLS together with macrophages and extracellular matrix form the synovial lining layer which separates the synovial fluid compartment from the synovial sublining region. To mimic this architecture *in vitro*, FLS were grown in so-called micromasses consisting of a pre-formulated Matrigel matrix. Therefore, cells were mixed with the matrix and dropped to the middle of a coated culture well. The round shaped structure developed after 17-21 days in medium supplied with the desired stimuli. As demonstrated in previous investigations, RA-FLS spontaneously form a lining layer-like structure in this micromass cell-culture system showing great similarities with the hyperplastic lining layer in the joints of RA patients (Kiener et al, 2010). Hence, the 3-D micromass culture represents an attractive *in vitro* model allowing to explore the effects of stimulatory and inhibitory agents.

To investigate the effects of NaHS on the cellular architecture within the synovium, micromass cultures were treated with either PBS, IL-1 β or IL1 β + NaHS on day three, seven, 10, 13 and 15. On day 17 cultures were fixed, sectioned and stained with hematoxylin and eosin (H&E).

This study is the first to describe that also OA-FLS spontaneously form a multi-cellular lining layer on the surface of micromass cultures (Figure 21A). Stimulation with IL-1 β -induced hyperplasia of this lining (Figure 21B) and this effect could be completely inhibited by NaHS treatment (Figure 21C). Quantification of lining layer thickness (Figure 21D) showed a significant difference between NaHS treated and non-treated IL-1 β -activated FLS. Hence, treatment with NaHS antagonized the effects of IL-1 β on the architecture of micromass cultures.

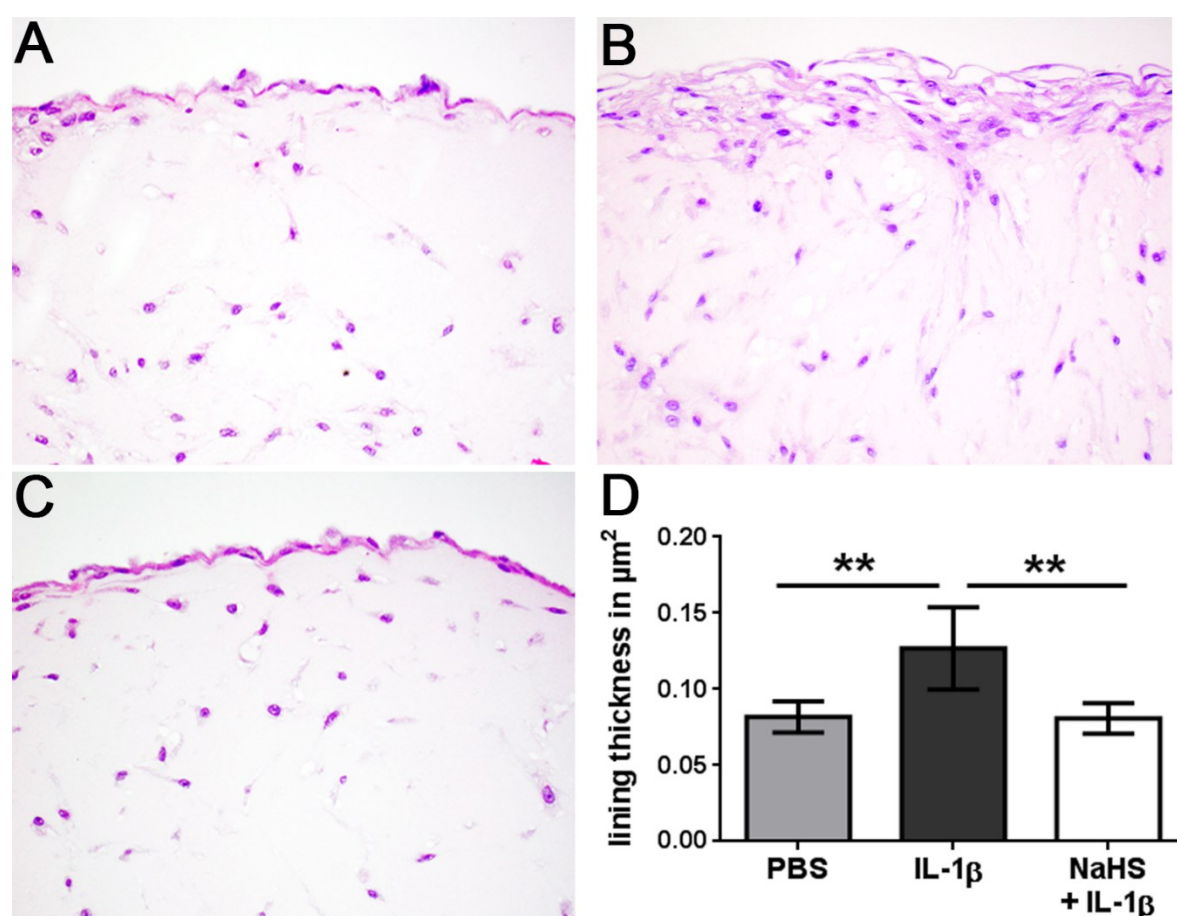


Figure 21 FLS grown in 3-D micromass culture develop lining hyperplasia when activated which could be inhibited by NaHS treatment

FLS from 3 patients were used to create a total 27 micromass cultures – 9 cultures per patient - which were then treated with either PBS (n=9), IL-1 β (n=9) or IL1 β + NaHS (n=9) on day three, seven, 10, 13 and 15. After 17 days, 3-D cultures were fixed, sectioned and stained with hematoxylin and eosin. Representative cultures of one patient treated with (A) PBS, (B) IL-1 β or (C) NaHS + IL-1 β are shown. Original magnification x 1000. (D) Quantification of lining layer thickness in 27 micromasses using Osteomeasure software. **P < 0.01

3.7.1 Phosphorylation of Akt is induced by NaHS treatment in FLS grown in 3-D micromass cultures

Since in previous experiments phosphorylation of Akt had been observed to be induced by NaHS treatment (3.6) it was of interest if Akt activation is induced by NaHS treatment also when FLS are cultured in micromasses. Therefore the micromasses described above were immunohistochemically stained for p-Akt. In PBS treated micromasses the basal phosphorylation of Akt was found to be very low, whereas in NaHS treated cultures an increase of p-Akt staining was detected predominantly in the lining layer (Figure 22). Stimulation with IL-1 β induced only little Akt phosphorylation in the lining layer which was lower than in NaHS treated micromasses. Hence, NaHS treatment can induce the activation of Akt even in 3-D cultured FLS more closely resembling physiological conditions than conventional 2-D culture systems.

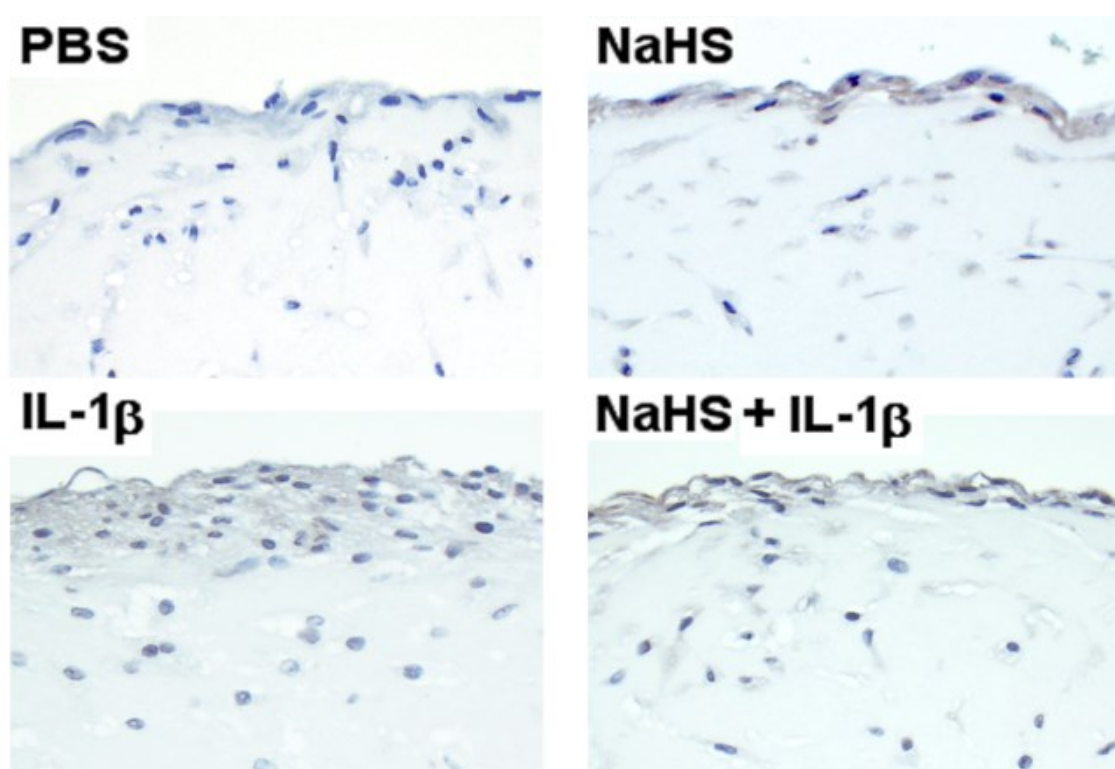


Figure 22 NaHS treatment induced Akt phosphorylation in micromass cultures

Micromass cultures were treated with either PBS (n=9), NaHS (n=9), IL-1 β (n=9) or IL-1 β + NaHS (n=9) on day three, seven, 10, 13 and 15 were fixed, sectioned and stained after 17 days of culturing. The phosphorylation of Akt (brown) was visualized by immunohistochemistry. The nuclei (purple) were stained with hemalaun. Representative pictures were taken with Axioskop MOT2 Microscope with CellF software. Original magnification x 1000.

3.7.2 *IL-1 β -induced stimulation of MMP-2 production is inhibited by NaHS treatment*

Additionally, micromasses were stained for the matrix degrading enzyme MMP-2 which showed a pronounced expression after IL-1 β stimulation (Figure 23). NaHS treatment alone did not seem to alter MMP-2 expression compared to PBS treated micromasses (Figure 23). However, it reduced not only the hyperplasia of the lining layer but also almost completely inhibited the IL-1 β -induced expression of MMP-2.

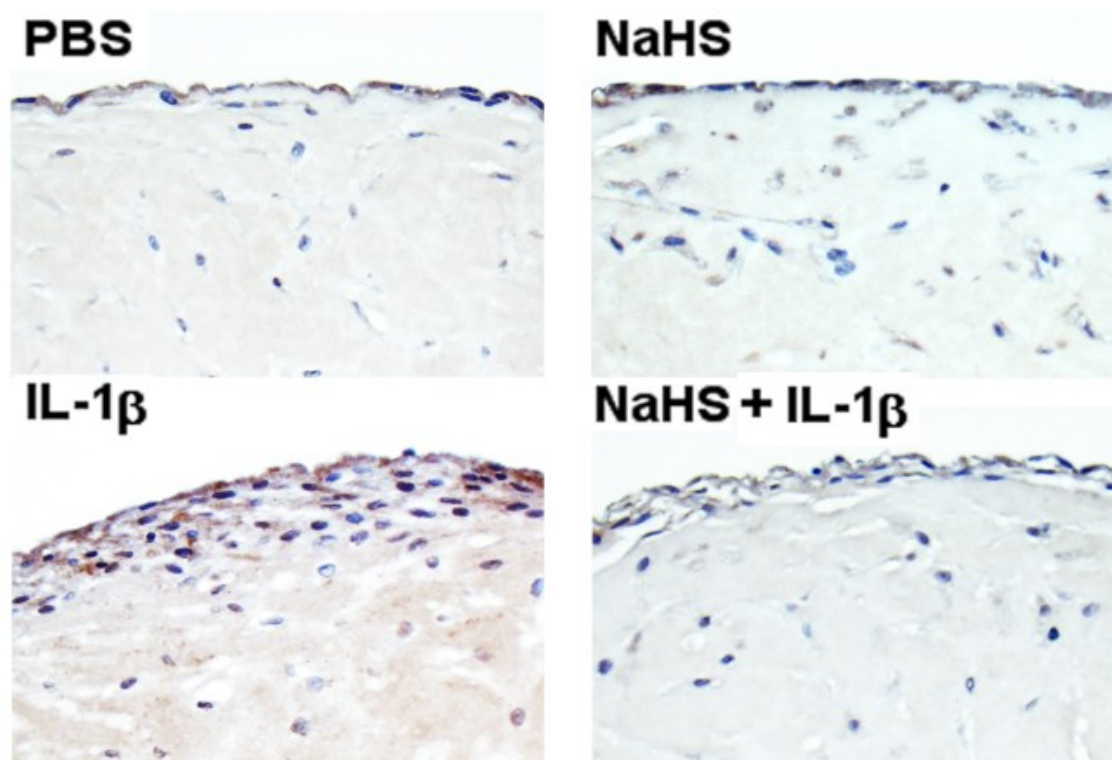


Figure 23 NaHS treatment reduced IL-1 β -induced MMP-2 production in FLS micromasses
Micromass cultures were treated with either PBS (n=9), NaHS (n=9), IL-1 β (n=9) or IL-1 β + NaHS (n=9) on day three, seven, 10, 13 and 15 and subsequently fixed and sectioned after 17 days of culturing. Micromasses were immunohistochemically stained for MMP-2. The nuclei were stained with hemalaun. Original magnification x 1000.

3.8 NaHS affects serum cytokine levels in healthy mice challenged with LPS

To study the effects of sulfur treatment *in vivo* a treatment protocol for animal trials was designed. First, dose escalation experiments were performed to determine the amount of NaHS that could be applied to mice without toxic effects (data not shown). In a pilot experiment four mice were injected three times i.p. with 0.4 mM NaHS diluted in 100 μ l PBS on day zero, two and five. Six mice were injected solely with 100 μ l PBS. On day six all mice received 100 μ g LPS and were sacrificed two h later. Serum cytokine levels were quantified by ELISA.

NaHS treatment seemed to reduce serum levels of TNF- α , IL-4 and IL-23, although only the reduction of IL-23 reached the level of statistical significance (Figure 24). Hence, these data indicated that NaHS might influence disease severity and/or outcome in a model of inflammatory arthritis.

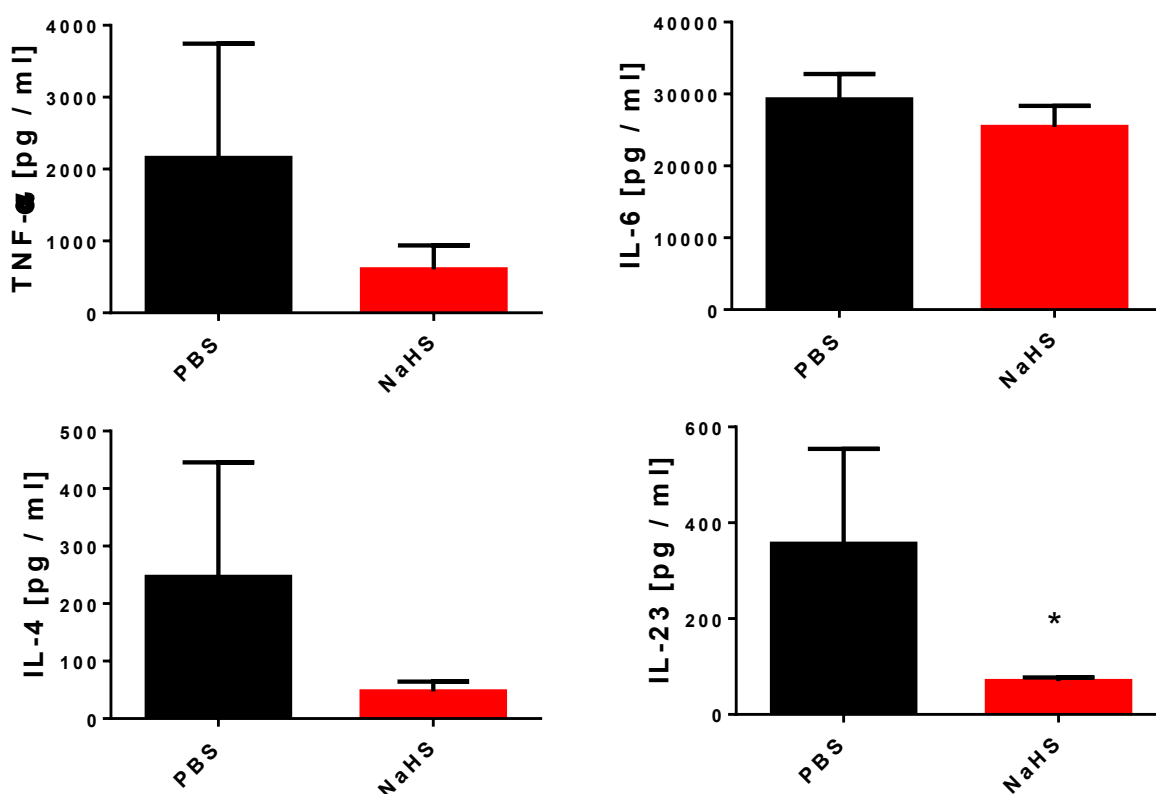


Figure 24 NaHS treatment reduced serum cytokine levels in LPS-triggered mice

Mice were treated either with PBS (n=6) or 0.4 mM NaHS in 100 μ l PBS (n=4) on day zero, two or five. On day six, mice were injected with 100 μ g LPS and sacrificed after two h. Serum cytokine levels of TNF- α , IL-6, IL-4 and IL-23 were quantified by ELISA. IL-23 was significantly decreased in NaHS-treated mice. *P < 0.05

3.9 NaHS treatment of mice with collagen-induced arthritis

The overall anti-inflammatory effects of NaHS treatment seen on FLS *in vitro* and from preliminary *in vivo* experiments further encouraged us to investigate the consequences of hydrogen sulfide treatment in an *in vivo* model of arthritis. Collagen-induced arthritis is a murine model for RA particularly useful to investigate treatment specific effects on the activation of adaptive immunity (Firestein, 2009). Hallmarks of CIA are the infiltration of synovium, pannus formation and increased production of pro-inflammatory cytokines and matrix degrading enzymes. For the induction of arthritis, 200 μg bovine type II collagen in 100 μl of complete Freund's adjuvant were injected intradermally (i.d.) at the base of the tail; 21 days later animals received a boost immunization. Disease onset occurred approximately one week after the boost. Male DBA/1 mice were treated eight times with 100 μl of a 0.4 mM NaHS solution in a prophylactic treatment protocol starting 3 days prior to the first immunization. As a control, mice with CIA were treated with PBS eight times or were left untreated. The treatment regimen is illustrated in Figure 25.

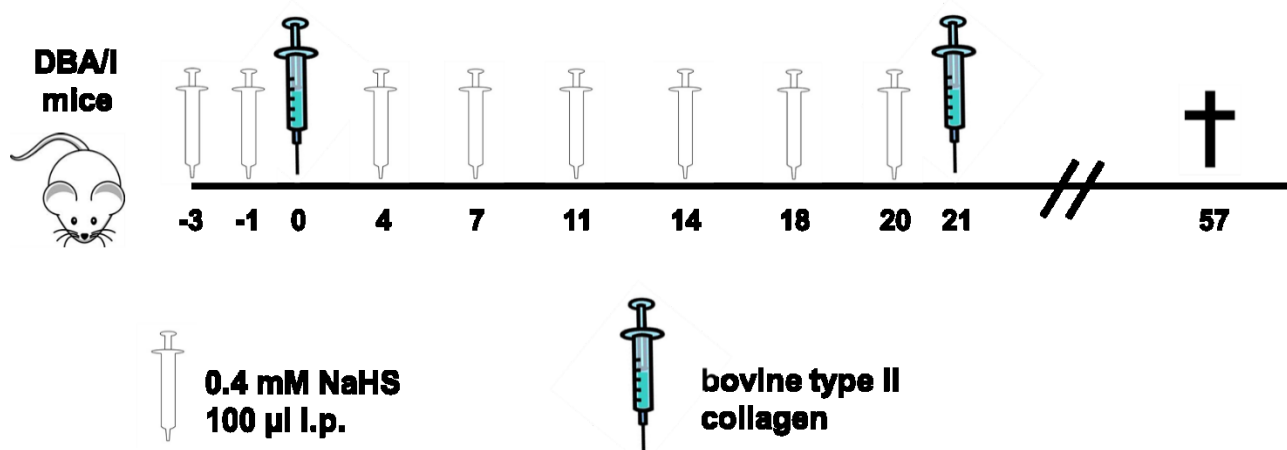


Figure 25 Schematic illustration of the treatment schedule for collagen-induced arthritis

For induction of disease, DBA/1 mice were injected with bovine collagen II in 100 μl of complete Freund's adjuvant. NaHS treatment was applied eight times (two times a week) starting one week before disease induction until the boost on day 21. Arthritis onset was approximately one week after the boost. Clinical evaluation of weight, grip strength and swelling was assessed at day 0 or 21, respectively. Mice were sacrificed on day 57 and blood, organs and paws were collected for further investigation.

3.9.1 Hydrogen sulfide treatment does not affect levels of anti-collagen IgG antibodies

When injected with bovine collagen type II, mice develop high titer anti-collagen antibodies. For the investigation of possible inhibitory effects of NaHS treatment on the generation of anti-collagen antibodies, blood was taken on day 29 after induction and serum levels of IgG were analysed by ELISA.

We found that anti-collagen IgG levels from NaHS treated mice did not differ from PBS treated or untreated controls (Figure 26). In contrast, control mice that did not receive collagen had no IgG antibodies against it. Hence, the disease induction was effective in CIA mice but NaHS treatment did not influence serum levels of anti-collagen antibodies.

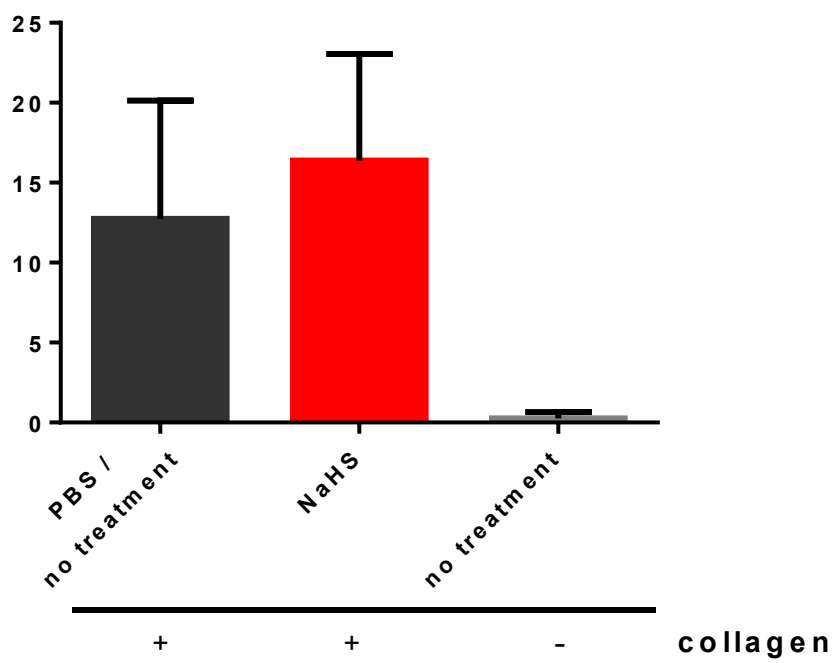


Figure 26 IgG antibody levels expressed as arbitrary units in the serum of DBA/1 mice. Serum was collected on day 29 and IgG anti-collagen antibodies were measured by ELISA. Mice with CIA were either treated with NaHS (n=6) or PBS or were left untreated (n=5); healthy animals (n=4) served as negative controls.

3.9.2 Hydrogen sulfide does not influence clinical outcome but seems to increase incidence of arthritis

Clinical evaluation of animals was performed during the experiment. Paw swelling and grip strength were assessed according to afore mentioned criteria as outlined in the methods section (see 4.8.3) and are summarized in Figure 27A&B. In addition, weight was assessed once a week and percentage change was calculated and plotted in a graph (Figure 27C). NaHS treatment had no significant impact on clinical parameters but showed a negative trend by increasing paw swelling (Figure 27A) and reducing grip strength (Figure 27B) of CIA mice.

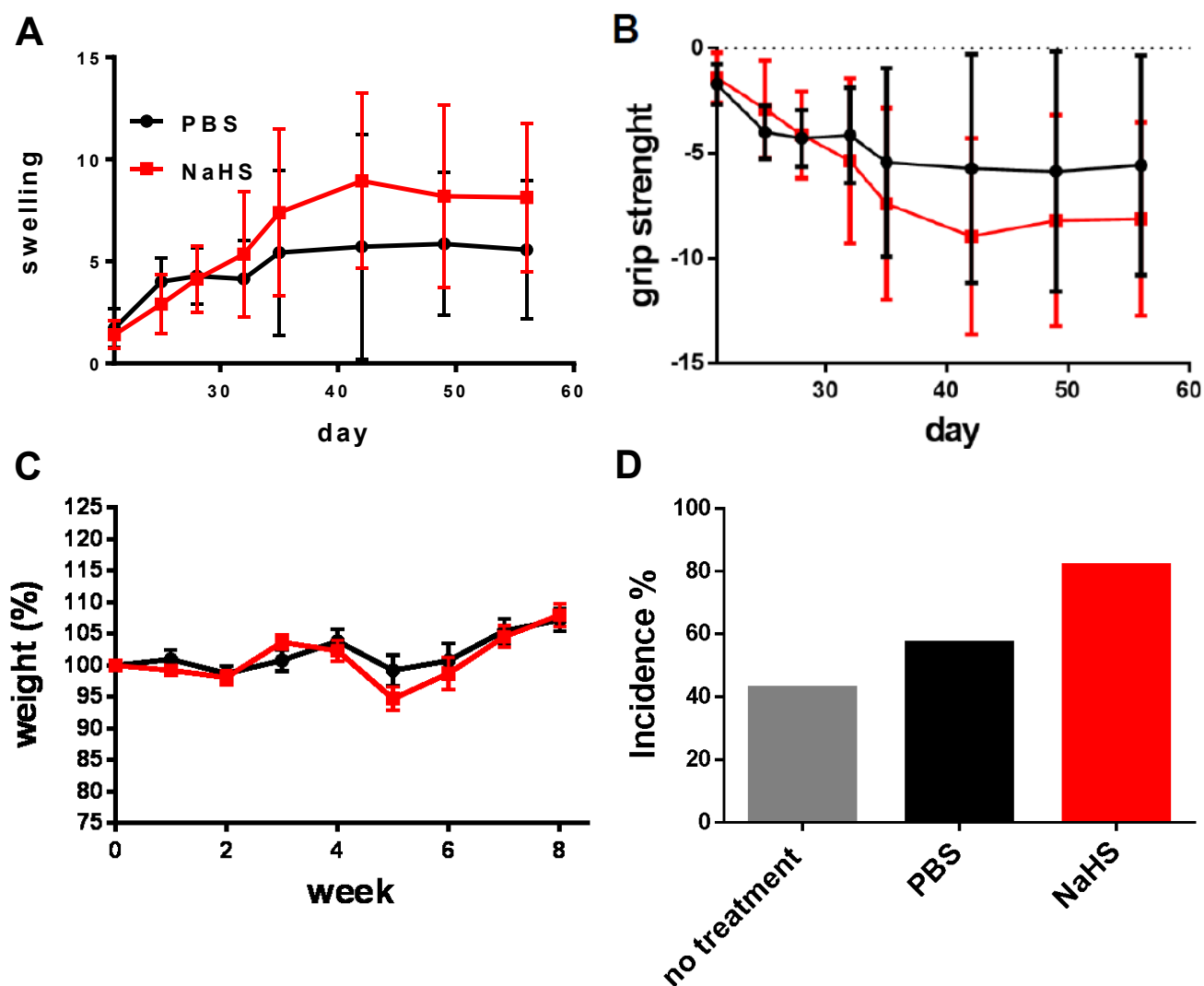


Figure 27 NaHS treatment did not influence outcome of CIA but increased disease incidence

Mice developing arthritis were scored for (A) paw swelling and (B) grip strength from day 21 until the end of the experiment. (C) Weight was assessed every week starting on day 0 and percentage of weight loss or gain was calculated. (D) Incidence was calculated and illustrated in a graph. Three to four out of seven animals in untreated or PBS treated mice developed the disease, respectively. Incidence in NaHS treated animals was higher with nine out of 11 mice developing arthritis.

NaHS treatment increased the incidence of disease (Figure 27D) to 81% compared to PBS (57%) or untreated controls (42%). For further histological and immunological analyses PBS-treated and untreated controls were merged to increase group size.

3.9.3 NaHS treatment significantly increases number of osteoclasts but does not influence other histological parameters

During arthritis, a variety of histological changes can be observed within paws of CIA mice. Characteristic features of CIA comprise bone erosion, infiltration of immune cells, increase in number of osteoclasts as well as cartilage degeneration.

To investigate possible effects of hydrogen sulfide on disease induced joint destruction, we performed histological evaluations of both hind paws.

NaHS treatment significantly increased numbers of osteoclasts (Figure 28A) compared to controls. However, no effects were seen on erosion (Figure 28B), inflammation (Figure 28C) or cartilage loss (Figure 28D).

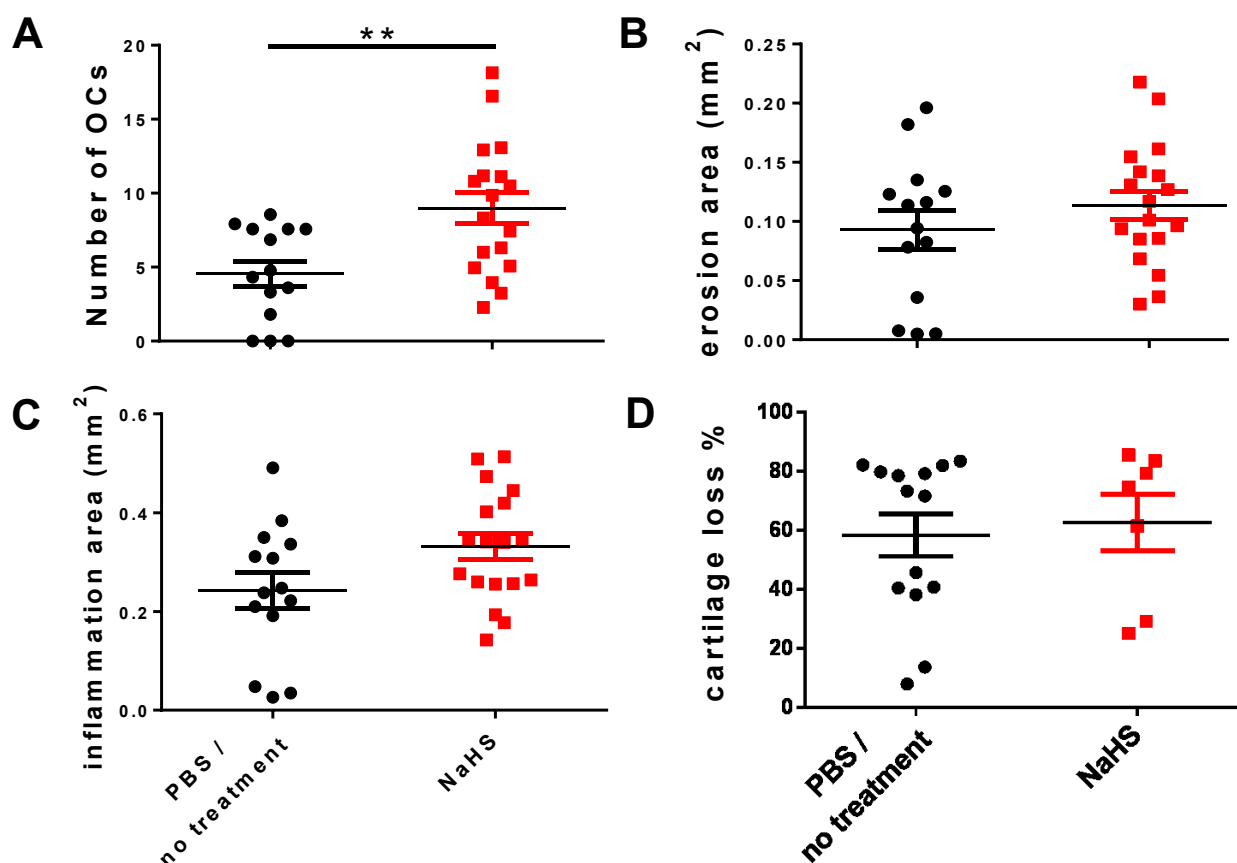


Figure 28 Histological evaluation of hind paws of CIA mice

(A) Osteoclasts have more than two nuclei and are TRAP positive cells. The number of osteoclasts was divided by tissue area. Erosion area (B) was calculated by division of erosion area by tissue area. The area of inflammation (C) was generated by the division of the area of inflammation by tissue area. Toluidine blue staining was used to evaluate cartilage degeneration (D). The area of total cartilage divided by the area of destained cartilage gave rise to the percent of cartilage loss. (A) **P < 0.01

3.9.4 NaHS treatment does not affect immune cell composition in lymph nodes of mice with collagen-induced arthritis

Furthermore, effects of NaHS treatment on immune cell distribution in lymphoid organs were investigated. Therefore, lymph nodes were collected and isolated immune cells were stained for several surface markers listed in the methods section (see 4.8.5) following which they were analysed by flow cytometry. NaHS treatment did not significantly influence numbers of CD4+ (Figure 29A) or CD8+ (Figure 29B) T-cells, B220+ B-cells (Figure 29C) and CD11b+ myeloid lineage cells (Figure 29D).

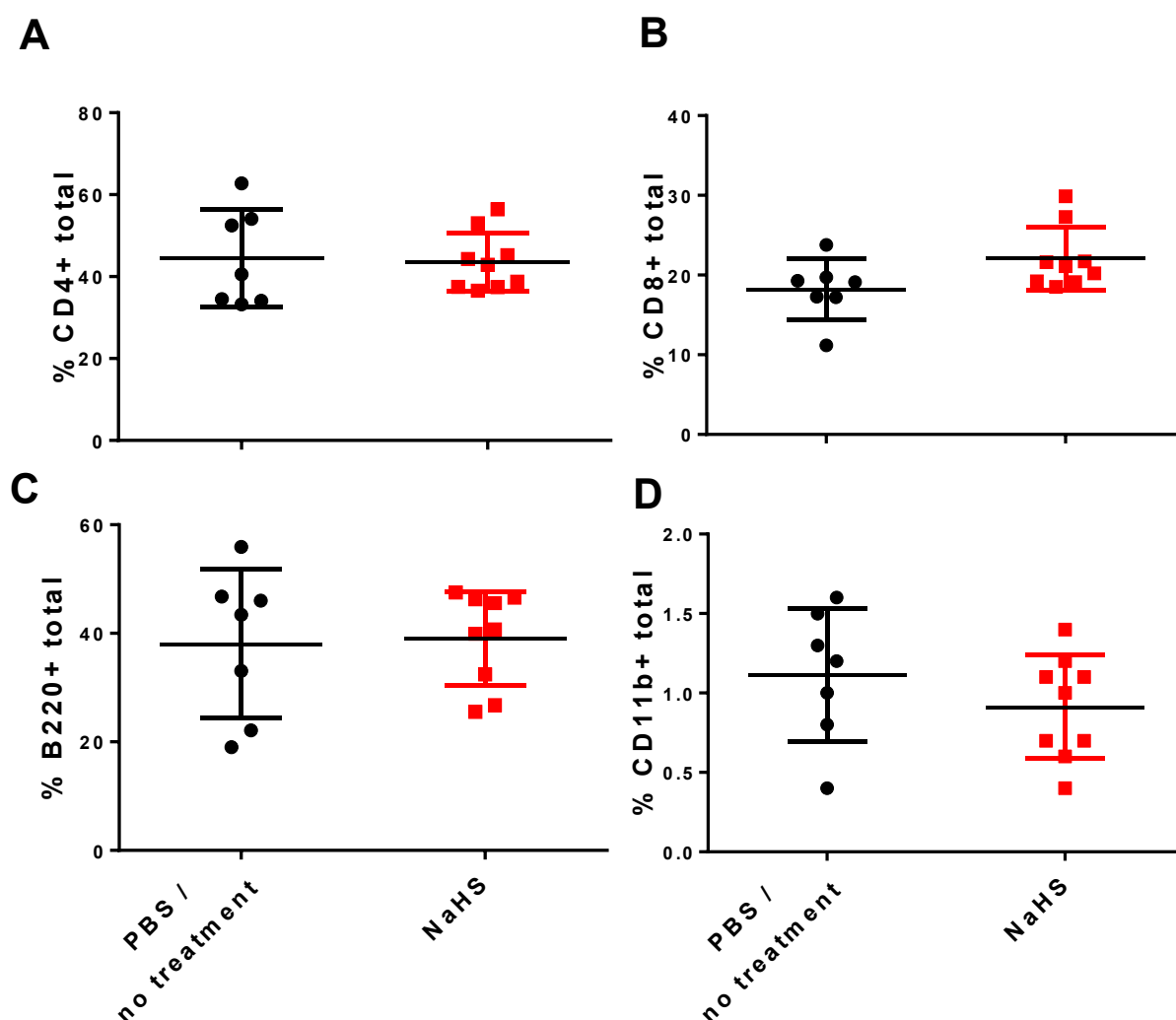


Figure 29 Flow cytometry analysis of immune cell composition in lymph nodes of NaHS treated mice and control mice

Extracted lymphoid cells were stained for (A) CD4, (B) CD8, (C) B220 or (D) CD11b and examined by flow cytometry. There was no significant difference between NaHS treated mice (n=9) and control animals (n=7).

3.10 NaHS treatment of mice with K/BxN serum transfer arthritis

Since we found little to no effect of hydrogen sulfide treatment on an *in vivo* model of adaptive immunity like CIA, our next goal was to investigate possible effects of NaHS on the effector phase of inflammatory arthritis. Therefore, we decided to employ the K/BxN serum transfer arthritis model (Monach et al, 2008). Acute arthritis was induced by injecting twice i.p. 150 μ l of serum from K/BxN mice into C57BL/6 mice. Thereby, autoantibodies directed against glucose-6-phosphate isomerase (GPI) lead to the development of disease with usually 100% incidence (Monach et al, 2008).

According to the semi-therapeutic protocol, NaHS treatment was applied i.p. five times starting one day prior to the first serum injection. The experiment was stopped at day nine. The experimental setup is outlined in Figure 30.

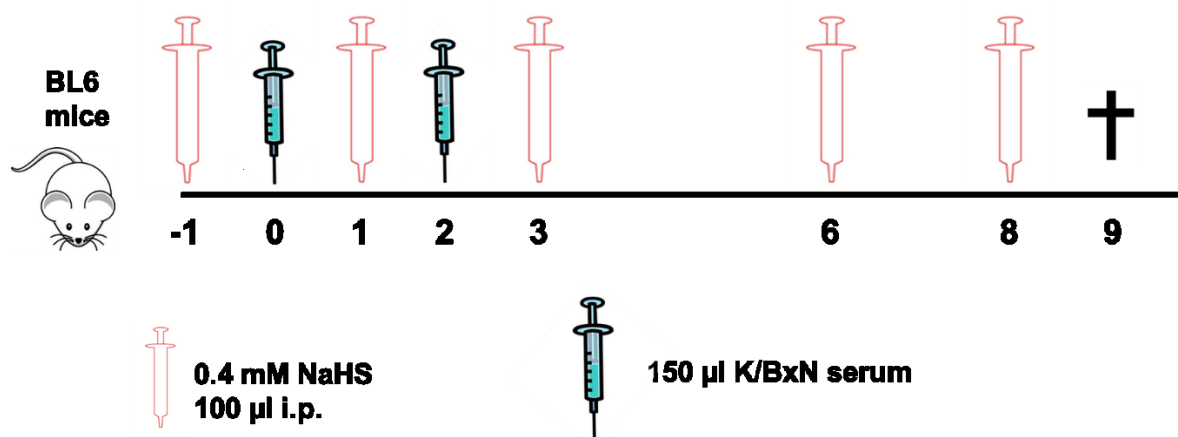


Figure 30 Schematic illustration of the treatment schedule for serum transfer arthritis

C57BL/6 mice were twice injected i.p. with 150 μ l serum of K/BxN mice on day 0 and day 2. NaHS treatment (0.4 mM in 100 μ l PBS) was applied on days -one, one, three, six and eight. Control mice received 100 μ l PBS. An acute arthritis developed after the serum boost. Clinical scores were evaluated during the experiment on days three, six, seven and eight. The experiment was terminated on day nine and blood, spleen and paws were collected for further investigations.

3.10.1 NaHS treatment does not influence disease severity or clinical outcome

During the experiment the clinical status of each animal was evaluated by analysing paw swelling and grip strength according to previously mentioned criteria (see 4.8.3) on day three, six, seven and eight.

The incidence of disease was 100% in both groups (data not shown) and we did not find significant differences between NaHS and PBS treated animals (Figure 31).

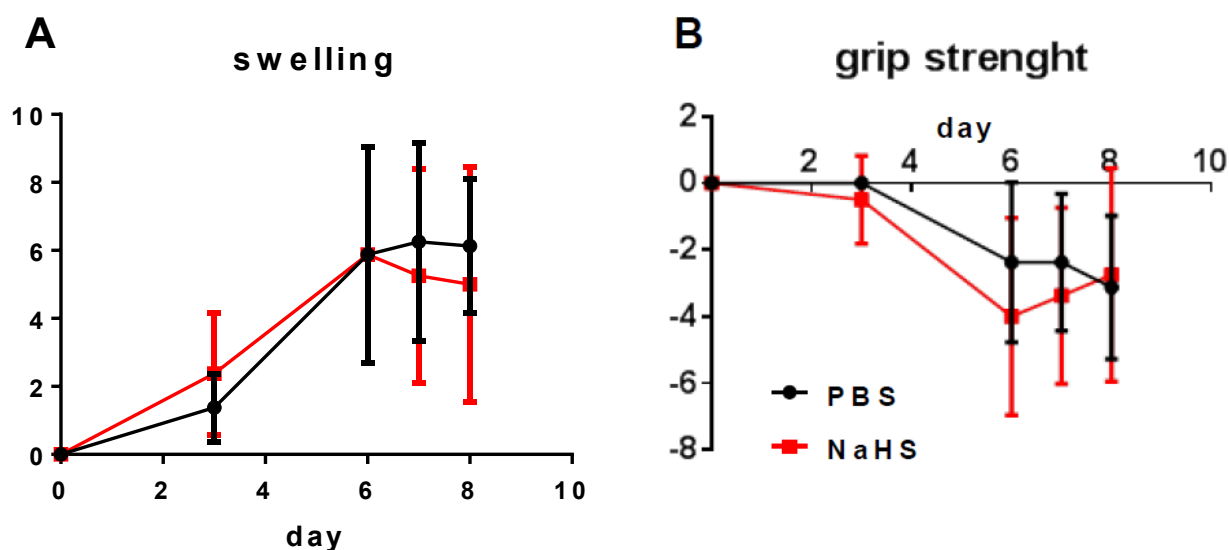


Figure 31 NaHS treatment has no significant effect on disease severity or outcome

Each paw was scored for (A) swelling and (b) grip strength on day three, six, seven and eight. Afterwards the sores of all four paws were added and plotted against time. The graphs comprise data from eight mice per group. NaHS treated mice (red graphs) were compared to PBS treated animals (black graphs).

3.10.2 NaHS treatment substantially reduces bone erosion and cartilage loss but has less impact on joint inflammation

Arthritis leads to pathological changes in murine joints which are detectable shortly after disease onset. To investigate possible effects of hydrogen sulfide on disease induced joint destruction, we evaluated histology of right hind paws of mice with serum transfer arthritis. Paws were paraffin embedded, sectioned and stained with H&E, toluidine blue and for the expression of TRAP. Parameters used for evaluation included osteoclast counts, area of bone erosion, area of inflammation as well as cartilage loss. The area of evaluation is marked in Figure 34 (see 5.8.5).

NaHS treatment led to a reduction of bone erosion and number of osteoclasts (Figure 32A&B) but had only little effect on inflammation (Figure 32C). Cartilage degradation was also found to be positively manipulated by sulfur treatment (Figure 32D). Hence, NaHS treatment primarily seemed to affect osteoclast-induced joint destruction and cartilage loss rather than inflammation.

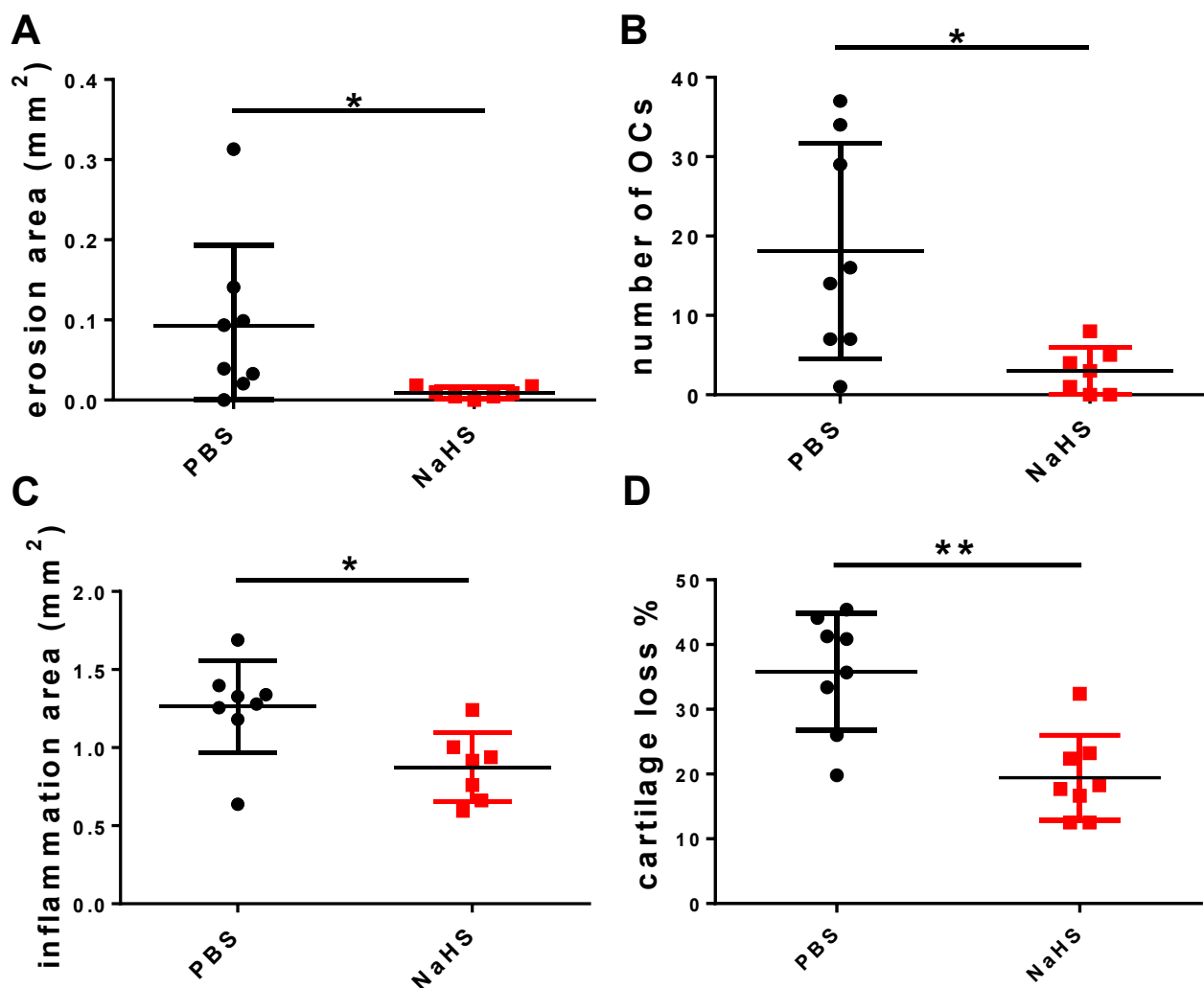


Figure 32 Hydrogen sulfide influences joint degradation in mice with serum transfer arthritis

Effects of NaHS treatment on pathological alterations of right hind paws of mice with serum transfer arthritis were investigated by evaluation of (A) area of erosion, (B) number of OCs, (C) area of inflammation and (D) cartilage loss. (A) *P < 0.05; (B) *P < 0.05; (C) *P < 0.05; (D) **P < 0.01

3.10.3 NaHS treatment increases inflammatory monocytes in blood

In serum transfer arthritis effector cells such as neutrophils, monocytes or macrophages play an important role in the induction of disease. To investigate possible effects of NaHS on the distribution of these cells, blood and splenocytes were collected, stained with myeloid lineage markers, and analysed by flow cytometry.

Remarkably, NaHS treatment significantly increased the number of inflammatory monocytes (CD11b⁺ Ly6G^{int} Ly6C⁺ Cd115⁺) in blood of mice with serum transfer arthritis (Figure 33).

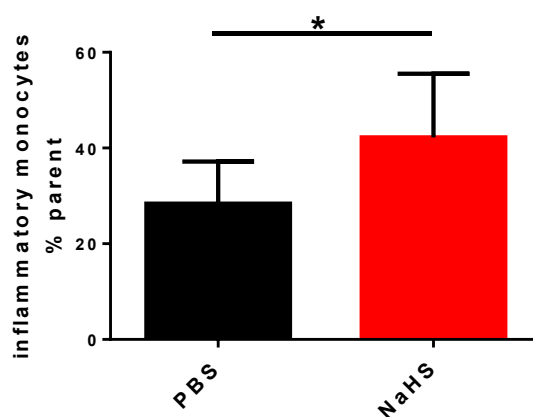


Figure 33 Numbers of inflammatory monocytes in blood of serum transfer arthritis mice were increased after NaHS treatment

Immune cells were isolated and stained for markers of the myeloid lineage and analysed by flow cytometry. Numbers of inflammatory blood monocytes (CD11b⁺ Ly6G^{int} Ly6C⁺ Cd115⁺) were determined in PBS-treated (n=6) and NaHS-treated (n=8) mice. *P < 0.05

4 Discussion

4.1 The role of hydrogen sulfide in inflammatory response

Rheumatic and musculoskeletal diseases (RMDs) are the major cause of disability world-wide. Hydrogen sulfide is a gasotransmitter which has emerged as an important signaling molecule in various physiologic and pathophysiologic conditions with a very complex role in inflammation (Lowicka and Beltowski 2007; Francon and Forestier 2009; Benedetti et al, 2010; Kovacs et al, 2012; Wallace et al, 2012). Hydrogen sulfide is frequently applied to patients suffering from RMDs like osteoarthritis in form of sulfur bath therapies, but definite clinical evidence is still scarce (Fioravanti et al, 2012). Therefore this study focused on elucidating molecular mechanisms of hydrogen sulfide treatment on synovial fibroblasts which are considered to play a pivotal role in joint inflammation. In previous experiments 20 min exposure of patient derived FLS to 1 mmol/l NaHS led to increased IL-6 secretion in unstimulated FLS (Kloesch et al, 2012a) whereas one h NaHS treatment decreased spontaneous and IL-1 β -induced IL-6 synthesis (Kloesch et al, 2010), suggesting a time dependent effect.

According to these findings we could demonstrate that one h treatment with 1 mmol/l NaHS significantly reduced the amount of spontaneously secreted IL-6, IL-8 and RANTES by FLS derived from OA patients. Furthermore, the inhibitory effect was found to be transient, being no longer detectable after 12 h which can be explained by the short half-life of NaHS in aqueous solution (Li & Lancaster, 2013). The results were supported by the additional observation that H₂S was not toxic at the concentrations applied which is in line with previous findings that concentrations higher than 100 μ mol/l H₂S were detected in synovial fluids of RA patients (Whiteman & Winyard, 2011).

OA was long time considered to be a wear and tear disease with no or very little inflammatory involvement. However, in recent years it has become evident that also OA patients may show increased levels of inflammatory mediators and cartilage degrading enzymes and particularly the pro-inflammatory cytokine IL-1 β seems to play a prominent role in the pathogenesis of OA. To more closely mimic the pathophysiological conditions to which FLS are exposed in an inflamed joint, IL-1 β is frequently applied *in vitro* to stimulate production of cytokines and cartilage destructive factors (Abramson & Amin, 2002; Nawata et al, 1989). The IL-1 β -induced secretion of the cytokine IL-6 as well as chemokines IL-8 and RANTES was strongly reduced by NaHS treatment. In addition, the expression of matrix degrading enzymes MMP-2 and -14 were markedly reduced by NaHS treatment. MMP-2 is activated by binding membrane-anchored MMP-14 and forms a membrane bound complex which displays matrix degrading potential (Konttinen et al, 1998; Pap et al, 2000). MMP-2, besides several types of collagens, degrades precursors of TNF- α and IL-1 β (Amalinei et al, 2010).

4.2 Hydrogen sulfide interferes with signaling pathways

These findings encouraged us to further investigate the potential effects of NaHS on known signal transduction pathways regulating MMPs (Choi et al, 2004; Herath et al, 2013; Hong et al, 2005; Lai et al, 2013; Lambert et al, 2001; Park et al, 2002) and cytokines (Georganas et al, 2000). MAPkinase signal transduction involves the activation of kinases at three levels: (a) MAPK kinase kinases (MAP3Ks), (b) MAPK kinases (MKKs) and (c) the MAPkinases ERK, p38 and JNKs. Once activated through phosphorylation by MKKs, MAPKs can migrate from the cytosol to the nucleus where they phosphorylate and activate important transcription factors. H₂S has been shown in previous investigations to interfere with MAPkinases (Kloesch et al, 2010; Kloesch et al, 2012a; Kloesch et al, 2012b). In FLS from RA patients, especially p38 MAPkinase isoforms α , β , γ and δ were described to be activated and mediate FLS aggressiveness (Bottini & Firestein, 2013). The inhibition of p38 α and β was found to decrease the secretion of pro-inflammatory cytokines by RA-FLS (Korb et al, 2006). Although in our experimental setting NaHS affected only phosphorylation of p38 δ MAPkinase, it significantly reduced the IL-1 β -induced activation of several other MAPkinases, particularly MKK6 (upstream of p38), MSK2 (downstream of p38) and GSK-3 which interacts with inflammatory pathways as well as the Wnt/ β -catenin pathway.

The protein kinase B, encoded by the genes Akt1-3 is part of the PI3K/Akt pathway regulating a variety of cellular functions e.g. survival (Garcia et al, 2010; Miyashita et al, 2003; Zhang et al, 2001), angiogenesis (Cai et al, 2007) or even migration and invasion (Fan et al, 2013) in synovial fibroblasts or endothelial cells. Our study is the first to demonstrate that NaHS treatment leads to increased phosphorylation of Akt in FLS. It is evident, however, that also the activation of NF- κ B, which can be induced by hydrogen sulfide, acts as a pro-survival factor. Activation of members of the ERK pathway (ERK2 & MSK2) but not of the p38 and JNK pathway were additionally observed after NaHS treatment of unstimulated FLS. Thus, on the one hand hydrogen sulfide obviously has the capacity to increase phosphorylation (activation) of several signal transduction molecules in unstimulated (i.e. non-inflammatory) FLS, while on the other hand it partially suppresses MAP-K activation in IL-1 β stimulated (i.e. inflammatory) FLS, acting as an IL-1 β antagonist. This further confirms the notion of the complex role hydrogen sulfide apparently plays in inflammation and inflammatory diseases.

4.3 Hydrogen sulfide inhibits IL-1 β -induced experimental hyperplasia of FLS in micromass cultures

The synovial lining layer which separates the synovial fluid compartment from the synovial sublining region consists of a network of FLS together with macrophages and extracellular matrix. Therefore, FLS cultured in spherical micromasses composed of Matrigel matrix are an interesting system to analyse the effects of NaHS treatment on cell migration, morphology and activation.

The data obtained in this culture system demonstrated that also OA-FLS form a condensed lining layer-like structure as shown in previous investigations for RA-FLS (Kiener et al, 2010). Furthermore, stimulation with IL-1 β resulted in hyperplasia of this lining layer like structure which is consistent with findings obtained previously with TNF- α stimulated RA-FLS (Kiener et al, 2010). Remarkably, the stimulatory effect of IL-1 β was completely blocked in cultures treated with NaHS which further supports our findings obtained in conventional cultures. We assume that this pronounced effect may result from the NaHS-induced manipulation of several signal transduction pathways such as the MAPkinase and the NF- κ B pathway. Although a detailed investigation on this issue has not yet been performed we could demonstrate that NaHS induced Akt phosphorylation also in lining FLS confirming data obtained in conventional cultures by spot blot assays. This leads us to assume that the effects of NaHS in 3-D cultures are quite similar to those seen under conventional assay conditions. In line with this assumption NaHS treatment almost completely inhibited IL-1 β -induced expression of MMP-2.

4.4 Effects of hydrogen sulfide treatment in animal models of arthritis

Based on the data obtained with primary human FLS we were interested to investigate the potential anti-inflammatory effects of hydrogen sulfide *in vivo*. Indeed, we could observe partial reduction of cytokine levels in mice that had been challenged with LPS. To further elucidate the therapeutic potency of NaHS treatment two murine models of arthritis were employed. Collagen-induced arthritis is the most widely used model of inflammatory arthritis in which both the adaptive and the innate immune system are involved

Surprisingly, prophylactic NaHS treatment starting before disease induction had no influence on severity of disease nor outcome of CIA. Therefore we assumed that sulfur treatment does not affect B- and T-cells which was supported by flow cytometric analysis of splenocytes and lymphocytes and the lack of effect on production of anti-collagen antibodies which are the pathogenetic key players in this model.

Therefore, we decided to continue our investigations in the serum transfer arthritis model which largely reflects the effector phase of arthritis in which mainly the innate immune system is involved (Monach et al, 2008). Although NaHS treatment did not influence clinical scores of serum transfer arthritis mice, bone erosion, number of osteoclasts and cartilage loss were significantly reduced. These findings are in line with recently published data that NaHS treatment inhibits osteoclastogenesis, both in murine bone marrow cells (Lee et al, 2013) and human CD11b+ cells (Gambari et al, 2014).

4.5 Concluding remarks

Our data propose anti-inflammatory properties of hydrogen sulfide on activated synovial fibroblasts that seem to result from selective manipulation of the MAPkinase and the PI3K/Akt pathway. The data obtained in serum transfer arthritis experiments revealed that NaHS has pronounced anti-osteoclastogenic properties which is in line with recently published work addressing the role of hydrogen sulfide on osteoclastogenesis *in vitro*. Taken together, while the effects of hydrogen sulfide in the regulation of inflammatory processes appear to be rather complex its role in osteoclastogenesis and bone metabolism suggests beneficial effects that should be further explored. Hence, newly developed slow releasing H₂S donors which show a more linear release of H₂S might lead to a breakthrough in sulfur science and are interesting candidates for future research aimed at developing novel drugs for treatment of bone diseases such as RA or osteoporosis.

5 Methods and Materials

5.1 Cell-Culture and treatment

For the development of primary FLS, synovial tissue was isolated from OA patients undergoing total joint replacement and cells were allowed to adhere to tissue culture flasks. Macrophage-like cells have a limited life span *in vitro* and are overgrown by FLS after a few passages. Primary FLS used in this study had been obtained previously and were stored in liquid nitrogen (Kiener et al, 2000; Kloesch et al, 2010).

After thawing, cells were cultured until confluency in Dulbecco's modified Eagle's medium (DMEM) supplemented with 10% heat-inactivated fetal bovine serum (FBS), 1% non-essential amino acids (NEAA), and penicillin / streptomycin in a humidified atmosphere of 5% CO₂ and 95% air. 24 h prior to each experiment, cells were seeded in the appropriate density. FLS were used between passage four and 14. If not stated otherwise, cells were treated with 1 mM NaHS freshly prepared in phosphate buffered saline (PBS) and diluted appropriately. In some experiments cells were stimulated with 10 ng/ml of IL-1 β .

5.2 Apoptosis Assay Using Flow Cytometry

Following treatment, FLS were harvested with Trypsin-EDTA, prepared for staining by washing with annexin labeling buffer containing 10 mM HEPES / NaOH, pH 7.4, 140 mM NaCl and 2.5 mM CaCl₂ and labeled with annexin V for 10 min. Afterwards, cells were stained with labeling buffer containing 0.001 g/l 7-Aminoactinomycin (7-AAD) and processed in flow cytometry. For induction of apoptosis, FLS were treated with 1 joule (J) / cm² UV light at 254 nm.

5.3 Real-time RT PCR

5.3.1 RNA Isolation

Total RNA was isolated from cultured cells using TriFast. After vortexing the solution was incubated for 5 min at room temperature (RT). Chloroform was added following another incubation step for 10 min RT. Afterwards the cell suspension was centrifuged (10 min, 13.000 rpm, 4°C). The equal volume of Isopropanol was added to the supernatant followed by incubation for 10 min at -20°C. Subsequently, the solution was centrifuged (10 min, 13.000 rpm, 4°C) and the Isopropanol was discarded. In the following washing step 1 ml of 70% Ethanol was added, centrifuged (10 min, 13.000 rpm, 4°C) and discarded. The pellet was air-dried and dissolved in aqua dest. After DNase digestion, RNA was precipitated over

night at -20°C by addition of sodium acetate (0.3 molar, pH 5.2), 96% ethanol and 5 µg glycogen as carrier.

5.3.2 Reverse Transcription

Reverse transcription was performed by adding 9 µl of pre-diluted total RNA to 1 µl of oligo-dt primer. After incubation for 5 min at 75°C, 15 µl of master mix composed of AMV reaction buffer, dNTPs, AMV and dH₂O was added to each sample. After addition of the mix, the solution was incubated for one hour at 42°C, followed by a heat inactivation step at 95°C for two min. The resulting cDNAs were diluted with 25 µl H₂O and were stored at -20°C. The quality of reverse transcription was controlled by performing real-time RT-PCR with *GAPDH*-specific primers.

In contrast to conventional PCR with only end-point detection, real-time RT-PCR is a method to measure the amount of cDNA during exponential phase of each cycle. Besides its high sensitivity it allows easy quantification of gene expression without post-PCR processing (e.g. agarose gel electrophoresis). SYBR Green was used as a reporter dye in our assays. When binding to the minor groove of double stranded DNA the emission of the fluorescent dye increases. The production of amplicons is proportional to the increase in fluorescent signal. Quantitative RT-PCR was performed in a total volume of 20 µl containing PCR master mix, reference dye, primer mix, dH₂O and 1 µl sample. At the beginning, samples were denatured at 95°C for 7 min. Amplification was performed for 40 cycles at 20 sec at 95°C (denaturation), 30 sec at 55 - 60°C (annealing) and 15 sec at 72°C (extension). All samples were analysed in duplicates. House-keeping gene *GAPDH* was used as a normalizing control for relative quantification.

Table 1 Oligonucleotide sequences for q RT-PCR

gene	sense	antisense	Ref Seq
GAPDH	5'-CGG GGC TCT CCA GAA CAT C-3'	5'-CTC CGA CGC CTG CTT CAC-3'	NM_002046.3
IL-6	5'-AGA GGC ACT GGC AGA AAA-3'	5'-TGC AGG AAC TGG ATC AGG AC-3'	NM_000600.3
MMP-2	5'-GCG ACA AGA AGT ATG GCT TC-3'	5'-TGC CAA GGT CAA TGT CAG GA-3'	
MMP-3	5'-CTC ACA GAC CTG ACT CGG TT-3'	5'-CAC GCC TGA AGG AAG AGA TG-3'	
MMP-14	5'-CAA CAC TGC CTA CGA GAG GA-3'	5'-GTT CTA CCT TCA GCT TCT GG-3'	

Oligonucleotides for quantitative expression analysis were designed using the primer 3 program or derived from Konttinen *et al.* 1999 (Konttinen et al, 1999). Gene sequences of *GAPDH* and *IL-6* were derived from Ensembl Human Genome Browser. The specificity of each primer set was tested by conventional PCR following gel electrophoresis and sequencing of the PCR product. The amplification efficiency was tested using serial dilutions. All primer sequences are summarized in Table 1.

5.4 Enzyme-linked Immunosorbent Assay

Quantitative detection of human cytokines and chemokines out of cell culture supernatant was performed by using either instant or self-coating ELISAs obtained from eBioscience (former Bender MedSystems).

Briefly, a 96-well plate was coated over night with a primary antibody (Ab) specific for the desired cytokine or chemokine. One ml of cell culture supernatant was centrifuged to eliminate cellular particles and the purified supernatant was diluted with the appropriate amount of sample diluent. 50-100 μ l of diluted sample or standard, depending on the assay, were added over night or at least for two hours. Afterwards the plate was washed and a biotin-conjugated detection Ab was added to each well and allowed to incubate for 1 hr. Following washing, a streptavidin-HRP antibody was added and incubation continued for 30 minutes. Unbound streptavidin-HRP was removed by intensive washing, before a substrate solution reactive to HRP was added forming a colored product in proportion to the amount of bound cytokine. The reaction was stopped by the addition of 50 μ l H_2SO_4 (1 mol/l) and the absorbance (450 nm) was measured by a microplate reader.

5.5 Proteome Profiler Array

Phosphorylation of 26 different MAPkinases or other serine/threonine kinases was analysed by spot blot assay. Cell lysates were prepared according to the manufacturer's instructions. Afterwards, protein concentrations were measured by Bradford assay and properly diluted samples were mixed with 20 μ l of reconstituted detection Ab cocktail and incubated for one h. Nitrocellulose membranes were then probed overnight at 4°C and subsequently incubated with horseradish peroxidase-linked Streptavidin. Proteins were visualized by chemiluminescence using the imaging system ChemiDoc XRS or on photographic film after an exposure of 8 min. Pixel densities were quantified using the imaging system GeneGnome or Image J software.

Changes in kinase activation were quantified by normalizing treated samples to PBS-treated control samples. For calculations Microsoft Excel 2013 was used.

5.6 Western-Blotting

Cells were harvested with Trypsin, lysed in sample buffer supplemented with DTT (100 mM), sonicated and incubated for five min at 95°C. After size-specific separation on a 10% polyacrylamide-SDS gel, proteins were transferred to a 0.2 µm nitrocellulose membrane by electroblotting. The membrane was then blocked for one hour in PBS wash solution supplemented with 0.1% Tween 20 and 5% dry milk. Subsequently, the blots were probed overnight (4°C) with the primary Ab. After washing the membrane was incubated for one hour with HRP-conjugated anti-rabbit IgG or anti-mouse IgG secondary Ab. Lumi-Light Western blotting substrate was applied for 5 min.

The results were visualized by chemiluminescence and detected by an imaging system (GeneGnome). A summary of primary Abs is listed in Table 2. Final quantification of pixel densities were done by GeneGnome or Image J software.

Table 2 Primary antibodies for Western blot analysis

Target	Origin	Company
α-tubulin	mouse	Sigma-Aldrich
β-Actin	rabbit	Sigma-Aldrich
p44/42 MAP Kinase (ERK1/2) (137F5)	rabbit	Cell Signaling
phospho-p44/42 MAP Kinase (ERK1/2) (Thr202/Tyr204)	rabbit	Cell Signaling
p38 MAP Kinase	rabbit	Cell Signaling
phospho-p38 MAP Kinase (Thr180/Tyr182)	rabbit	Cell Signaling
NF-κB p65 (C22B4)	rabbit	Cell Signaling
phospho-NF-κB p65 (Ser536)	rabbit	Cell Signaling
phospho-Akt	rabbit	Cell Signaling
phospho-MSK1	rabbit	Cell Signaling
phospho-MKK3/6	rabbit	Cell Signaling
phospho-GSK-3β	rabbit	Cell Signaling
phospho-JNK	rabbit	Cell Signaling

5.7 Micromass Cultures

Three-dimensional (3-D) cultures were constructed as described previously (Kiener et al, 2006; Kiener et al, 2010). Briefly, cultured FLS were released from the culture dish, enumerated and pelleted. The pellet was resuspended in ice-cold Matrigel Matrix at a density of 5×10^6 cells / ml. The solution was transferred one drop each to the middle of a poly-2-hydroxyethylmethacrylate (poly-HEMA) pre-coated culture well. Afterwards, micromass culture medium composed of standard medium supplemented with 1% ITS liquid media supplement, bovine serum albumin (1.250 g/l) and vitamin C (0.176 g/l) was added to each well. The medium was changed three times a week. The floating micromasses were treated and incubated as described in the results section. Micromasses were fixed with 2% paraformaldehyde in PBS. After dehydration and paraffin-embedding the cultures were sectioned at 4 μ m thickness and hematoxylin and eosin staining was performed.

5.7.1 Immunohistochemistry

Slides were deparaffinized, rehydrated and subjected to antigen retrieval. After blocking unspecific binding sites with rabbit IgG Vectastain ABC kit for 20 min, the primary Ab specific for IL-6, MMP-2 or p-Akt diluted in assay diluent, was applied and incubated over night at 4°C. Following 45 min incubation with the secondary Ab, a H₂O₂ block was performed. Finally the ABC substrate was added and color was developed using 3,3'-diaminobenzidine tetrahydrochloride for a maximum of 10 min. Slides were counterstained with hemalaun. As a control, mouse serum was applied to one slide instead of the primary Ab. Light microscopy images were captured and images were processed using Adobe Photoshop CS5 software.

5.8 Animal Models

Experimental models for RA provide a better understanding of the etiology of disease and possible treatment strategies (Bendele, 2001). DBA/1 and C57BL/6 mice were purchased from Charles River Laboratories (Sulzfeld, Germany). Mice were housed under standard pathogen free conditions and were fed standard sNIFF diet. Animals were habituated to the animal facility of the Medical University Vienna for one week before experimental procedures were started.

5.8.1 Collagen-induced Arthritis

DBA/1OlaHsd inbred male mice of 6-8 weeks of age purchased from Harlan Laboratories were used in CIA experiments.

The effect of NaHS treatment was analysed by applying a prophylactic protocol (Table 3). Mice were treated by i.p. injection of either 100 μ l PBS, or 0.2 mmol/l (1 μ mol / kg) or 0.4

mmol/l (2 μ mol / kg) NaHS on day -3, -1, 4, 7, 11, 14, 18 and 20. For the induction of arthritis, mice were intravenously injected with 100 μ g bovine collagen type II in 100 μ l Freund's complete adjuvant (CFA) and 2 mg / ml *mycobacterium tuberculosis* on day 0. Lyophilized bovine collagen was dissolved by incubating on a rotator overnight in 5 ml of 50 mmol/l acetic acid. 21 days later, animals received a boost injection of 100 μ g bovine collagen type II in 100 μ l IFA. Already one week before the boost injection, the first disease symptoms could be recognized. 60 days after the first immunization, mice were sacrificed and serum, spleens, lymph nodes and paws were collected.

Table 3 Sulfur treatment of mice with CIA

number of mice	Substance	concentration (mM)	disease induction
7	-	-	yes
7	PBS	-	yes
12	NaHS	0.2	yes
12	NaHS	0.4	yes
7	NaHS	0.4	no
7	-	-	yes

5.8.2 Serum transfer arthritis

C57BL/6 inbred male mice of 6-8 weeks of age purchased from Harlan Laboratories were used for serum transfer arthritis experiments. K/BxN mice expressing the T cell receptor transgene KRN and the MHC class II molecule Ag⁷ spontaneously develop severe arthritis. By injecting the serum of these mice, arthritis can be transferred to other mouse strains (Monach et al, 2008). For disease induction C57BL/6 mice were injected i.p. with 150 μ l K/BxN serum on day 0 following a boost injection on day 2.

Mice (n=8 per group) were treated with 100 μ l of a 0.4 mmol/l NaHS solution or PBS which was injected i.p. one day before the disease induction (-1), one day before the boost (1) and on days 3, 6 and 8. One day after the boost mice developed an acute monophasic arthritis. In an additional experiment mice were treated only twice, on days -1 and 1. The experiments was terminated on day 9 and serum, spleens and paws were collected.

5.8.3 Clinical evaluation

Arthritis symptoms were evaluated by two independent observers. Paw swelling at each limb using a score of 0 to 3 (0: no swelling; 1: mild- ; 2: moderate- ; 3: severe swelling) and the grip strength of each paw scored from 0 to -3 (0: normal grip strength; -1: moderately- ; -2: severely reduced grip strength; -3: no grip strength) were monitored either two times a week starting day 21 after induction of CIA or on day three, six, seven and eight after induction of serum transfer arthritis (Bluml et al, 2011). In addition, weight of DBA/1 mice enrolled in CIA experiments was monitored starting day 0.

5.8.4 Sample Collection

Mice were sacrificed by cervical dislocation after anesthetization with ether. Lymphoid tissues, blood and paws were collected for histological and immunological analyses. Paws were dissected, decalcified and paraffin embedded.

Spleen and lymph nodes were collected and splenocytes and lymphocytes were extracted by filtering in 5 ml PBS. The cell solution was then transferred to 15 ml Falcon tubes and the filter was washed with another 5 ml of PBS. The tubes were centrifuged for 7 min at 1.300 rpm at 4°C and the supernatants were discarded. For isolation of splenocytes, erylysis using ACK erylysis buffer had to be performed. Therefore 1 ml of buffer was added to the detached cells and the solution was incubated for 5 min on ice. The reaction was stopped by adding 5 ml ice-cold PBS. After another centrifugation step at the above mentioned conditions, the supernatant was discarded and cells were resuspended in 5 ml pre-warmed DMEM supplemented with 10% FBS. Splenocytes and lymphocytes were analysed by flow cytometry.

Blood was collected for flow cytometry and serum analysis by ELISA. Serum was generated by centrifuging at 1.500 rpm for seven min at 4°C and stored at -80°C.

5.8.5 Histological and Immunological Analysis

Paws were stained with H&E, toluidine blue and for tartrate-resistant acid phosphatase (TRAP) and were analysed by standard histological techniques for signs of bone erosions, cartilage degradation, inflammation and number of osteoclasts.

The area considered in our analysis is illustrated in Figure 34.

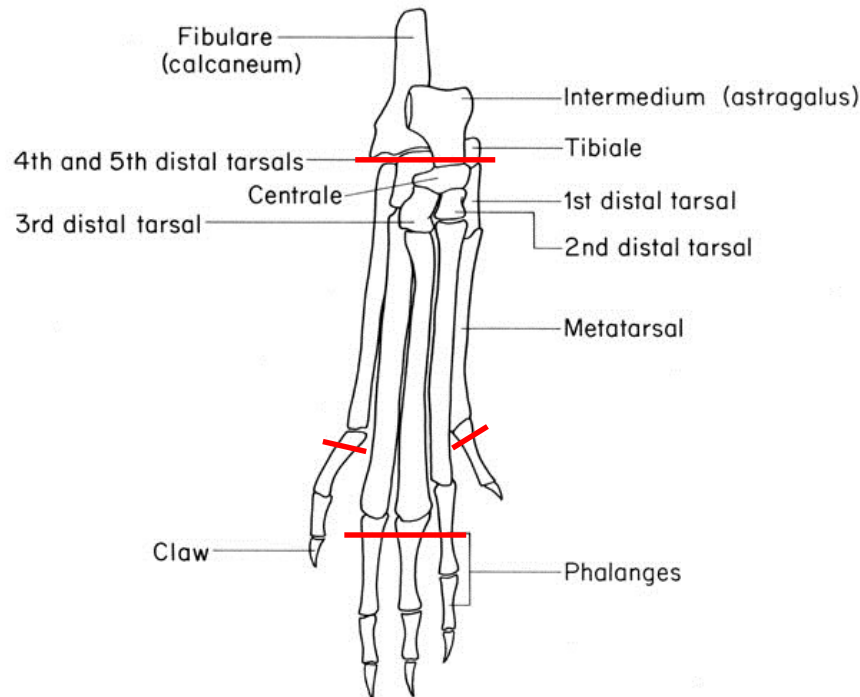


Figure 34 Schematic illustration of a right hind paw from *mus musculus* (Cook, 1965)

The area between the red lines was analysed for histological alterations.

Levels of TNF- α , IL-6, IL-1 β , IL-4, MIP-2, IL-17 and IgG anti-collagen Abs were quantified out of murine serum by ELISA (see 5.4 for details).

The distribution of immune cells of blood and lymphoid organs were assessed by flow cytometry. Lymph nodes from CIA mice were stained for B- and T-cells, effector cells and Foxp3⁺ regulatory T-cells. Blood cells and splenocytes of mice with serum transfer arthritis were stained for effector cells only. Antibodies were obtained from eBioscience and are listed in table 4.

Table 4 Antibodies used in flow cytometry

Target	antibody	Color
T-cells	CD62L	FITC
	CD44	PE
	CD4	Per CP
	CD3	APC
	CD69	APC Cy7
	CD8	PE Cy7
B-cells	B220	APC Cy7
	CD27	PE Cy7
	IgG	APC
	IgM	PE
	PNA	FITC
Regulatory T-cells	CD25	PE
	CD4	PE Cy5
	CCR6	APC
	GITR	PE Cy7
	CD8	APC Cy7
	Foxp3 (intracellular)	Alexa Fluor 488
Effector cells	Ly6G	FITC
	CD115	PE
	CD11b	Per CP
	F4/80	APC
	CD11c	APC Cy7
	Ly6C	PE Cy7

5.9 Statistical Analysis

All statistic evaluations were performed using Microsoft Excel and GraphPad Prism version 5.04. Data are expressed as the mean \pm standard error of the mean (SEM). Homogeneous distribution of variances was analysed by f-tests. For normally distributed data an unpaired Student's *t*-test with Welch's correction was used. In case of heterogeneous variances, a log transformation of data sets was applied prior to analysis. For the statistical analysis of results gained from the animal model a two-tailed Fisher exact test or a two-tailed Mann-Whitney test was applied. The levels of statistically significant differences were $p < 0.05$ (*), $p < 0.01$ (**), $p < 0.001$ (***) and $p < 0.0001$ (****).

5.10 Chemicals and Reagents

Table 5 Chemicals and reagents used for this work

Solution / Reagents / Kit	Description	Company
3,3'- Diaminobenzidinetetrahydrochloride	10 mg	Sigma-Aldrich
7-Aminoactinomycin (7-AAD)		Fluka Biochemica
Acetic acid		Sigma-Aldrich
Ammonia solution	25%	Merck
Ammoniumpersulphate (APS)	10%	Applichem
Annexin V		Eubio
Aqua bidest.		Fresenius Kabi
Bovine serum albumin (BSA)		Carl Roth GmbH
Chloroform		Carl Roth GmbH
Collagen type II; bovine	10 mg	MDbioproducts
Complete Freund's adjuvant (CFA)		BD Biosciences
Dimethyl sulfoxide (DMSO)	Minimum 99.5% GC	Sigma-Aldrich
dNTP Set 1	25 µM	Carl Roth GmbH
Dulbecco's modified eagle's medium (DMEM)	4500 mg glucose / l, L- glutamine, NaHCO ₃ and pyridoxine	Sigma-Aldrich
ELISA Ready-SET-Go!	hIL-6, mTNF-α, mL-6, mIL-1β, mL-4, mL-17	eBioscience
Eosin G solution	1%	Carl Roth GmbH
Ethanol	100%	Merck
Fetal Bovine Serum (FBS)		Sigma-Aldrich
Glycogen		PeqLab
Human Instant ELISA	IL-6	Bender MedSystems
Hydrochloride acid solution	HCl 1Mol / l (1N)	Kwizda
Hydrogen Peroxide (H ₂ O ₂)	30%	Merck
Interleucin-1β	10 µg / ml	Prospec
Isopropanol	99% + H ₂ O 0.05%	Sigma-Aldrich
ITS + Premix		BD Biosciences
L(+)-ascorbic acid	≥ 99%	Carl Roth GmbH
Lipopolysaccharide (LPS)	<i>Escherichia coli</i> 055:B5	Sigma-Aldrich
Lumi-Light Western substrate		Roche
Matrigel Matrix		BD Biosciences

Mayer's hemalaun solution		Merck
Methanol		Merck
Mycobacterium Tuberculosis		BD Biosciences
Natriumhydrogensulfid (NaHS)		Sigma-Aldrich
n-Butyl acetate		Merck
Non-essential amino acid (NEAA) solution	100%	Sigma-Aldrich
Oligonucleotides	Stock solution 100 µM	Eurofins MWG
Penicillin / Streptomycin	50 U + 0.05 mg / ml	Sigma-Aldrich
PeqGold protein marker		PeqLab
PeqGold TriFast		PeqLab
Pertex		Medite
Phorbol 12-Myristate 13-Acetate (PMA)		Sigma-Aldrich
Phosphate Buffered Saline (PBS)	10x	Gibco
Poly (2-hydroxyethylmethacrylate)		Sigma-Aldrich
Roti®-Histofix	4%	Carl Roth GmbH
Roti®-Mark prestained protein marker		Carl Roth GmbH
Rotiphorese® gel 40		Carl Roth GmbH
Sodium Acetate		Sigma-Aldrich
Sodium chloride		Merck
Sulfuric acid		Sigma-Aldrich
Tetramethylethylenediamine (Temed)	99%	Carl Roth GmbH
TRIS (hydroxymethyl)-aminomethane		Merck
Tris-Acetate-EDTA buffer	10x	Sigma-Aldrich
Trypsin-EDTA solution	0.25%	Sigma-Aldrich
Tween 20		Merck

5.11 Buffers and solutions

ACK erylysis solution

8,29 g NH₄Cl

1 g KHCO₃

200 µl EDTA (pH 8.0)

fill up to 1 l with dH₂O

Annexin labeling buffer (ALB)

10 mM HEPES/NaOH, pH 7.4 (Carl Roth GmbH)

140 mM NaCl (Merck)

2.5 mM CaCl₂ (Merck)

Blocking solution

100 ml PBST

5 g milk powder (Carl Roth GmbH)

Blotting buffer (10x)

58.2 g Tris (Carl Roth GmbH)

29.3 g Glycin (Carl Roth GmbH)

0.375 g SDS (Carl Roth GmbH)

Blotting solution

100 ml blotting buffer (10x)

200 ml Methanol (Carl Roth GmbH)

Ad at 1000 ml with H₂O

DNase digestion

Baseline-Zero DNase 1 U / µl (Epicentre)

10 x Baseline-Zero DNase reaction buffer (Epicentre)

10 x Baseline-Zero DNase stop buffer (Epicentre)

Freezing medium (for 50 ml)

45 ml DMEM + 10% FBS

5ml DMSO

Polyacrylamide gel (10%):

Running gel (2x): 2.5 ml running gel buffer

- 4.1 ml dH₂O
- 3.3 ml Acrylamide
- 100 µl APS
- 4 µl TEMED

Stacking gel (2x): 750 µl running gel buffer

- 1.8 ml dH₂O
- 450 µl Acrylamide
- 30 µl APS
- 3 µl TEMED

PBST

- 100 ml PBS (10x)
- 1 ml Tween 20 (Merck)
- Ad 1000 ml with H₂O

Real-time PCR Master Mix

F-415L DyNAmo Flash SYBR Green qPCR Kit (Finnzymes)
and F416L DyNAmo ColorFlash SYBR Green qPCR Kit

Reverse Transcriptase Master Mix

- AMV reverse transcriptase F-570L (Finnzymes)
- 10 x AMV reaction buffer F-570B (Finnzymes)
- dNTPs

Running gel buffer

- 1.5 M Tris-HCl buffer (Bio-Rad Laboratories)
- 0.4 g SDS (Carl Roth GmbH)
- pH 8.8

Sample buffer for WB

- 500 µl Roti[®]-Load 1 (Carl Roth GmbH)
- 500 µl H₂O

SDS running buffer (5x)

15.1 g Tris (Carl Roth GmbH)

72 g Glycin (Carl Roth GmbH)

5 g SDS (Carl Roth GmbH)

Stacking gel buffer

100 ml 0.5 M Tris-HCl buffer (Bio-Rad Laboratories)

0.4 g SDS (Carl Roth GmbH)

pH 6.8

5.12 Equipment

Axioskop MOT2 Microscope (Zeiss) **with CellF software** (Olympus)

BioBan LAF Cabinet (Angelantoni Industries)

Centrifuge 5415R and 5810R (Eppendorf)

Chemiluminescence detector Gene Genome (Syngene)

CO₂ incubator (Binder)

Combispin FVL-2400N (PeqLab)

EcoLab water bath (AL-Labortechnik)

Facscanto II, with Facsdiva software (BD Biosciences)

Microplate reader 680 (Bio-Rad)

Microscope inverse IT400 trino plan (VWR)

Osteomeasure software (OsteoMetrics)

pH meter (Orion)

Pipetboy (Integra Biosciences)

Pipettes (Eppendorf; Gilson; PeqLab)

Power supply PowerPac 200 and 1000 (Bio-Rad)

Real-time PCR cyclers MX3000P (Stratagene)

Rotilabo[®] blotting paper 1 mm (Carl Roth GmbH)

Roti[®]-NC nitrocellulose membrane 0.2 mm (Carl Roth GmbH)

RNA/DNA Calculator Spectrophotometer (Gene Quant)

Thermomixer Dry Block Heating Shaker 1.5 ml (Eppendorf)

Trans-Blot SD semi-dry transfer cell (Bio-Rad)

Scale Adventurer-Pro (OHAUS)

Semi Dry Maxi blotting system (Biozym)

Sonicator (Brandelin Electric)

Ultra low temperature freezer U410 Premium (New Brunswick Scientific)

6 References

Abramson SB, Amin A (2002) Blocking the effects of IL-1 in rheumatoid arthritis protects bone and cartilage. *Rheumatology* **41**: 972-980

Abramson SB, Attur M (2009) Developments in the scientific understanding of osteoarthritis. *Arthritis research & therapy* **11**: 227

Afif H, Benderdour M, Mfuna-Endam L, Martel-Pelletier J, Pelletier JP, Duval N, Fahmi H (2007) Peroxisome proliferator-activated receptor gamma1 expression is diminished in human osteoarthritic cartilage and is downregulated by interleukin-1beta in articular chondrocytes. *Arthritis research & therapy* **9**: R31

Alaaeddine N, Di Battista JA, Pelletier JP, Kiansa K, Cloutier JM, Martel-Pelletier J (1999) Inhibition of tumor necrosis factor alpha-induced prostaglandin E2 production by the antiinflammatory cytokines interleukin-4, interleukin-10, and interleukin-13 in osteoarthritic synovial fibroblasts: distinct targeting in the signaling pathways. *Arthritis and rheumatism* **42**: 710-718

Altman R, Asch E, Bloch D, Bole G, Borenstein D, Brandt K, Christy W, Cooke TD, Greenwald R, Hochberg M, et al. (1986) Development of criteria for the classification and reporting of osteoarthritis. Classification of osteoarthritis of the knee. Diagnostic and Therapeutic Criteria Committee of the American Rheumatism Association. *Arthritis and rheumatism* **29**: 1039-1049

Amalinei C, Caruntu ID, Giusca SE, Balan RA (2010) Matrix metalloproteinases involvement in pathologic conditions. *Romanian journal of morphology and embryology = Revue roumaine de morphologie et embryologie* **51**: 215-228

Andruski B, McCafferty DM, Ignacy T, Millen B, McDougall JJ (2008) Leukocyte trafficking and pain behavioral responses to a hydrogen sulfide donor in acute monoarthritis. *American journal of physiology Regulatory, integrative and comparative physiology* **295**: R814-820

Arend WP, Dayer JM (1995) Inhibition of the production and effects of interleukin-1 and tumor necrosis factor alpha in rheumatoid arthritis. *Arthritis and rheumatism* **38**: 151-160

Bartok B, Firestein GS (2010) Fibroblast-like synoviocytes: key effector cells in rheumatoid arthritis. *Immunological reviews* **233**: 233-255

- Begovich AB, Carlton VE, Honigberg LA, Schrodi SJ, Chokkalingam AP, Alexander HC, Ardlie KG, Huang Q, Smith AM, Spoerke JM, Conn MT, Chang M, Chang SY, Saiki RK, Catanese JJ, Leong DU, Garcia VE, McAllister LB, Jeffery DA, Lee AT, Batliwalla F, Remmers E, Criswell LA, Seldin MF, Kastner DL, Amos CI, Sninsky JJ, Gregersen PK (2004) A missense single-nucleotide polymorphism in a gene encoding a protein tyrosine phosphatase (PTPN22) is associated with rheumatoid arthritis. *American journal of human genetics* **75**: 330-337
- Bendele A (2001) Animal models of rheumatoid arthritis. *Journal of musculoskeletal & neuronal interactions* **1**: 377-385
- Benedetti S, Canino C, Tonti G, Medda V, Calcaterra P, Nappi G, Salaffi F, Canestrari F (2010) Biomarkers of oxidation, inflammation and cartilage degradation in osteoarthritis patients undergoing sulfur-based spa therapies. *Clinical biochemistry* **43**: 973-978
- Benetti LR, Campos D, Gurgueira SA, Vercesi AE, Guedes CE, Santos KL, Wallace JL, Teixeira SA, Florenzano J, Costa SK, Muscara MN, Ferreira HH (2013) Hydrogen sulfide inhibits oxidative stress in lungs from allergic mice in vivo. *European journal of pharmacology* **698**: 463-469
- Blackburn WD (1996) Management of osteoarthritis and rheumatoid arthritis: prospects and possibilities. *The American journal of medicine* **100**: 24S-30S
- Bluml S, Binder NB, Niederreiter B, Polzer K, Hayer S, Tauber S, Schett G, Scheinecker C, Kollias G, Selzer E, Bilban M, Smolen JS, Superti-Furga G, Redlich K (2010) Antiinflammatory effects of tumor necrosis factor on hematopoietic cells in a murine model of erosive arthritis. *Arthritis and rheumatism* **62**: 1608-1619
- Bluml S, Bonelli M, Niederreiter B, Puchner A, Mayr G, Hayer S, Koenders MI, van den Berg WB, Smolen J, Redlich K (2011) Essential role of microRNA-155 in the pathogenesis of autoimmune arthritis in mice. *Arthritis and rheumatism* **63**: 1281-1288
- Boegard T, Jonsson K (1999) Radiography in osteoarthritis of the knee. *Skeletal radiology* **28**: 605-615
- Bottini N, Firestein GS (2013) Duality of fibroblast-like synoviocytes in RA: passive responders and imprinted aggressors. *Nature reviews Rheumatology* **9**: 24-33

Cai WJ, Wang MJ, Moore PK, Jin HM, Yao T, Zhu YC (2007) The novel proangiogenic effect of hydrogen sulfide is dependent on Akt phosphorylation. *Cardiovascular research* **76**: 29-40

Caliendo G, Cirino G, Santagada V, Wallace JL (2010) Synthesis and biological effects of hydrogen sulfide (H₂S): development of H₂S-releasing drugs as pharmaceuticals. *Journal of medicinal chemistry* **53**: 6275-6286

Chen D, Pan H, Li C, Lan X, Liu B, Yang G (2011) Effects of hydrogen sulfide on a rat model of sepsis-associated encephalopathy. *Journal of Huazhong University of Science and Technology Medical sciences = Hua zhong ke ji da xue xue bao Yi xue Ying De wen ban = Huazhong keji daxue xuebao Yixue Yingdewen ban* **31**: 632-636

Chen W, Liu N, Zhang Y, Qi Y, Yang J, Deng Z, Li X, Xie X (2013) [Exogenous hydrogen sulfide protects against myocardial injury after skeletal muscle ischemia/reperfusion by inhibiting inflammatory cytokines and oxidative stress in rats]. *Nan fang yi ke da xue xue bao = Journal of Southern Medical University* **33**: 554-558

Choi YA, Lee DJ, Lim HK, Jeong JH, Sonn JK, Kang SS, Baek SH (2004) Interleukin-1beta stimulates matrix metalloproteinase-2 expression via a prostaglandin E₂-dependent mechanism in human chondrocytes. *Experimental & molecular medicine* **36**: 226-232

Clements KM, Price JS, Chambers MG, Visco DM, Poole AR, Mason RM (2003) Gene deletion of either interleukin-1beta, interleukin-1beta-converting enzyme, inducible nitric oxide synthase, or stromelysin 1 accelerates the development of knee osteoarthritis in mice after surgical transection of the medial collateral ligament and partial medial meniscectomy. *Arthritis and rheumatism* **48**: 3452-3463

Colmegna I, Weyand CM (2011) Haematopoietic stem and progenitor cells in rheumatoid arthritis. *Rheumatology* **50**: 252-260

Contassot E, Beer HD, French LE (2012) Interleukin-1, inflammasomes, autoinflammation and the skin. *Swiss medical weekly* **142**: w13590

Cook M (1965) *The Anatomy of the Laboratory Mouse*.

Ding B, Padyukov L, Lundstrom E, Seielstad M, Plenge RM, Oksenberg JR, Gregersen PK, Alfredsson L, Klareskog L (2009) Different patterns of associations with anti-citrullinated protein antibody-positive and anti-citrullinated protein antibody-negative rheumatoid arthritis in the extended major histocompatibility complex region. *Arthritis and rheumatism* **60**: 30-38

Doss F, Menard J, Hauschild M, Kreutzer HJ, Mittlmeier T, Muller-Steinhardt M, Muller B (2007) Elevated IL-6 levels in the synovial fluid of osteoarthritis patients stem from plasma cells. *Scandinavian journal of rheumatology* **36**: 136-139

Ekmekcioglu C, Strauss-Blasche G, Holzer F, Marktl W (2002) Effect of sulfur baths on antioxidative defense systems, peroxide concentrations and lipid levels in patients with degenerative osteoarthritis. *Forschende Komplementarmedizin und klassische Naturheilkunde = Research in complementary and natural classical medicine* **9**: 216-220

Fan W, Zhou ZY, Huang XF, Bao CD, Du F (2013) Deoxycytidine kinase promotes the migration and invasion of fibroblast-like synoviocytes from rheumatoid arthritis patients. *International journal of clinical and experimental pathology* **6**: 2733-2744

Fan Z, Bau B, Yang H, Aigner T (2004) IL-1beta induction of IL-6 and LIF in normal articular human chondrocytes involves the ERK, p38 and NFkappaB signaling pathways. *Cytokine* **28**: 17-24

Ferraccioli G, Bracci-Laudiero L, Alivernini S, Gremese E, Tulusso B, De Benedetti F (2010) Interleukin-1beta and interleukin-6 in arthritis animal models: roles in the early phase of transition from acute to chronic inflammation and relevance for human rheumatoid arthritis. *Molecular medicine* **16**: 552-557

Fioravanti A, Giannitti C, Bellisai B, Iacoponi F, Galeazzi M (2012) Efficacy of balneotherapy on pain, function and quality of life in patients with osteoarthritis of the knee. *International journal of biometeorology* **56**: 583-590

Firestein GS (2009) Rheumatoid arthritis in a mouse? *Nature clinical practice Rheumatology* **5**: 1

Flood J (2010) The role of acetaminophen in the treatment of osteoarthritis. *The American journal of managed care* **16 Suppl Management**: S48-54

Fournier C (2005) Where do T cells stand in rheumatoid arthritis? *Joint, bone, spine : revue du rhumatisme* **72**: 527-532

Francon A, Forestier R (2009) [Spa therapy in rheumatology. Indications based on the clinical guidelines of the French National Authority for health and the European League Against Rheumatism, and the results of 19 randomized clinical trials]. *Bulletin de l'Academie nationale de medecine* **193**: 1345-1356; discussion 1356-1348

Gabriel SE, Michaud K (2009) Epidemiological studies in incidence, prevalence, mortality, and comorbidity of the rheumatic diseases. *Arthritis research & therapy* **11**: 229

Gambari L, Lisignoli G, Cattini L, Manferdini C, Facchini A, Grassi F (2014) Sodium hydrosulfide inhibits the differentiation of osteoclast progenitor cells via NRF2-dependent mechanism. *Pharmacological research : the official journal of the Italian Pharmacological Society* **87C**: 99-112

Garcia S, Liz M, Gomez-Reino JJ, Conde C (2010) Akt activity protects rheumatoid synovial fibroblasts from Fas-induced apoptosis by inhibition of Bid cleavage. *Arthritis research & therapy* **12**: R33

Georganas C, Liu H, Perlman H, Hoffmann A, Thimmapaya B, Pope RM (2000) Regulation of IL-6 and IL-8 expression in rheumatoid arthritis synovial fibroblasts: the dominant role for NF-kappa B but not C/EBP beta or c-Jun. *Journal of immunology* **165**: 7199-7206

Giuliani D, Ottani A, Zaffe D, Galantucci M, Strinati F, Lodi R, Guarini S (2013) Hydrogen sulfide slows down progression of experimental Alzheimer's disease by targeting multiple pathophysiological mechanisms. *Neurobiology of learning and memory* **104**: 82-91

Gu Q, Wang B, Zhang XF, Ma YP, Liu JD, Wang XZ (2013) Contribution of hydrogen sulfide and nitric oxide to exercise-induced attenuation of aortic remodeling and improvement of endothelial function in spontaneously hypertensive rats. *Molecular and cellular biochemistry* **375**: 199-206

Guerne PA, Zuraw BL, Vaughan JH, Carson DA, Lotz M (1989) Synovium as a source of interleukin 6 in vitro. Contribution to local and systemic manifestations of arthritis. *The Journal of clinical investigation* **83**: 585-592

Herath TD, Wang Y, Seneviratne CJ, Darveau RP, Wang CY, Jin L (2013) The expression and regulation of matrix metalloproteinase-3 is critically modulated by *Porphyromonas gingivalis* lipopolysaccharide with heterogeneous lipid A structures in human gingival fibroblasts. *BMC microbiology* **13**: 73

Hettinga DL (1979) I. Normal Joint Structures and their Reaction to Injury*. *The Journal of orthopaedic and sports physical therapy* **1**: 16-22

Hirano T (2010) Interleukin 6 in autoimmune and inflammatory diseases: a personal memoir. *Proceedings of the Japan Academy Series B, Physical and biological sciences* **86**: 717-730

Hong IK, Kim YM, Jeoung DI, Kim KC, Lee H (2005) Tetraspanin CD9 induces MMP-2 expression by activating p38 MAPK, JNK and c-Jun pathways in human melanoma cells. *Experimental & molecular medicine* **37**: 230-239

Hu Y, Cheng W, Cai W, Yue Y, Li J, Zhang P (2013) Advances in research on animal models of rheumatoid arthritis. *Clinical rheumatology* **32**: 161-165

Hughes MN, Centelles MN, Moore KP (2009) Making and working with hydrogen sulfide: The chemistry and generation of hydrogen sulfide in vitro and its measurement in vivo: a review. *Free radical biology & medicine* **47**: 1346-1353

Imada K, Oka H, Kawasaki D, Miura N, Sato T, Ito A (2010) Anti-arthritic action mechanisms of natural chondroitin sulfate in human articular chondrocytes and synovial fibroblasts. *Biological & pharmaceutical bulletin* **33**: 410-414

Irigoyen P, Lee AT, Wener MH, Li W, Kern M, Batliwalla F, Lum RF, Massarotti E, Weisman M, Bombardier C, Remmers EF, Kastner DL, Seldin MF, Criswell LA, Gregersen PK (2005) Regulation of anti-cyclic citrullinated peptide antibodies in rheumatoid arthritis: contrasting effects of HLA-DR3 and the shared epitope alleles. *Arthritis and rheumatism* **52**: 3813-3818

Ispanovic E, Haas TL (2006) JNK and PI3K differentially regulate MMP-2 and MT1-MMP mRNA and protein in response to actin cytoskeleton reorganization in endothelial cells. *American journal of physiology Cell physiology* **291**: C579-588

Iwanaga T, Shikichi M, Kitamura H, Yanase H, Nozawa-Inoue K (2000) Morphology and functional roles of synoviocytes in the joint. *Archives of histology and cytology* **63**: 17-31

Jackson R (1990) Waters and spas in the classical world. *Medical history Supplement*: 1-13

Joosten LA, Abdollahi-Roodsaz S, Heuvelmans-Jacobs M, Helsen MM, van den Bersselaar LA, Oppers-Walgreen B, Koenders MI, van den Berg WB (2008) T cell dependence of chronic destructive murine arthritis induced by repeated local activation of Toll-like receptor-driven pathways: crucial role of both interleukin-1beta and interleukin-17. *Arthritis and rheumatism* **58**: 98-108

Julia A, Marsal S (2013) The genetic architecture of rheumatoid arthritis: from susceptibility to clinical subphenotype associations. *Current topics in medicinal chemistry* **13**: 720-731

Kao JK, Hsue YT, Lin CY (2007) Role of new population of peripheral CD11c(+)CD8(+) T cells and CD4(+)CD25(+) regulatory T cells during acute and remission stages in rheumatoid arthritis patients. *Journal of microbiology, immunology, and infection = Wei mian yu gan ran za zhi* **40**: 419-427

Kapoor M, Martel-Pelletier J, Lajeunesse D, Pelletier JP, Fahmi H (2011) Role of proinflammatory cytokines in the pathophysiology of osteoarthritis. *Nature reviews Rheumatology* **7**: 33-42

Karagülle M.Z. ZNT, O. Aslan, E. Başak, A. Mutlu (1996) Effects of thermal sulphur bath cure on adjuvant arthritic rats. *Phys Rehab Kur Med* **06**: 53-57

Kiener HP, Brenner MB (2005) Building the synovium: cadherin-11 mediates fibroblast-like synoviocyte cell-to-cell adhesion. *Arthritis research & therapy* **7**: 49-54

Kiener HP, Hofbauer R, Tohidast-Akrad M, Walchshofer S, Redlich K, Bitzan P, Kapiotis S, Steiner G, Smolen JS, Valent P (2000) Tumor necrosis factor alpha promotes the expression of stem cell factor in synovial fibroblasts and their capacity to induce mast cell chemotaxis. *Arthritis and rheumatism* **43**: 164-174

Kiener HP, Lee DM, Agarwal SK, Brenner MB (2006) Cadherin-11 induces rheumatoid arthritis fibroblast-like synoviocytes to form lining layers in vitro. *The American journal of pathology* **168**: 1486-1499

Kiener HP, Watts GF, Cui Y, Wright J, Thornhill TS, Skold M, Behar SM, Niederreiter B, Lu J, Cernadas M, Coyle AJ, Sims GP, Smolen J, Warman ML, Brenner MB, Lee DM (2010) Synovial fibroblasts self-direct multicellular lining architecture and synthetic function in three-dimensional organ culture. *Arthritis and rheumatism* **62**: 742-752

Kloesch B, Liszt M, Broell J (2010) H₂S transiently blocks IL-6 expression in rheumatoid arthritic fibroblast-like synoviocytes and deactivates p44/42 mitogen-activated protein kinase. *Cell biology international* **34**: 477-484

Kloesch B, Liszt M, Krehan D, Broell J, Kiener H, Steiner G (2012a) High concentrations of hydrogen sulphide elevate the expression of a series of pro-inflammatory genes in fibroblast-like synoviocytes derived from rheumatoid and osteoarthritis patients. *Immunology letters* **141**: 197-203

Kloesch B, Liszt M, Steiner G, Broll J (2012b) Inhibitors of p38 and ERK1/2 MAPkinase and hydrogen sulphide block constitutive and IL-1 β -induced IL-6 and IL-8 expression in the human chondrocyte cell line C-28/I2. *Rheumatology international* **32**: 729-736

Knauper V, Will H, Lopez-Otin C, Smith B, Atkinson SJ, Stanton H, Hembry RM, Murphy G (1996) Cellular mechanisms for human procollagenase-3 (MMP-13) activation. Evidence that MT1-MMP (MMP-14) and gelatinase a (MMP-2) are able to generate active enzyme. *The Journal of biological chemistry* **271**: 17124-17131

Konttinen YT, Ainola M, Valleala H, Ma J, Ida H, Mandelin J, Kinne RW, Santavirta S, Sorsa T, Lopez-Otin C, Takagi M (1999) Analysis of 16 different matrix metalloproteinases (MMP-1 to MMP-20) in the synovial membrane: different profiles in trauma and rheumatoid arthritis. *Annals of the rheumatic diseases* **58**: 691-697

Konttinen YT, Ceponis A, Takagi M, Ainola M, Sorsa T, Sutinen M, Salo T, Ma J, Santavirta S, Seiki M (1998) New collagenolytic enzymes/cascade identified at the pannus-hard tissue junction in rheumatoid arthritis: destruction from above. *Matrix biology : journal of the International Society for Matrix Biology* **17**: 585-601

- Korb A, Tohidast-Akrad M, Cetin E, Axmann R, Smolen J, Schett G (2006) Differential tissue expression and activation of p38 MAPK alpha, beta, gamma, and delta isoforms in rheumatoid arthritis. *Arthritis and rheumatism* **54**: 2745-2756
- Kovacs C, Pecze M, Tihanyi A, Kovacs L, Balogh S, Bender T (2012) The effect of sulphurous water in patients with osteoarthritis of hand. Double-blind, randomized, controlled follow-up study. *Clinical rheumatology* **31**: 1437-1442
- Kurko J, Besenyi T, Laki J, Glant TT, Mikecz K, Szekanecz Z (2013) Genetics of rheumatoid arthritis - a comprehensive review. *Clinical reviews in allergy & immunology* **45**: 170-179
- Lai WW, Hsu SC, Chueh FS, Chen YY, Yang JS, Lin JP, Lien JC, Tsai CH, Chung JG (2013) Quercetin inhibits migration and invasion of SAS human oral cancer cells through inhibition of NF-kappaB and matrix metalloproteinase-2/-9 signaling pathways. *Anticancer research* **33**: 1941-1950
- Lambert CA, Colige AC, Munaut C, Lapiere CM, Nusgens BV (2001) Distinct pathways in the over-expression of matrix metalloproteinases in human fibroblasts by relaxation of mechanical tension. *Matrix biology : journal of the International Society for Matrix Biology* **20**: 397-408
- Lauder SN, Carty SM, Carpenter CE, Hill RJ, Talamas F, Bondeson J, Brennan P, Williams AS (2007) Interleukin-1beta induced activation of nuclear factor-kappab can be inhibited by novel pharmacological agents in osteoarthritis. *Rheumatology* **46**: 752-758
- Lee SK, Chung JH, Choi SC, Auh QS, Lee YM, Lee SI, Kim EC (2013) Sodium hydrogen sulfide inhibits nicotine and lipopolysaccharide-induced osteoclastic differentiation and reversed osteoblastic differentiation in human periodontal ligament cells. *Journal of cellular biochemistry* **114**: 1183-1193
- Leibetseder V, Strauss-Blasche G, Holzer F, Marktl W, Ekmekcioglu C (2004) Improving homocysteine levels through balneotherapy: effects of sulphur baths. *Clinica chimica acta; international journal of clinical chemistry* **343**: 105-111

- Li L, Whiteman M, Guan YY, Neo KL, Cheng Y, Lee SW, Zhao Y, Baskar R, Tan CH, Moore PK (2008) Characterization of a novel, water-soluble hydrogen sulfide-releasing molecule (GYY4137): new insights into the biology of hydrogen sulfide. *Circulation* **117**: 2351-2360
- Li P, Schwarz EM (2003) The TNF-alpha transgenic mouse model of inflammatory arthritis. *Springer Seminars in Immunopathology* **25**: 19-33
- Li Q, Lancaster JR, Jr. (2013) Chemical foundations of hydrogen sulfide biology. *Nitric oxide : biology and chemistry / official journal of the Nitric Oxide Society* **35**: 21-34
- Liacini A, Sylvester J, Li WQ, Zafarullah M (2002) Inhibition of interleukin-1-stimulated MAP kinases, activating protein-1 (AP-1) and nuclear factor kappa B (NF-kappa B) transcription factors down-regulates matrix metalloproteinase gene expression in articular chondrocytes. *Matrix biology : journal of the International Society for Matrix Biology* **21**: 251-262
- Ling S, Cheng A, Pumpens P, Michalak M, Holoshitz J (2010) Identification of the rheumatoid arthritis shared epitope binding site on calreticulin. *PloS one* **5**: e11703
- Liu Y, Kalogeris T, Wang M, Zuidema MY, Wang Q, Dai H, Davis MJ, Hill MA, Korthuis RJ (2012) Hydrogen sulfide preconditioning or neutrophil depletion attenuates ischemia-reperfusion-induced mitochondrial dysfunction in rat small intestine. *American journal of physiology Gastrointestinal and liver physiology* **302**: G44-54
- Liu YY, Nagpure BV, Wong PT, Bian JS (2013) Hydrogen sulfide protects SH-SY5Y neuronal cells against d-galactose induced cell injury by suppression of advanced glycation end products formation and oxidative stress. *Neurochemistry international* **62**: 603-609
- Lowicka E, Beltowski J (2007) Hydrogen sulfide (H₂S) - the third gas of interest for pharmacologists. *Pharmacological reports : PR* **59**: 4-24
- Madhok R, Crilly A, Watson J, Capell HA (1993) Serum interleukin 6 levels in rheumatoid arthritis: correlations with clinical and laboratory indices of disease activity. *Annals of the rheumatic diseases* **52**: 232-234
- Majithia V, Geraci SA (2007) Rheumatoid arthritis: diagnosis and management. *The American journal of medicine* **120**: 936-939

Mani S, Untereiner A, Wu L, Wang R (2013) Hydrogen Sulfide and the Pathogenesis of Atherosclerosis. *Antioxidants & redox signaling*

Martel-Pelletier J, Alaaeddine N, Pelletier JP (1999) Cytokines and their role in the pathophysiology of osteoarthritis. *Frontiers in bioscience : a journal and virtual library* **4**: D694-703

McAlindon TE, Bannuru RR, Sullivan MC, Arden NK, Berenbaum F, Bierma-Zeinstra SM, Hawker GA, Henrotin Y, Hunter DJ, Kawaguchi H, Kwok K, Lohmander S, Rannou F, Roos EM, Underwood M (2014) OARSI guidelines for the non-surgical management of knee osteoarthritis. *Osteoarthritis and cartilage / OARS, Osteoarthritis Research Society* **22**: 363-388

Mitsushashi H, Yamashita S, Ikeuchi H, Kuroiwa T, Kaneko Y, Hiromura K, Ueki K, Nojima Y (2005) Oxidative stress-dependent conversion of hydrogen sulfide to sulfite by activated neutrophils. *Shock* **24**: 529-534

Miyashita T, Kawakami A, Tamai M, Izumi Y, Mingguo H, Tanaka F, Abiru S, Nakashima K, Iwanaga N, Aratake K, Kamachi M, Arima K, Ida H, Migita K, Origuchi T, Tagashira S, Nishikaku F, Eguchi K (2003) Akt is an endogenous inhibitor toward tumor necrosis factor-related apoptosis inducing ligand-mediated apoptosis in rheumatoid synovial cells. *Biochemical and biophysical research communications* **312**: 397-404

Miyazawa K, Mori A, Miyata H, Akahane M, Ajisawa Y, Okudaira H (1998) Regulation of interleukin-1beta-induced interleukin-6 gene expression in human fibroblast-like synoviocytes by p38 mitogen-activated protein kinase. *The Journal of biological chemistry* **273**: 24832-24838

Monach PA, Mathis D, Benoist C (2008) The K/BxN arthritis model. *Current protocols in immunology / edited by John E Coligan [et al]* **Chapter 15**: Unit 15 22

Monfort J, Pelletier JP, Garcia-Giralt N, Martel-Pelletier J (2008) Biochemical basis of the effect of chondroitin sulphate on osteoarthritis articular tissues. *Annals of the rheumatic diseases* **67**: 735-740

Nawata Y, Eugui EM, Lee SW, Allison AC (1989) IL-6 is the principal factor produced by synovia of patients with rheumatoid arthritis that induces B-lymphocytes to secrete

immunoglobulins. *Annals of the New York Academy of Sciences* **557**: 230-238, discussion 239

Ngian GS (2010) Rheumatoid arthritis. *Australian family physician* **39**: 626-628

O'Dell JR (2004) Therapeutic strategies for rheumatoid arthritis. *The New England journal of medicine* **350**: 2591-2602

Olofsson P, Holmdahl R (2007) Pristane-induced arthritis in the rat. *Methods in molecular medicine* **136**: 255-268

Palazzo C, Ravaud JF, Papelard A, Ravaud P, Poiraudeau S (2014) The burden of musculoskeletal conditions. *PloS one* **9**: e90633

Pap T, Shigeyama Y, Kuchen S, Fernihough JK, Simmen B, Gay RE, Billingham M, Gay S (2000) Differential expression pattern of membrane-type matrix metalloproteinases in rheumatoid arthritis. *Arthritis and rheumatism* **43**: 1226-1232

Park MJ, Park IC, Hur JH, Kim MS, Lee HC, Woo SH, Lee KH, Rhee CH, Hong SI, Lee SH (2002) Modulation of phorbol ester-induced regulation of matrix metalloproteinases and tissue inhibitors of metalloproteinases by SB203580, a specific inhibitor of p38 mitogen-activated protein kinase. *Journal of neurosurgery* **97**: 112-118

Rainbow R, Ren W, Zeng L (2012) Inflammation and Joint Tissue Interactions in OA: Implications for Potential Therapeutic Approaches. *Arthritis* **2012**: 741582

Roman-Blas JA, Stokes DG, Jimenez SA (2007) Modulation of TGF-beta signaling by proinflammatory cytokines in articular chondrocytes. *Osteoarthritis and cartilage / OARS, Osteoarthritis Research Society* **15**: 1367-1377

Romano M, Sironi M, Toniatti C, Polentarutti N, Fruscella P, Ghezzi P, Faggioni R, Luini W, van Hinsbergh V, Sozzani S, Bussolino F, Poli V, Ciliberto G, Mantovani A (1997) Role of IL-6 and its soluble receptor in induction of chemokines and leukocyte recruitment. *Immunity* **6**: 315-325

Rosengren S, Boyle DL, Firestein GS (2007) Acquisition, culture, and phenotyping of synovial fibroblasts. *Methods in molecular medicine* **135**: 365-375

Rosloniec EF, Cremer M, Kang A, Myers LK (2001) Collagen-induced arthritis. *Current protocols in immunology / edited by John E Coligan [et al]* **Chapter 15**: Unit 15 15

Shammas RM, Ranganath VK, Paulus HE (2010) Remission in rheumatoid arthritis. *Current rheumatology reports* **12**: 355-362

Sidhapuriwala JN, Ng SW, Bhatia M (2009) Effects of hydrogen sulfide on inflammation in caerulein-induced acute pancreatitis. *Journal of inflammation* **6**: 35

Sokolove J, Lepus CM (2013) Role of inflammation in the pathogenesis of osteoarthritis: latest findings and interpretations. *Therapeutic advances in musculoskeletal disease* **5**: 77-94

Strand V, Kimberly R, Isaacs JD (2007) Biologic therapies in rheumatology: lessons learned, future directions. *Nature reviews Drug discovery* **6**: 75-92

Szabó C (2007) Hydrogen sulphide and its therapeutic potential. *Nature reviews Drug discovery* **6**: 917-935

Tan PL, Farmiloe S, Yeoman S, Watson JD (1990) Expression of the interleukin 6 gene in rheumatoid synovial fibroblasts. *The Journal of rheumatology* **17**: 1608-1612

Truong DH, Mihajlovic A, Gunness P, Hindmarsh W, O'Brien PJ (2007) Prevention of hydrogen sulfide (H₂S)-induced mouse lethality and cytotoxicity by hydroxocobalamin (vitamin B(12a)). *Toxicology* **242**: 16-22

Venn G, Nietfeld JJ, Duits AJ, Brennan FM, Arner E, Covington M, Billingham ME, Hardingham TE (1993) Elevated synovial fluid levels of interleukin-6 and tumor necrosis factor associated with early experimental canine osteoarthritis. *Arthritis and rheumatism* **36**: 819-826

Viatte S, Plant D, Raychaudhuri S (2013) Genetics and epigenetics of rheumatoid arthritis. *Nature reviews Rheumatology* **9**: 141-153

Wallace JL, Ferraz JG, Muscara MN (2012) Hydrogen sulfide: an endogenous mediator of resolution of inflammation and injury. *Antioxidants & redox signaling* **17**: 58-67

Wang M, Shen J, Jin H, Im HJ, Sandy J, Chen D (2011) Recent progress in understanding molecular mechanisms of cartilage degeneration during osteoarthritis. *Annals of the New York Academy of Sciences* **1240**: 61-69

Wang R (2003) The gasotransmitter role of hydrogen sulfide. *Antioxidants & redox signaling* **5**: 493-501

Warencya MW, Goodwin LR, Benishin CG, Reiffenstein RJ, Francom DM, Taylor JD, Dieken FP (1989) Acute hydrogen sulfide poisoning. Demonstration of selective uptake of sulfide by the brainstem by measurement of brain sulfide levels. *Biochemical pharmacology* **38**: 973-981

Whiteman M, Haigh R, Tarr JM, Gooding KM, Shore AC, Winyard PG (2010a) Detection of hydrogen sulfide in plasma and knee-joint synovial fluid from rheumatoid arthritis patients: relation to clinical and laboratory measures of inflammation. *Annals of the New York Academy of Sciences* **1203**: 146-150

Whiteman M, Li L, Rose P, Tan CH, Parkinson DB, Moore PK (2010b) The effect of hydrogen sulfide donors on lipopolysaccharide-induced formation of inflammatory mediators in macrophages. *Antioxidants & redox signaling* **12**: 1147-1154

Whiteman M, Winyard PG (2011) Hydrogen sulfide and inflammation: the good, the bad, the ugly and the promising. *Expert review of clinical pharmacology* **4**: 13-32

Williams RO (2004) Collagen-induced arthritis as a model for rheumatoid arthritis. *Methods in molecular medicine* **98**: 207-216

Zanardo RC, Brancaleone V, Distrutti E, Fiorucci S, Cirino G, Wallace JL (2006) Hydrogen sulfide is an endogenous modulator of leukocyte-mediated inflammation. *FASEB journal : official publication of the Federation of American Societies for Experimental Biology* **20**: 2118-2120

Zhang D, Bar-Eli M, Meloche S, Brodt P (2004) Dual regulation of MMP-2 expression by the type 1 insulin-like growth factor receptor: the phosphatidylinositol 3-kinase/Akt and Raf/ERK pathways transmit opposing signals. *The Journal of biological chemistry* **279**: 19683-19690

Zhang G, Wang P, Yang G, Cao Q, Wang R (2013a) The inhibitory role of hydrogen sulfide in airway hyperresponsiveness and inflammation in a mouse model of asthma. *The American journal of pathology* **182**: 1188-1195

Zhang HG, Wang Y, Xie JF, Liang X, Liu D, Yang P, Hsu HC, Ray RB, Mountz JD (2001) Regulation of tumor necrosis factor alpha-mediated apoptosis of rheumatoid arthritis synovial fibroblasts by the protein kinase Akt. *Arthritis and rheumatism* **44**: 1555-1567

Zhang Q, Fu H, Zhang H, Xu F, Zou Z, Liu M, Wang Q, Miao M, Shi X (2013b) Hydrogen sulfide preconditioning protects rat liver against ischemia/reperfusion injury by activating Akt-GSK-3beta signaling and inhibiting mitochondrial permeability transition. *PloS one* **8**: e74422

Zhang W, Moskowitz RW, Nuki G, Abramson S, Altman RD, Arden N, Bierma-Zeinstra S, Brandt KD, Croft P, Doherty M, Dougados M, Hochberg M, Hunter DJ, Kwok K, Lohmander LS, Tugwell P (2007) OARSI recommendations for the management of hip and knee osteoarthritis, part I: critical appraisal of existing treatment guidelines and systematic review of current research evidence. *Osteoarthritis and cartilage / OARS, Osteoarthritis Research Society* **15**: 981-1000

Zhi L, Ang AD, Zhang H, Moore PK, Bhatia M (2007) Hydrogen sulfide induces the synthesis of proinflammatory cytokines in human monocyte cell line U937 via the ERK-NF-kappaB pathway. *Journal of leukocyte biology* **81**: 1322-1332

7 Curriculum Vitae

Name: Daniela Sieghart

E-mail: daniela.sieghart@meduniwien.ac.at

Date of birth: May 7, 1986

Place of birth: Vienna, Austria

Nationality: Austrian

Maiden name: Krehan

Education:

September 1996 – June 2004:

Public grammar school (A level)

3, Wohlmutstrasse, A-1020 Vienna

Tertiary education:

September 2004 – June 2008:

University of Applied Sciences and Biotechnology Vienna (fh-campus wien)

Vienna BioCenter II, 2A, Viehmarktgasse, A-1030 Vienna

Diploma thesis:

July 2007 – March 2009

Children's Cancer Research Institute (CCRI)

6, Kinderspitalgasse, A-1090 Vienna

Topic: *PAX5* aberrations in childhood acute lymphoblastic leukemia

Doctoral thesis:

May 2009 – September 2014

Ludwig Boltzmann Institute for Rheumatology, Balneology and Rehabilitation

14, Kurbadstrasse, A-1100 Vienna

Medical University Vienna, Department of Internal Medicine III, Division of Rheumatology,

18-20, Währinger Gürtel, A-1090 Vienna

Topic: Investigations on the effects of sodium hydrogen sulfide on human fibroblast-like synoviocytes and in two murine models of arthritis

Publications:

Pichler H, Mörlicke A, Mann G, Teigler-Schlegel A, Niggli F, Nebral K, König M, Inthal A, Krehan D, Dworzak MN, Janousek D, Harbott J, Schrappe M, Gadner H, Strehl S, Haas OA, Panzer-Grümayer R, Attarbaschi A (2010) Berlin-Frankfurt-Münster (BFM) Study Group, Prognostic relevance of dic(9;20)(p11;q13) in childhood B-cell precursor acute lymphoblastic leukaemia treated with Berlin-Frankfurt-Münster (BFM) protocols containing an intensive induction and post-induction consolidation therapy. *British Journal of Haematology* **149**: 93-100

Nebral K, Krehan D, Strehl S (2011) Expression of PAX5 splice variants: a phenomenon of stress-induced, illegitimate splicing? *British Journal of Haematology* **155**: 277-80

Kloesch B, Liszt M, Krehan D, Broell J, Kiener H, Steiner G (2012a) High concentrations of hydrogen sulphide elevate the expression of a series of pro-inflammatory genes in fibroblast-like synoviocytes derived from rheumatoid and osteoarthritis patients. *Immunology letters* **141**: 197-203

Sieghart D, Liszt M, Wanivenhaus A, Broell H, Kiener H, Kloesch B, Steiner G Hydrogen sulfide decreases IL-1 β -induced activation of fibroblast-like synoviocytes from patients with osteoarthritis. *Journal of Cellular and Molecular Medicine* (in press)

Congress Participations:**2009 November**

Annual meeting of the Austrian Society of Rheumatology (ÖGR); Graz, Austria

Poster presentation: Effects of an exogenous H₂S-donor (NaHS) on osteoarthritic fibroblast-like synoviocytes

2010 November

Annual meeting of the ÖGR; Wien, Austria

Poster presentation: Effects of hydrogen sulfide on activated T helper 1 leukemic cell line Jurkat as model for rheumatoid arthritis

2014 September

Annual meeting of the ÖGMBT; Vienna, Austria

Oral presentation: Hydrogen sulfide reduces IL-1 β -induced activation of fibroblast-like synoviocytes derived from patients with osteoarthritis

Memberships in the scientific community:

Young Scientist Association of the MUW (YSA) since 2011.

Austrian Association of Molecular Life Sciences and Biotechnology (OEGMBT) since 2013.